Faculdade de Engenharia da Universidade do Porto

Automatic Classification of Ulcers Through Visual Image

Rita Maria Almeida Frade

Master in Biomedical Engineering

Supervisor: Ricardo Vardasca, PhD
Co-supervisor: Joaquim Gabriel Mendes, PhD

19 June, 2017

U.PORTO
FEUP FACULDADE DE ENGENHARIA UNIVERSIDADE DO PORTO

MEB - MESTRADO EM ENGENHARIA BIOMÉDICA **2016/2017**

A Dissertação intitulada

"Automatic Classification of Ulcers Through Visual Image"

foi aprovada em provas realizadas em 27-06-2017

o júri

Presidente Prof. Doutor Miguel Fernando Paiva Velhote Correia
Professor Auxiliar do Departamento de Engenharia Eletrotécnica e de Computadores da FEUP - U.Porto

Prof. Doutor Miguel Tavares Coimbra
Professor Auxiliar do Faculdade de Ciências da U. Porto

Doutor Ricardo Ângelo Rosa Vardasca
Investigador externo do Departamento de Engenharia Mecânica da FEUP - U.Porto

O autor declara que a presente dissertação (ou relatório de projeto) é da sua exclusiva autoria e foi escrita sem qualquer apoio externo não explicitamente autorizado. Os resultados, ideias, parágrafos, ou outros extratos tomados de ou inspirados em trabalhos de outros autores, e demais referências bibliográficas usadas, são corretamente citados.

Autor - Rita Maria Almeida Frade

Faculdade de Engenharia da Universidade do Porto

Abstract

Globally, Chronic Wounds (CW) are health condition, which constitutes a threat to the public health and economy having a detrimental effect on patient's quality of life and high costs in treatments. CW do not perform a well-ordered reparative process thus, the anatomic and functional integrities of the damaged tissue are not restored, being of extreme importance the establishment of an appropriate treatment based on an accurate characterisation of the state of the healing process.

Over the years, several ulcer risk assessment tools have been created, such as: scales, which depend on visual examination being highly subjective; invasive methods that use manual procedures for depicting the shape, area, depth and volume of wounds, are time consuming, susceptible to human errors and can lead to wound contamination; and non-invasive methods such as optical based techniques which provide three-dimensional information about the lesion, being expensive, time consuming and require user training.

There have been made several efforts to use image processing techniques for an objective and automatic analysis of CW images.

This research study aims to create a methodology based in a mobile application which incorporates an algorithm that characterises chronic ulcers providing information about its area and tissue composition.

A MATLAB methodology and an Android mobile application were developed, tested and evaluated in 200 diabetic foot ulcers, allowing greater characterisation of 97% of the ulcers analysed with high correlation with the clinical assessment (R^2=1), reducing subjectivity, avoiding wound contamination probability and smaller costs when compared to conventional solutions.

Key words: Chronic wounds; characterisation; image processing; wound assessment; wound healing.

Resumo

Globalmente, as Feridas Crónicas (FC) são um problema de saúde que constitui uma ameaça para a saúde pública e economia, tendo um efeito prejudicial na qualidade de vida dos pacientes e elevados custos em tratamento. As FC não realizam um processo de reparação ordenado, por esse motivo, as integridades anatómica e funcional dos tecidos danificados não são reestabelecidas, tendo uma importância elevada a determinação de um tratamento apropriado baseado numa caracterização exata do estado do processo de cicatrização.

Ao longo dos anos, têm sido criadas várias ferramentas de avaliação de risco de úlcera, tais como: escalas, que dependem de inspeção visual sendo altamente subjetivas; métodos invasivos que incluem técnicas manuais para obter a forma, área, profundidade e volume de feridas, são demorados, suscetíveis a erros humanos e podem levar a contaminação da úlcera; e métodos não invasivos como técnicas baseadas em sistemas óticos que fornecem informação tridimensional sobre as lesões, tendo um custo elevado, obrigam a que os utilizadores sejam treinados para a sua utilização e a obtenção da caracterização é muito demorada.

Por estes motivos, tem sido verificado um interesse crescente em usar técnicas de processamento de imagem para obter uma análise objetiva e automática de imagens de úlceras.

Este projeto de investigação tem como finalidade a criação de uma metodologia baseada numa aplicação móvel que incorpora um algoritmo de caracterização de úlceras crónicas, fornecendo informação relativamente à sua área e composição tecidular.

Uma metodologia em MATLAB e uma aplicação *Android* foram desenvolvidas, testadas e avaliadas em 200 úlceras de pés diabéticos, permitindo uma ótima caracterização de 97% das úlceras analisadas com alta correlação relativamente à caracterização realizada por clínicos (R^2=1), reduzindo a subjetividade, evitando a contaminação da lesão e com menor custos associados quando comparada com as soluções mais convencionais.

Palavras-chave: Avaliação de feridas; caracterização; cicatrização de feridas; feridas crónicas; processamento de imagem.

Acknowledgments

First of all, I would like to thank Prof. Dr. *Ricardo Vardasca*, my mentor of dissertation, for the will, patience and the constant availability shown to assist me in certain aspects throughout this work.

Secondly, I want to thank Prof. Dr. *Joaquim Gabriel Mendes*, my co-supervisor for the encouragement and kindness of allowing me to work in the L003 laboratory during this year.

Next, I would like to thank Dr. *Rui Morais Carvalho* and all of the physicians and nurses at the D*iabetic Foot Clinic* in *Centro Hospitalar do Porto* for the kindness, motivation and readiness to help and answer all of my questions since the start of this study. I want to leave here a special thanks to every single one of the patients who kindly agreed to participate in my study at *Diabetic Foot Clinic* in *Centro Hospitalar do Porto*.

I would like to acknowledge the Project NORTE-01-0145-FEDER-000022 - SciTech - Science and Technology for Competitive and Sustainable Industries, cofinanced by Programa Operacional Regional do Norte (NORTE2020), funded through the Fundo Europeu de Desenvolvimento Regional (FEDER) and the FCT - Foundation for Science and Technology under the project (PEst-OE/EME/LA0022/2013).

Last but not the least, I thank my family, specially my mother, for believing in me and showing her pride for every difficulty surpassed and goals achieved, and friends who supported and motivated me throughout this adventure.

Contents

List of figures

List of tables

Abbreviations and Symbols

2-D	Two-dimensional
3-D	Three-dimensional
BMI	Body Mass Index
CHT	Circle Hough Transform
CIE	Commission *Internationale de l'Éclairage*
CW	Chronic wound
dB	Decibel
EPUAP	European Pressure Ulcer Advisory Panel
FC	*Feridas crónicas*
FDA	Food and Drug Administration
FOV	Field of view
HSI	Hue, Saturation and Intensity colour space
JavaCV	Java Computer Vision Library
JPEG	Joint Photographics Experts Group
JPG	Joint Photographics Group
LED	Light-Emitting Diode
MAVIS	Measurement of Area and Volume Instrument system
MOWA	Mobile Wound Analyzer
MSS	Manchester Scar Scale
NPUAP	National Pressure Ulcer Advisory Panel
OpenCV	Open Source Computer Vision Library
PDF	Portable Document Format
PNG	Portable Network Graphics

POSAS	Patient and Observer Scar Assessment Scale
PU	Pressure ulcer
PUSH	Pressure ulcer scale for healing
RGB	Red, Green, Blue colour model
ROI	Region of interest
SBSES	Stony Brook Scar Evaluation Scale
SNR	Signal to Noise Ratio
SPG	Stereophotogrammetry
SSS	Seattle Scar Scale
SVM	Support vector machine
TNP	Topical negative pressure
UT	University of Texas
VSS	Vancouver Scar scale
XML	Extensible Markup Language

Chapter 1

Introduction

1.1 - Background and objectives

The skin is the largest organ in the human body acting as an efficient physical and chemical barrier in the organism, being crucial in the survival and maintenance of human life. When compromised, or destroyed, this barrier requires immediate intervention to ensure the return of its normal functions (Lanza *et al.*, 2007; Fung, 2001; Langer and Vacanti, 1993; Benbow, 2006), since skin degeneration and loss associated with chronic wounds (CW) can result in significant morbidity and mortality, due to a disruption of the homeostatic function and susceptibility to infection (Langer and Vacanti 1993).

A wound is defined as a disruption of normal anatomic structure and function, resulting from pathologic processes that begin internally or externally to the involved organ(s). Factors as the patient age, wound size, depth and location and the presence of local and/or systemic diseases lead to wound healing time variation. Homeostasis, inflammation, proliferation and angiogenesis, and remodelling are the main events of the complex highly orchestrated process defined as normal wound healing. Acute wounds experience this series of overlapping phases but CW do not (Benbow, 2006; Whittington and Briones, 2004; Zhan and Miller, 2003; Langemo, 2005; Dargaville *et al.*, 2013).

Besides the financial impact caused by the high costs associated with the treatments and prevention, studies report that CW have a negative impact on patient's psychological and social functioning (Fung, 2001; Langer and Vacanti, 1993; Benbow, 2006; Whittington and Briones, 2004) causing pain and immobility, followed by privation of sleep which leads to lack of energy and of self-esteem, worries and frustrations and thus, leading to their isolation.

When compared to healthy people, individuals with CW have a significantly poorer quality of life due to the regularity of dressing changes, which clearly affects patient's daily routine. On the other hand, due to lack of adequate sleep, these individuals experience a daily feeling of continued fatigue. However, the consequences of having a CW have a massive impact not only on the patient's

social life but also in the lives of their caregivers. The loss of independence associated with functional debility can lead to variations in general health and wellbeing as altered eating habits, social isolation and as a result, depression and a continuing reduction in activity. These issues, plus the absence of mobility, influences the occurrence of further lesions, worsens their severity and limits their ability to heal (Langer and Vacanti, 1993; Benbow, 2006; Whittington and Briones, 2004); Zhan and Miller, 2003; Langemo, 2005).

Ulcers are one of the most common cases of CW. There are many different types of ulcers (venous, arterial, neuropathic, lymphatic, and infectious) with different causes (Dargaville *et al.*, 2013). Ulcers resultant of vascular disease are the most dominant type particularly the venous ones, which accounts for over two-thirds of all types of ulcers, being the most usual type (Benbow, 2006; Whittington and Briones, 2004; Zhan and Miller, 2003; Langemo, 2005).

Relatively to the three types of CW approached in this dissertation, during 2014, it is estimated that developed countries have spent approximately $USD88218 per patient in order to treat scars/burns.

According to the Portuguese society of Diabetology (Sociedade Portuguesa de Diabetologia, 1997), about 415 million (8.8%) of the worldwide population was diagnosed with Diabetes Mellitus in 2015. Being the Portuguese population incidence of 1 million people (13.3% of the total population), with a national annual total spending of 1.7 billion euros with this disease.

Furthermore, the Directorate-General of Health (DGS, 1899) estimated that in 2016, the prevalence of pressure ulcers was of 11.5% in the Portuguese population.

The follow up of the wound healing process is typically performed through scoring scales completed by clinical observation in order to provide comparable semi-quantitative information and thus stimulate better management of funds. However, this is highly dependent on the observer and thus, extremely subjective, jeopardising the quantification of the observations as well as the comparison of results between healthcare centres (Torra, 1997), therefore, its use is restricted (Xu, 2004). After these scales were created, contact methods to evaluate wound depth, area and volume were designed and developed. However, these methods are extremely invasive to the patient and introduce errors. Efforts to automatically assess wounds have been made globally through image processing techniques and smartphones/tablets applications to reduce healthcare costs, patient suffering and improve the assessment of the lesions.

1.2 - Objectives

The aim of this research is to create a methodology that performs chronic wound characterisation according to its area and tissue colour, without promoting wound contamination, patient discomfort, time consumption and subjectivity. This purpose was satisfied by first creating a MATLAB image processing methodology and then incorporating it in an Android mobile application.

In order to fulfil the aim of this project, secondary goals were also established:

- Perform the segmentation of the calibration marker in the image;
- Achieve the segmentation of the chronic ulcer in the image;
- Calculate ulcer area in cm^2;

- Characterise the tissue composition of the ulcer bed relatively to the percentage of unhealthy and healthy granulating tissues, necrotic tissue and white tissue.

1.3 - Dissertation outline

This document is organised in six sections.

The first section, this section, the theme and a characterisation of the problem and its context are introduced as well as the description of the aim and goals. It ends with the description of the report structure.

The Literature review addresses the scientific background of the research. This section is divided in three subsections: Qualitative assessment, Quantitative assessment and Wound care. The first part of the chapter addresses the scales used in medical environment to assess three types of CW: burn/scar, pressure ulcer and diabetic ulcer. These scales are a visual and intuitive starting point of the choice of the most adequate treatment for the patient. The Quantitative assessment, contemplates the necessity of a more accurate follow up of the healing process of a chronic wound. Two types of techniques used to quantify a wound are described: visual characterisation and physical characterisation methods, being the physical methods divided in two sections, namely invasive methods and non-invasive methods. In the invasive methods are described several methods currently used for predicting invasively the depth, area and volume of ulcers; in the non-invasive subsection are described methods created to obtain more accurately the same measures as the invasive approaches such as imaging techniques and image processing methodologies. Further, a review of the existing mobile applications that perform wound assessment is presented by the end of the subchapter. In the Wound care section are described the most common dressings and treatments applied to wounds based on their assessment relatively to appearance, tissue composition, probability of infection and amount of exudate.

The 3rd chapter presents the methodology comprising the sample, software and equipment used, the techniques chosen to process the images and the parameters' values and the mobile application design as well as the methods used to evaluate the obtained outcomes. The tested and low successful image processing techniques tried are also described.

The achieved results are outlined in the 4th chapter relatively to the image pre-processing, ulcer and marker segmentation, ulcer area calculation and tissue characterisation phases of both the methodology created in MATLAB and the one included in the Android mobile application. The cases where the methodology did not succeed are presented for both the markers and the ulcers.

In the Discussion, the algorithms that were tested are assessed, comparisons are established between the work limitations of both methodologies, being presented suggestions of solutions for the weaknesses of each method.

In the last section, Conclusion, the main conclusions are described along with a proposal of further work.

The structure of this dissertation and the links between different parts of this document can be seen in Figure 1.1.

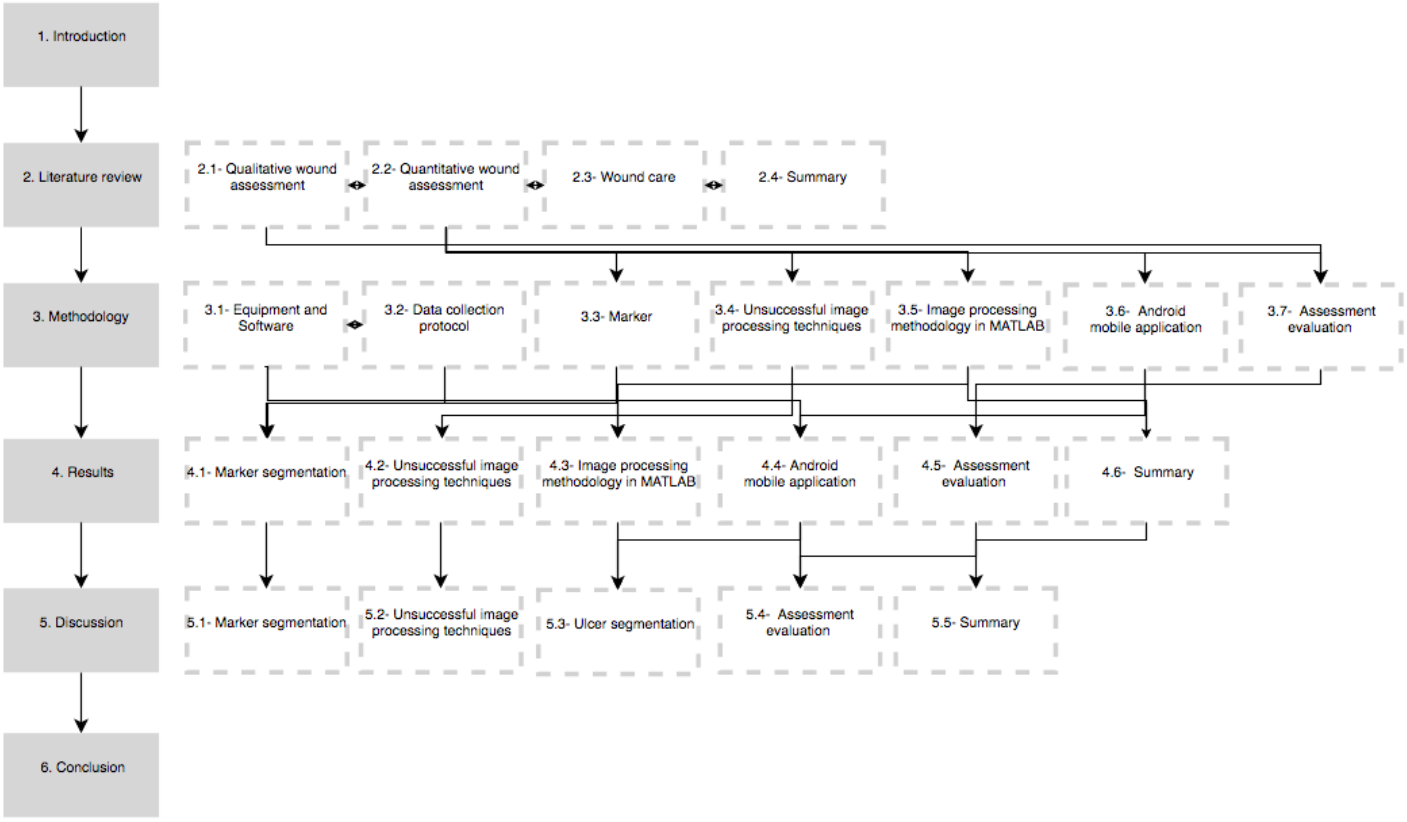

Figure 1.1- Document Outline.

Chapter 2

Literature review

There are several approaches for wound assessment being globally classified as qualitative or quantitative and each has advantages and disadvantages. In this chapter, the most globally accepted techniques of the two types of wound assessment are described as well as the treatments/wound care performed according to the wound characterisation.

2.1 - Qualitative wound assessment

2.1.1 -Cutaneous wound

Acute cutaneous wounds, including burn wounds are a health and economical concern in the global community, which may lead, in the most severe cases to death.

The efficacy of a treatment directly depends on the achieved adequate characterisation therefore, regular assessment of the wound is of extreme importance in order to determine wound healing based on the percentage reduction/increase in wound area over time (Flanagan, 2003; Margolis *et al.*, 2003) and to adjust wound management. However, wound assessment is a very complex process including wound location, wound appearance and tissue type, wound size, odour, identification of aspects that contribute to wound healing delay (presence of serous fluid, pus or exudate, signals of infection or maceration, etc.), pain and the condition of the adjacent skin (Collier, 2003).

The treatment of the cutaneous lesion, particularly when a significant part of tissue is lost, has the goal of leading to the closure of the wound (Xu, 2004). In order to evaluate the response to treatments and to assess its outcomes, numerous techniques have been developed to measure scars (Berardesca and Wilhelm, 1995). Although, new treatments are increasingly becoming more available, there is no international agreement on what is the best method to assess the effects of these treatments. The follow up of the wound healing process is achieved manly through clinical observation (Berardesca and Wilhelm, 1995).

The following scales (2.1.1.1 to 2.1.1.6) were developed for the characterisation of cutaneous wounds.

2.1.1.1 - Vancouver Scar Scale (VSS)

Initially described in 1990 by Sullivan *et al.* (Sullivan *et al.*, 1990), the Vancouver Scar Scale (VSS) is possibly the most documented method to assess burns/scars (Nedelec *et al.*, 2000; Sullivan *et al.*, 1990).

This scale evaluates four variables: vascularity, pigmentation, pliability and height/thickness. Both vascularity and height are rated from 0 to 3, pigmentation has 3 possible scores (0, 1 and 2) and pliability is rated between 0 and 5, giving a possible total score that goes from 0 to 13 points, being 13 the score for the worst scenario.

One drawback of this scale is that patient perception of the wound is not taken into account in to the final score of his/her respective scars (Nguyen *et al.*, 2015) (Table 2.1).

Vascularity	**Score**	**Pigmentation**	**Score**	**Pliability**	**Score**	**Height**	**Score**
Normal	0	Normal	0	Normal	0	Flat	0
Pink	1	Hypopigmentation	1	Supple	1	<2mm	1
Red	2	Hyperpigmentation	2	Yielding	2	2-5mm	2
Purple	3			Firm	3	>5mm	3
				Ropes	4		
				Contracture	5		

Table 2.1- The Vancouver scar scale. Adapted from (Fearmonti *et al.*, 2010).

The VSS proved not to be adequate for large and irregular scars which are characterised by a not homogenous pliability, colour and hypertrophy (Roques and Teot, 2007; Bayat *et al.* 2003). Therefore, this scale is strongly investigator-dependent, using pure word descriptions, and it does not locate the test site within the scar, which is indispensable for a follow-up (Draaijers *et al.*, 2004; Van de Kar *et al.*, 2005).

The numeric scoring of each variable is also questionable, since not all parameters are considered to be equally important for each patient or physician. Another problem, already documented by Sullivan *et al.* (Sullivan *et al.*, 1990), was the nonexistence of records of pain and itching and the functional and psychological sequelae of scars.

Due to these limitations, several adjustments to the VSS have been proposed in the literature along the years (Nguyen *et al.*, 2015).

2.1.1.2 - The Seattle Scar Scale (SSS)

In 1997 the Seattle scar scale (SSS) was proposed by Yeong *et al.* (Yeong *et al.*, 1997) as a numeric scale based on 24 standardised colour pictures. This scale assesses thickness, border height, scar surface and colour. The score of the parameters of the scale are the same (Surface irregularity (–1 to 4), thickness (–1 to 4), border height (–1 to 4) and colour (–1 to 4)), giving a total sum between –4 and 16 points, increasing the severity with the increase of the given score, with zero indicating normal (Yeong *et al.*, 1997).

The SSS allows negative values for certain parameters such as hypopigmentation or atrophy. The negative values help to differentiate diverse scar types but they also lead to “improved” total

scores and poor interpretation of scar severity (Van der Wal *et al.*, 2012). This limitation and the absence of attention to symptoms have hindered the wide adoption of the SSS (Nguyen *et al.*, 2015).

2.1.1.3 - The Hamilton Scar Scale

The Hamilton Scale was developed in 1998 by Crowe *et al.* (Crowe *et al.*, 1998), being a photographic assessment tool for scars (Crowe *et al.*, 1998). Based on photographs only, observers are requested to rate numerous parameters including thickness, surface irregularity, vascularity and colour. Relatively to attribution of scores, both surface irregularity, colour and vascularity are rated from 0 to 4 and thickness has 4 possible scores (0, 1, 2 or 3) giving a possible total score that goes from 0 to 15 points, being 15 the score for the worst scenario possible (Table 2.2).

The Hamilton Scale depends only on photographs rather than real scars to perform the assessment process, which can potentially distort the observer's interpretation, thus leading to errors in the assessment (Van der Wal *et al.*, 2012).

Table 2.2 - Hamilton scar scale. Based on (Smith *et al.*, 1988; Crowe *et al.*, 1998; Brusselaers *et al.*, 2010).

Surface irregularity	Score	Thickness	Score	Colour	Score	Vascularity	Score
Smooth	0	None	0	Normally pigmented/mature	0	Normal or paler	0
1/4 irregular	1	Slight	1	Light to medium pink	1	Slightly darker	1
1/2 irregular	2	Moderate	2	Deep pink to light red	2	Darker	2
3/4 irregular	3	Severe	3	Medium to deep red	3	Much darker	3
Majority of the scar irregular	4			Purplish	4	Hyper pigmented	4

One remarkable aspect is the fact that the controversial negative scores used in the SSS were not applied, but the parameter of scar irregularity was introduced, which is not scored in the most used assessment scar scale, the VSS (Crowe *et al.*, 1998; Van der Wal *et al.*, 2012). A big advantage of this scale is its good reliability, even when used by inexperienced observers, which proves that training is not a necessity for its use (Crowe *et al.*, 1998; Van der Wal *et al.*, 2012). However, likely other scales, the Hamilton Scale lacks an assessment of subjective symptoms (Nguyen *et al.*, 2015).

2.1.1.4 - Manchester Scar Scale (MSS)

The MSS was projected by Beausang *et al.* (Beausang *et al.*, 1998), in 1998 with the goal of assessing five scar parameters: scar colour, radiance (matte or shiny), distortion, texture and scar contour (Table 2.3). All of the parameters were taken into account in this scale, which have a possible score from 1 to 4, with the exception of the parameter Matte vs. shiny that is rated as 1 or 2. These parameters are combined with a visual analogue scale to determine an overall score proportional to scar severity (Nguyen *et al.*, 2015).

Colour	Score	Matte vs shiny	Score	Contour	Score	Distortion	Score	Texture	Score
Perfect	1	Matte	1	Flush with surrounding skin	1	None	1	Normal	1
Slightly mismatch	2	Shiny	2	Slightly proud	2	Mild	2	Just palpable	2
Obvious mismatch	3			Hypertrophic	3	Moderate	3	Firm	3
Gross mismatch	4			Keloid	4	Severe	4	Hard	4

Table 2.3- Manchester scar scale (Fearmonti *et al.*, 2010).

On contrary to the VSS, the MSS combines vascularity and pigmentation in the parameter "colour mismatch" of the adjacent tissue, which leads to better interrater agreement when compared with the other (Sullivan *et al.*, 1990).

However, the MSS has been criticised for being more suited to the assessment of linear scars and for a lack of accounting for symptoms (Van der Wal *et al.*, 2012).

2.1.1.5 - Patient and Observer Scar Assessment Scale (POSAS)

The VSS is mainly focused on scar severity from a healthcare professional's point of view, but there was acknowledgement that the inclusion of a patient-based assessment was also essential, this limitation served as base for the creation of the POSAS (Powers *et al.*, 1999; Martin *et al.*, 2003), whose introduction in 2004 was a turning point in the assessment of scars through the use of scales (Draaijers *et al.*, 2004).

The POSAS is the first scale that comprises two numeric scales: The Observer Scar Assessment Scale (observer scale) and the Patient Scar Assessment Scale (patient scale). The Observer Scale includes thickness, pigmentation, vascularity, pliability and relief while the Patient Scale includes stiffness, itching, irregularity, thickness, pain, and colour. Each item is rated between 1 and 10, being a score of 10 the worst imaginable scar or sensation and the lowest scores (5 in the observer scale and 6 in the patient scale) are for normal skin (Draaijers *et al.*, 2004). The patient scale is completed by the patient whereas the observer scale has to be marked by the observer (Table 2.4).

Table 2.4- Patient and observer scar assessment scale (Hyunjoo *et al.*, 2015).

Vascularity	o	o	o	o	o	o	o	o	o	o	
Pigmentation	o	o	o	o	o	o	o	o	o	o	Hypo _ Mixed _ Hyper _
Thickness	o	o	o	o	o	o	o	o	o	o	
Relief	o	o	o	o	o	o	o	o	o	o	
Pliability	o	o	o	o	o	o	o	o	o	o	
Total score Observer Scar Scale :											
Patient Scar Assessment Scale											
No, no complaints	1	2	3	4	5	6	7	8	9	10	*Yes, worst imaginable*
Is the scar painful?	o	o	o	o	o	o	o	o	o	o	
Is the scar itching?	o	o	o	o	o	o	o	o	o	o	
No, as normal skin	1	2	3	4	5	6	7	8	9	10	*Yes, very different*
Is the color of the scar different?	o	o	o	o	o	o	o	o	o	o	
Is the scar more stiff?	o	o	o	o	o	o	o	o	o	o	
Is the thickness of the scar different?	o	o	o	o	o	o	o	o	o	o	
Is the scar irregular?	o	o	o	o	o	o	o	o	o	o	

The POSAS takes into account the subjective symptoms of pain and pruritus and increases the objective information used in the VSS (Draaijers *et al.*, 2004), but as the other scales, it does not include functional measurements about the influence of pain or pruritus in patient's quality of life (Roques and Teot, 2007).

2.1.1.6 - Stony Brook Scar Evaluation Scale (SBSES)

Proposed by Singer *et al.* (Singer *et al.*, 2007) in 2007, it is based on five scar parameters including width, elevation or height, colour, suture or hatch marks and overall appearance (Singer *et al.*, 2007). Each parameter is rated by 0 or 1 (Table 2.5) for the presence or absence of the following: width greater than 2 mm at any point of the scar, raised or depressed scar, a darker coloration than the surrounding skin, any hatch or staple marks and an overall poor appearance. The total score ranges from 0 (worst) to 5 (best) (Singer *et al.*, 2007).

Table 2.5- The Stony Brook Scar Evaluation Scale (Fearmonti *et al.*, 2010).

Width	Score	Height	Score	Colour	Score	Hatch marks	Score	Overall appearance	Score
>2mm	0	Elevated/depressed in relation to surrounding skin	0	Darker than surrounding skin	0	Present	0	Poor	0
≤ 2mm	1	Flat	1	Same colour or lighter than surrounding skin	1	Absent	1	Good	1

The main goal of the SBSES was to measure short-term instead of long-term wound outcomes, so it was recently recommended for being used in research (Sullivan *et al.*, 1990; Fearmonti *et al.*, 2010). Therefore, its use is restricted for pathologic scar assessment.

Most of the above described scales do not incorporate subjective symptoms (pain or pruritus) in their assessment (Crowe *et al.*, 1998; Van der Wal *et al.*, 2012; Flanagan, 1993; Van Zuijlen *et al.*, 2002), do not considers nutrition as a risk factor (Flanagan, 1997) and do not records the location of the ulcer, foot deformities and/or patient-related factors (emotional upset, poor foot care, denial) (Oyibo *et al.*, 2001).

Numerous researchers point out that future scales should contain a patient-based component (missing in scales such as the SBSBES, the SSS and the Hamilton scale), since the presence of itching and pain is more disturbing than the appearance of the scar, and therefore these symptoms have a great impact on the quality of life and in the mental health (Van Loey and Van Son, 2003; Cheng *et al.*, 1996; Patterson *et al.*, 1993; Herndon *et al.*, 1986; Mazharinia *et al.*, 2007; Patterson *et al.* 2000; Sheffield *et al.*, 1988).

2.1.2 -Pressure ulcer (PU)

PU are characterised by the action of pressure, friction, or shearing leading to areas of skin and subcutaneous tissues breakdown (Benbow, 2006). The frequency (Whittington and Briones, 2004), cost (Zhan and Miller, 2003) and sufferance (Langemo, 2005) of patients confined to bed due to pressure ulcers turns this type of lesions in an important clinical problematic.

The time necessary for the wounds to heal, as well as its high prevalence among CW, increases the necessity of predicting the probability of a wound not healing early after starting a treatment. However, there is no consensus of which wound healing parameters permits accurately predict wound healing (Kantor and Margolis, 2000; Tallman *et al.*, 1997).

The optimal scale for wound risk assessment must have a high sensitivity and specificity in order to provide an acceptable prediction of the risk of wound development. Once its use is confined mainly to healthcare professionals, it should be simple to use, for that it is imperative that the parameters are clear and appropriate to apply in different healthcare settings (Torra, 1997).

Thereafter are presented the scales that are most commonly used for the assessment of PUs.

2.1.2.1 - Norton scale

The first PU risk assessment tool was created in 1962 by Doreen Norton (Norton *et al.*, 1962), with the aim of being used in elderly care environment. This scale qualifies five key risk factors separated: activity, physical condition, mobility, incontinent and mental condition (Table 2.6). Each parameter was scored from 1 to 4, thus, the range of possible total scores varies between 5 and 20, with a subjective cut-off score of 14, which equates to the individual being 'at risk'. In this tool, scores under 14 signify 'at risk' and scores under 12 signify 'high risk ', thus, the lowers scores represent the worst scenario (Norton *et al.*, 1962).

Table 2.6- Norton scale (Bell, 2005).

Physical condition	Score	Mental condition	Score	Activity	Score	Mobility	Score	Incontinent	Score
Very bad	1	Stupor	1	Stupor	1	Immobile	1	Doubly	1
Poor	2	Confused	2	Chair-bound	2	Very limited	2	Usually urine	2
Fair	3	Apathetic	3	Walk-help	3	Slightly limited	3	Occasional	3
Good	4	Alert	4	Ambulant	4	Full	4	Not	4

Despite in the original Norton scale nutritional factors and shearing forces were not contemplated and parameters are in need of a functional definition, this scale is widely used for clinical evaluation of pressure ulcer risk (Papanikolaou *et al.*, 2007; Bolton, 2007). Additionally, this tool has suffered several improvements in posterior versions as the incorporation of nutrition as a risk factor once it has been reported that it is important in the process of wound healing, as well as stratification of the degrees of risk (Wai-Han *et al.*, 1997; European Pressure Ulcer Advisory Panel, 2003).

2.1.2.2 - Braden scale

In the mid-1980s the Braden Scale was devised (Bergstrom *et al.*, 1987), shown in Table 2.7. The foundation for this tool was based on a "conceptual schema of aetiological factors" as well as the assumption that "pressure" and "tissue tolerance" are important aspects to be considered in the development of PUs (Bergstrom *et al.*, 1987). Six further parameters were identified as risk factors: sensory perception, moisture, activity, mobility, nutrition and friction and shear. In this tool, every parameter is rated between 1 and 4 with the exception of "Friction and shear" that has 3 possible scores (1, 2 and 3) (Bergstrom *et al.*, 1987). When using this tool, the range of possible total scores varies between 6 and 23 and low scores signify higher risk. The cut off points, which signify that an individual is 'at risk', varies between 16 and 18 (Bergstrom *et al.*, 1987).

Table 2.7- Braden scale (Bergstrom *et al.*, 1987).

Sensory perception	Score	Moisture	Score	Activity	Score	Mobility	Score	Nutrition	Score	Friction and shear	Score
Completely Limited	1	Constantly Moist	1	Bedfast	1	Completely Immobile	1	Very Poor	1	Problem	1
Very Limited	2	Very Moist	2	Chair fast	2	Very Limited	2	Probably Inadequate	2	Potential Problem	2
Slightly Limited	3	Occasionally Moist	3	Walks Occasionally	3	Slightly Limited	3	Adequate	3	No Apparent Problem	3
No Impairment	4	Rarely Moist	4	Walks Frequently	4	No Limitation	4	Excellent	4		

The main criticism to the Braden scale is the incapability of professionals to differentiate the parameters. For instance, 'mobility and activity', where 'mobility' is used by the authors to enquiry the capacity of the patient to relieve pressure through movement, whereas, 'activity' is applied to ascertain the frequency and duration of a patient's movement (Capobianco and McDonald, 1996). Even though, this scale has been found to have better predictive validity than single nursing judgment (Pancorbo *et al.*, 2006).

2.1.2.3 - Waterlow scale

Developed in 1987 by Judy Waterlow (Waterlow, 1988), this scale was created as an alternative to the Norton scale, once the author felt that the Norton scale did not address nutritional issues, underlying pathologies, or the risk of patients undergoing surgical procedures.

When compared to both the Norton and the Braden scales, the Waterlow scale recognises more risk factors in its assessment such as Body Mass Index (BMI), skin appearance in risk areas, sex and age, continence, mobility, appetite, neurological deficit and special risks (Waterlow, 1988; Waterlow, 1998) (Table 2. 8). Both BMI, skin appearance in risk areas, continence and appetite are rated from 0 to 3, sex and age and mobility has 6 possible scores (0 to 5), special risks are rated between 1 and 8 and lastly, neurological deficit has three possible scores (4-6, 5 and 8). The total score possible ranges between 4 and 40. In contrary to the Braden and Norton scales, in the Waterlow scale high scores signify high risk.

Table 2.8- Waterlow Scale (Agrawal and Chauhan, 2012).

Built/weight for height	**Score**	**Skin type- Visual risk areas**	**Score**	**Sex and age**	**Score**	**Special risks**	**Score**
Average–BMI 20-24.9	0	Healthy	0	Male	0	Multiple organ failure/terminal cachexia	8
Above average–BMI 25-29.9	1	Tissue paper/ Dry/Oedematous/Clammy /Pyrexia	1	Female	1	Single organ failure	5
Obese- BMI> 30	2	Discoloured (bruising/mottled)	2	14-49	1	Peripheral vascular disease	5
Below average-BMI< 20	3	Broken (established ulcer)	3	50-64	2	Anaemia= Hb<8	2
				65-74	3	Smoking	1
				75-80	4		
				81+	5		
Mobility	**Score**	**Continence**	**Score**	**Appetite**	**Score**	**Neurological deficit**	**Score**
Fully mobile	0	Complete/catheterised	0	Normal	0	Diabetes, MS, CVA	4-6
Restless/fidgety	1	Incontinent urine	1	Scarce/feeding tube	1	Motor/sensory/paraplegia	4-6
Apathetic	2	Incontinent faeces	2	Liquid IV	2	Major trauma	5
Restricted	3	Doubly continent (urine and faeces)	3	Anorexia/ absolute diet	3	Orthopaedic/spinal	5
Bedbound (e.g. traction)	4					On table >2 hours	5
Chair bound (e.g.	5					On table >6 hours	8

weel-chair)

The most obvious limitation of the Waterlow scale is the risk of over assessment, the fact that it has several parameters which, makes it complex to use and non-practical and is implied that women have higher risk of developing pressure ulcers than men (Edwards, 1995; Weststrate, *et al.*, 1998).

2.1.2.4 - Pressure ulcer scale for healing (PUSH)

The PUSH scale was designed in 1996 by National Pressure Ulcer Advisory Panel (NPUAP) as an instrument easy to use, clinically practical and biologically accurate, to follow PUs in different care situations. This scale was evaluated and accepted for measuring the healing process of venous and diabetic foot ulcers (Cuddigan, 1997; Thomas *et al.,* 1997; Stotts *et al.*, 2001).

In this scale, three factors are considered to evaluate the wound condition, namely its size (cm^2), the type of tissue existing in wound bed and the amount of exudate. Tissue type has four possible scores (0, 1, 2, 3 or 4), while the exudate amount parameter has possible scores that ranges between 0 and 3, finally, the length/width parameter has eleven possible scores between 0 and 10 as shown in Table 2.9 (Ferrell *et al.*, 2000). The scores of the three considered parameters are then added together to obtain a global score (Thomas *et al.,* 1997; Stotts *et al.*, 2001) and higher final scores mean a higher risk.

Table 2.9- Pressure ulcer scale for healing 3.0 (Cuddigan, 1997; Thomas *et al.,* 1997; Stotts *et al.*, 2001).

Length/ width (cm^2)	Score	Exudate amount	Score	Tissue type	Score
0	0	None	0	Closed	0
<0.3	1	Light	1	Epithelial tissue	1
0.3 – 0.6	2	Moderate	2	Granulation tissue	2
0.7 – 1.0	3	Heavy	3	Slough	3
1.1 – 2.0	4			Necrotic tissue	4
2.1 – 3.0	5				
3.1 – 4.0	6				
4.1 – 8.0	7				
8.1 – 12.0	8				
12.1 – 24.0	9				
>24.0	10				

The PUSH tool appears to be more easily incorporated into clinical practice routine than many other wound assessment instruments already introduced in this document, once it has fewer items, takes less time and effort to complete and does not requires intensive user training (McHorney and Tarlov, 1995).

Since the parameters measured by the PUSH tool are not only aetiology-specific, the instrument should theoretically be applicable not only to PUs but also to other wound types, where the three parameters are measureable. To date, studies (Ratliff and Rodeheaver, 2005; Hon *et al.*, 2010; Mackelbust, 1997; Gardner *et al.*, 2005) have validated the PUSH tool and shown that it is responsive for monitoring wound healing progress of pressure, diabetic and venous ulcers (Ratliff and Rodeheaver, 2005; Hon *et al.*, 2010).

2.1.2.5 - European Pressure Ulcer Advisory Panel scale (EPUAP)

Created in 1999, the EPUAP (European Pressure Ulcer Advisory Panel, 1999) scale resulted from a united effort of both European Pressure Ulcer Advisory Panel scale and National Pressure Ulcer Advisory Panel, being the PUs classified into four stages according to the ulcer's depth (Ferrell *et al.*, 2000; Berlowitz *et al.*, 1997; Mayfield *et al.*, 1998).

The EPUAP pressure ulcer classification distinguishes four grades and each grade is defined by the anatomic limit of soft-tissue damage: non-blanchable erythema corresponds to grade 1, blistering is included in grade 2, superficial lesions are classified as being grade 3 and deep lesions correspond to an ulcer with a grade 4 classification (European Pressure Ulcer Advisory Panel, 1999). The classification of 4th stage represents the higher risk and the 1st stage represent the lowest (Table 2.10). However, some authors (Defloor *et al.*, 2001; Schoonhoven, 2003) do not include non-blanchable erythema as a pressure stage.

Table 2.10- EPUAP scale. Based on (Thomas *et al.*, 1997; Stotts *et al.*, 2001).

Grade	Characteristics
1	The affected area of skin appears discoloured and is red in white people, and purple or blue in people with darker coloured skin. Oedema, induration. Warmth over a bony prominence.
2	Partial thickness skin loss involving epidermis, dermis or both. The ulcer is superficial and presents clinically as an abrasion or blister.
3	Full thickness loss of skin involving damage to or necrosis of, subcutaneous tissue that may extend down to, but not through, underlying fascia. Presents clinically as a deep crater with or without undermining
4	Full thickness skin loss with extensive destruction, tissue necrosis, or damage to muscle, bone, or supporting structures, for example, tendon or joint capsule. Undermining and sinus tracts may be associated with this stage of wound progression. Similar to grading a burn with the addition of a stage 4 that is deeper than a stage 3 ulcer or 3rd degree burn.

When an eschar is present, correct characterisation is not conceivable with this scale (Ferrell *et al.*, 2000; Berlowitz *et al.*, 1997; Mayfield *et al.*, 1998). On the other hand, the classification is based on a correct identification of the different tissue layers and the extent of tissue damage which demands training and experience from the user (Ferrell *et al.*, 2000; Berlowitz *et al.*, 1997; Mayfield *et al.*, 1998).

The most critical unresolved issues relatively to the formulation of assessment scales for pressure ulcers are:

- Pre-requisite of training

Most of the described scales are simple and easy-to-use however, was proved by the daily usage that these scales only provide usable measurements of the ulcer incidence and severity when used by trained healthcare professionals.

- Need for clarity

Scales such as the Norton and the Waterlow scales do not provide descriptions of their risk components, although this need has been recognised by Norton (Norton, 1996). The absence of explanatory observations leads to misjudgements when assigning scores to each parameter. Therefore, their usage requires informed clinical judgment, which turns it applicability restricted to the better-trained healthcare professionals.

- Predictive performance

The existing scales are over-sensitive to the number of patients assigned to the 'at-risk' group of pressure ulcer occurrence and under-sensitive to the number of patients assigned to the 'risk-free' group. Therefore, according to Bick and Stephens (Bick and Stephens, 2004) ulcer assessment should be performed in combination with clinical judgment (National Institute for Clinical Excellence, 2003; National Institute for Clinical Excellence, 2005).

- Definition of the critical threshold score

According to the existing literature (Clark and Farrar, 1992) there are no match in scores that define the "at risk "and "risk-free" status among the scales. The higher risk score varies from scale to scale. Furthermore, the disagreement about the proper cut-off score is pertinent, once healthcare professionals receive confusing signals about the best available evidence when applying risk assessment strategies and this may well produce variations in the appropriateness of the resultant healthcare preventive plans.

2.1.3 -Diabetic ulcer

Foot ulcers are one of the severe consequences of diabetes and main reasons of morbidity (Reiber *et al.*, 1998; Frykberg, 1991; Larsson *et al.*, 1993; Levin, 1993; Bose, 1979; Benotmane *et al.*, 2000; Van Houtum *et al.*, 1996; Boulton *et al.*, 2005; Ribu *et al.*, 2007). According to statistics, 25% of individuals with diabetes will have a foot ulcer during their life and 70% of those who healed ulcers are in risk of them to reappear in 5 years (Palumbo and Melton, 1985; Apelqvist *et al.*, 1993). There are several risk factors that result from the disease and lead to the development of diabetic foot ulcers, the main aspects are peripheral vascular disease, peripheral neuropathy, abnormal plantar pressure load and infection, which frequently leads to amputations (Edmonds *et al.*, 1982; Shaw and Boulton, 1997).

In order to reduce the impact of the disease, and thus, decrease the occurrence of major amputation, which was defined as a marker of the disease and its management, premature professional evaluation and treatment are obligatory (Jeffcoate and Van Houtum, 2004). Numerous assessment tools have been developed in order to classify ulcers with more accuracy, allowing the comparison of the results of routine management and treatments (Jeffcoate and Van Houtum, 2004; Oakley and Caterall, 1956; Shea, 1975; Jones *et al.*, 1987; Kaufman *et al.*, 1987).

Further, are presented the scales that are the most commonly used worldwide for the assessment of diabetic ulcers.

2.1.3.1 - Wagner scale

The most commonly acknowledged assessment method for diabetic wound is the Wagner scale (Wagner Jr., 1981; Wagner Jr., 1986), which was developed in the 1970s. This scale scores wounds from 0 to 5 mainly according to the depth and severity of the ulcer as shown in Table 2.11 (Wagner Jr., 1981; Wagner Jr., 1986).

The first four grades (grade 0, 1, 2, and 3) are based on the physical depth of the lesion in and through the soft tissues of the foot. The last two grades (grade 4 and 5) are completely distinct when compared with the previous because they are based on the extent of gangrene and loss of tissue in the foot (Mark and Warren, 2007).

Table 2.11- The Wagner scale (Wagner Jr., 1981; Wagner Jr., 1986).

Grade	Type of lesion
0	Pre- or post-ulcerative site
1	Superficial ulcer
2	Ulcer penetrating to tendon or joint capsule
3	Lesion involving deeper tissues
4	Forefoot gangrene
5	Whole foot gangrene involving more than two thirds of the foot

This scale is easy to memorise as a visual method, but does not comprises ulcer dimensions, peripheral neuropathy, peripheral arterial disease nor the level of infection (Wagner Jr., 1986). This is due to the fact that infection is only ascertained in the grade 3 (Wagner Jr., 1981; Wagner Jr., 1986). This scale fails to recognise and define vascular disease as one risk feature. Besides, infected superficial wounds or dysvascular wounds cannot be categorised by this scale (Wagner Jr., 1981; Wagner Jr., 1986).

The best use of the Wagner scale is with the assistance of systems such as a ruler, grid or measuring tape that allows an objective assessment (Wagner Jr., 1981; Wagner Jr., 1986).

2.1.3.2 - University of Texas Diabetic Wound Classification scale (UT)

The UT scale evaluates diabetic wounds via four stages and four grades, ulcer's depth, wound infection and ischemia in the lower-extremities (Oyibo *et al.*, 2001).

Relatively to the grades, grade 0 represents healing ulcers, grade 1 ulcers are superficial wounds through the epidermis or the epidermis and dermis, not penetrating on the tendon, capsule, or bone. Grade 2 wounds penetrate to tendon or capsule, without the bone and joints being involved. Grade 3 wounds penetrate to bone or into a joint.

Each wound grade consists of 4 stages: clean wounds (A), non-ischemic infected wounds (B), ischemic wounds (C), and infected ischemic wounds (D) (Table 2.12) (Oyibo *et al.*, 2001; Lavery *et al.*, 1996; Jain, 2012).

Table 2.12- The university of Texas diabetic wound classification system. Based on (Lavery *et al.*, 1996).

Stage	**Type of lesion**
A	No infection or ischemia
B	Infection present
C	Ischemia present
D	Infection and ischemia present

Grade	Type of lesion
0	Epithelialised wound
1	Superficial wound
2	Wound penetrates to tendon or capsule
3	Wound penetrates to bone or joint

Comparing the UT and the Wagner scale, the first is more descriptive and has shown a greater association with higher risk of amputation and likelihood of the healing process of ulcers, which is due to the combination of both grade and stage.

The assessment obtained with the UT scale can usually be predicted, at wounds of higher grade and stage, which are less likely to heal without revascularisation or amputation (Oyibo *et al.*, 2001; Lavery *et al.*, 1996). Being simple and easy to use, this scale shows good performance as predictor of clinical outcome, according to Oyibo *et al.* (Oyibo *et al.*, 2001) for groups rather than individual patients.

A comparison between all of the described scales during this section of the chapter is performed in Table 2.13.

Table 2.13- Comparison of all the scales mentioned in this report. Based on (Fearmonti *et al.*, 2010; Reichel, 1958; Mark and Warren, 2007; Jain, 2012; Beeckman *et al.*, 2007).

Type of wound	Scale	Inputs	Strengths	Limitations	Higher risk
Cutaneous	Vancouver Scar Scale (VSS)	Vascularity Height/thickness Pliability Pigmentation	Used widely in literature for outcome measure in burn studies.	Not applicable for large and irregular scars High score does not necessarily mean worse scenario Excludes pain and pruritus.	High scores
	Seattle Scar Scale	Surface irregularity Thickness Border height Colour	Proved to be a useful tool for evaluation of the 4 parameters considered	Allows negative scores Lack of attention to symptoms	High scores
	Hamilton Scale	Surface irregularity Thickness Colour Vascularity	Does not require training	Lack of an assessment of subjective symptoms	High scores
	Patient and Observer Scar Assessment Scale (POSAS)	The observer scale: Vascularity Pigmentation Thickness Relief Pliability The patient scale: Pain Itching Colour Stiffness Thickness Irregularity	Focuses on scar severity from clinician's and patient's points of view	Items represented may not adequately express patient's perceptions and concerns Cannot be used for young children	High scores
	Manchester Scar Scale (MSS)	Colour Matte vs shiny Contour Distortion Texture	Applicable to a wider range of scars	Arbitrary assessment and weighting of items	High scores
	Stony Brook Scar Evaluation Scale (SBSES)	Width Height Colour Hatch marks Overall appearance	Developed to assess short-term appearance of repaired lacerations	Does not include patient assessment Not designed for long-term scar assessment	Low scores
Pressure ulcer	Norton scale	Physical condition Mental condition Activity Mobility Incontinence	Widely used for clinical evaluation of pressure ulcer risk	Shearing force and nutrition are not incorporated in the scale. Overly simple	Low scores
	Braden scale	Activity Mobility Sensory perception	Good sensitivity and reasonable specificity levels	Difficulty in distinguish what the parameters mean	Low scores

		Nutrition Moisture Friction and shear			
	Waterlow scale	Build/weight for height Skin appearance in risk areas Sex and age Continence Mobility Appetite Neurological deficit Special risks.	Identifies significantly more risk factors than the Norton and Braden scale.	Has the assumption that women are at a higher risk of developing pressure ulcer than men. Risk of over assessment	High scores
	Pressure ulcer scale for healing (PUSH)	Length/ width Exudate amount Tissue type	Does not requires intensive user training Easy to use	Not widely used Has limited use in clinical practice and research	High scores
	European Pressure Ulcer Advisory Panel scale	Anatomic limit of soft-tissue damage.	Widely used to determine the severity of pressure ulcers.	Unambiguous descriptions of pressure ulcer grades Lack of distinction between moisture lesions.	High grade number
Diabetic ulcer	University of Texas Diabetic Wound Classification scale	Depth of ulcer penetration Presence of infection	Widely used to determine the severity of diabetic ulcers.	Do not include all the diabetic foot complications Cannot be used as a teaching tool.	High grade number and stage number
	Wagner scale	Physical depth of the lesion	Simple to use and easy to remember	Does not take the presence of neuropathy or the size of the lesion into account.	High grade number

2.2 - Quantitative wound assessment

2.2.1 -Visual characterisation of wounds

One of the characteristics that can be added in order to obtain a more accurate diagnosis of the state of a wound is its aspect. This additional information provides vital evidences that can be helpful when defining wound's severity and the prediction of healing (Oduncu *et al.*, 2004; Pereira *et al.*, 2013).

In 1983 was developed the Red-Yellow-Black (RYB) wound colour classification (Hellgren and Vincent, 1986) as a simple practical method of assessing wounds used by physicians in a descriptive manner (Oduncu *et al.*, 2004; Pereira *et al.*, 2013; Hellgren and Vincent, 1986; Ballerini *et al.*, 2010; Wannous *et al.*, 2010; Dorileo *et al.*, 2010; Zheng *et al.*, 2004; Cuzzel, 1988).

The colours are descriptive of tissue types in the wound bed (Hellgren and Vincent, 1986):

- Red wounds are usually granulating and healing.
- Yellow wounds have sloughy tissue adherent to the wound bed.
- Black wounds have necrotic tissue.

However, this method for colour classification of tissue has limitations (Cuzzel, 1988), such as: red wounds can be healing (granulated), over-granulated or infected and on the other hand, yellow wounds can contain slough or infected discharge.

In clinical practice the usage of the RYB wound bed assessment has shown good to moderate inter observer agreement (Lorentzen *et al.*, 1999; Vermeulen *et* al., 2007).

2.2.2 -Physical characterisation of wounds

Skin serves to protect against the entry of microorganisms and ultraviolet (UV) radiation, engage in thermoregulation, regulate water loss and as a component of the immune system (Harrist *et al.*, 1999).

Alterations in the integrity of skin may activate an inflammatory repair process (Martin and Parkhurst, 2004; Martin, 1997; Singer and Clark, 1999), which involves the complex combination of biological and molecular events during cell migration and proliferation and extracellular matrix deposition.

In order to the correct occurrence of the healing process, cellular responses to inflammatory mediators, growth factors and cytokines as well as to the proper mechanical forces must be precise (Martin, 1997; Singer and Clark, 1999; Vascotto *et al.*, 2005).

The process of wound healing comprehends four overlapping but well defined main phases, as described in Figure 2.1:

- Homeostasis

Formation of a fibrin clot at the site of endothelial injury and aggregation of platelets, which adhere to the injured endothelium and release chemokines, attracting the cellular components of the inflammatory phase (DiPietro *et al.*, 1998).

- Inflammation

The inflammatory cells (neutrophils, macrophages and lymphocytes) release pro-inflammatory cytokines, ingest foreign materials, increase vascular permeability and promote fibroblast activity (Polverini *et al.*, 1977; Hunt *et al.*, 1984).

- Proliferation

This phase is characterised by the occurrence of capillary growth and granulation tissue formation, cellular proliferation and abundant synthesis of collagen by fibroblasts leading to re-epithelialisation and construction of a preliminary dermis.

- Remodelling

In the last stage occurs the synthesis of type I collagen and differentiation of fibroblasts into myofibroblasts, allowing further wound contraction, thus decreasing the wound area.

This final phase of wound healing is a long process of tissue remodelling and increasing wound strength.

Different cell types, cytokines, and extracellular matrix molecules at the wound site interact with different systemic factors such as platelets, the coagulation cascade and humoral cell components, which combined enable the healing of wounds (Soo *et al.*, 2002).

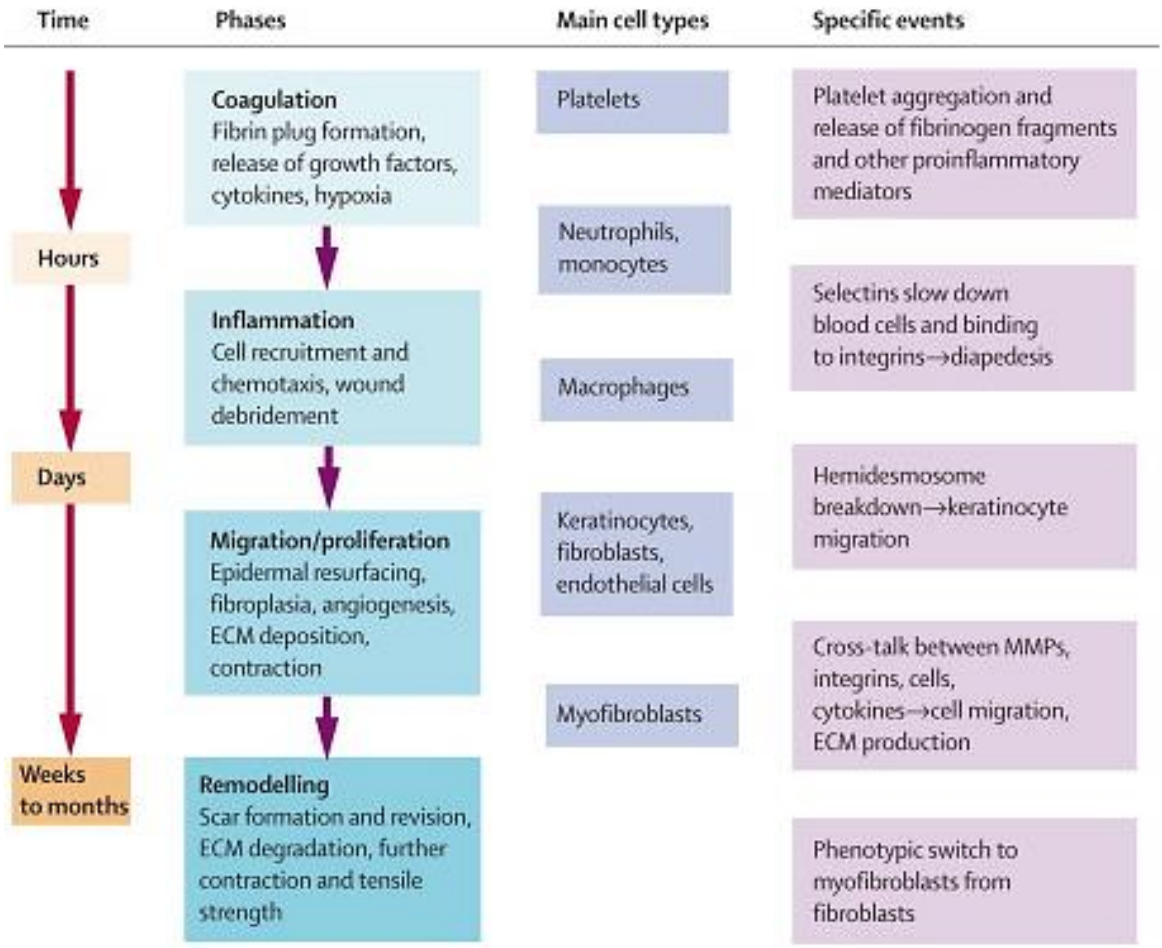

Figure 2.1- Phases of wound healing (Falanga, 2005).

During this process, wound depth and volume shrinkages due to the growth of the granulation tissue, on the other hand, wound area is reduced due to the production and migration of new epithelium (Flanagan, 2003).

Measures of ulcer size are therefore important indicators of healing, since it can give measurements of the wound that will serve as a reference point to precisely calculate the fraction of reduced/increased wound area over wound healing time (Flanagan, 2003; Margolis *et al.*, 2003).

Depth, length, circumference, width, area and volume are the dimensional aspects of an ulcer that can be assessed.

Several approaches for wound assessment through wound measurement have been created and all have their benefits and drawbacks. The most used methods described in the literature for measurement of area, volume and depth of the ulcers can be categorised as invasive or non-invasive.

2.2.2.1 - Invasive methods

The invasive methods require direct contact with the wound and can be separated by what is measured in its applicability: depth, area or volume.

However, these invasive methods have limitations and disadvantages as tissue injury, risk of local contamination, infection of other patients and/or the clinical team, failure to report information about the area, colour and presence of granulation tissue (Krouskop *et al.*, 2002).

- Depth
  - Depth Gauge

The introduction of a thin bar into the lesion until it reaches the deepest point, according to the clinician's evaluation, as shown in Figure 2.2, has become a usual clinical approach to measure the depth of a skin lesion. Then, the point that is equivalent to the probable skin surface height is signed on the bar and the distance from the start of the bar to the mark is measured by a ruler to provide the wound's depth (Callieri *et al.*, 2003).

Figure 2.2- Depth Gauge method (Shai and Maibach, 2005).

This technique is highly dependent on the ability of the clinician which makes it not easily reproducible (Callieri *et al.*, 2003).

- Area
  - The ruler method

This method allows the measurement of the maximal length by the maximal perpendicular width, through a not reusable paper ruler in order to afterward calculate wound area. However, this 2-D system works on the assumption that the wound has a geometric surface shape, as a rectangle (length x width), a circle (diameter x diameter) or an oval (maximum diameter x maximum diameter perpendicular to the first measurement) (Sterling, 1996; Plassmann, 1995) (Figure 2.3).

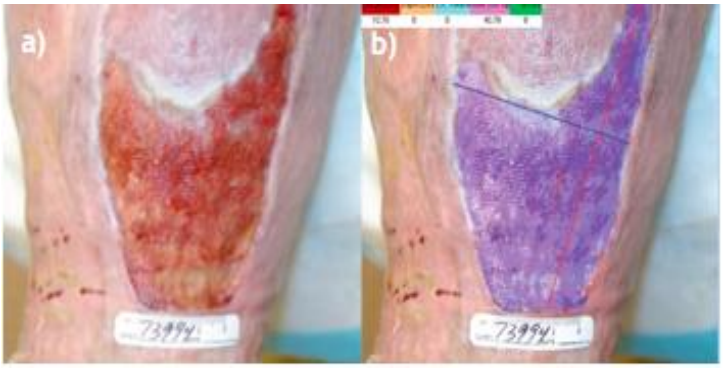

Figure 2.3- The ruler method a) Image of the wound b) Measurement of the length (red line) and width (blue line) of the wound through the ruler method (Wendelken *et al.*, 2011).

This method is simple to use, inexpensive and widely used in hospitals around the World, however, it has shown inconsistencies in measurements limited by subjective interpretation and inter observer variability (Gelfand, 2002; Sheehan, 2003), and since wounds of various shapes and area may fit into the same linear L × W dimensions, most of the wounds cannot be accurately measured if they are not rectangular or square shaped (Ahn and Salcido, 2008).

Furthermore, ruler-based techniques also carry the risk of wound contamination and inaccuracy and in certain situations can be painful to the patient (Thawer *et al.*, 2002).

- Acetate method

The practice of tracing the outline of a wound through a transparency appears to be the most popular and practicable method for area measurements. This technique has shown to be inexpensive, easy to learn and readily available.

The acetate method consists of applying a two-layer transparent acetate over the wound and then trace the wound edges with a permanent pen on the transparency sheet. The lower sheet that is in contact with the wound is thrown out into clinical waste and the top layer is stored within the patient files (Mani, 1999) (Figure 2.4). The area is approximated by counting the number of squares on the grid covered by the wound outline. The area can also be estimated with the use of a planimeter (Langemo *et al.*, 2001; Majeske, 1992; Mayrovitz and Soontupe, 2009).

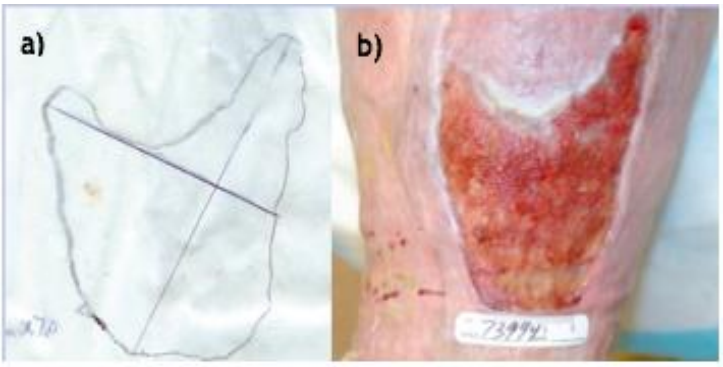

Figure 2.4- Acetate method a) Manual tracing of the wound b) Image of the wound (Wendelken *et al.*, 2011).

For the majority of cutaneous wounds, in spite of the errors introduced by flattening a curved surface, the wound area approximations and the healing obtained from contour delineation are reliable (Mani, 1999).

- Digital planimetry

Digital planimetry includes the same process to get the wound edge as the acetate method, i.e., a two-layer transparent acetate is applied on the wound and the perimeter is traced with a permanent pen on the top transparency sheet, then, the lower sheet which is in contact with the wound is discarded into clinical waste and the top layer will enable the characterisation of the wound, but instead of counting squares, the tracing is positioned on a digital tablet, and the edge is re-traced using a stylus (Sterling, 1996; Plassmann, 1995) (Figure 2.5). The underlying sensor then calculates the wound area.

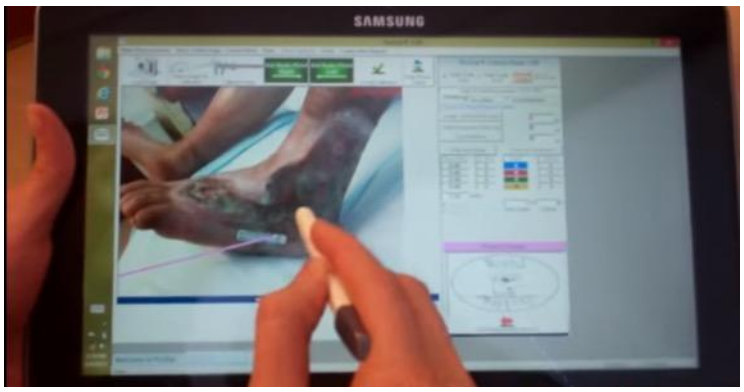

Figure 2.5- Digital planimetry of a wound (use of PictZar Digital Planimetry Software on a Windows 8 Tablet) (PictZar Digital Planimetry Software, 2007).

- Kundin gauge

This method consists of a commercially existing 3-D ruler used to estimate the area and volume of wounds (Kundin, 1985), see Figure 2.6. This method was developed as an easy basic tool that could be used with simple mathematical formulas to give accurate estimations of area and volume.

This tool is based on the use of three disposable paper rulers set at orthogonal angles to measure length, breadth or width, and depth of the wound, once it is an inexpensive plastic coated paper instrument designed to be thrown away after one time use, it can be placed on top of a wound to measure wound surface area or volume, thus minimising the risk of infection to the patient or nurse (Kundin, 1985; Kundin, 1989).

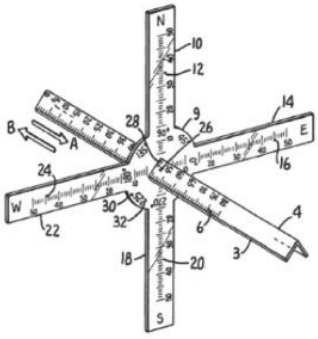

Figure 2.6- Kundin gauge (Kundin, 1985; Kundin, 1989).

To compensate for the irregular shapes of ulcers, values from the Kundin wound gauge are applied to mathematical formulas. For wound surface area, the formula involves an ellipse (with the area calculated as A=length x breadth x 0.785) and for wound volume, it involves an elliptical paraboloid (being the volume calculated as V= A x depth x 0.327) (Kundin, 1985; Baranoskl and Ayello, 2004). Although simple, ruler-based methods do not provide very consistent results being highly inaccurate for non-regular or big wounds and have also the risk of wound infection (Thawer *et al.*, 2002).

- Volume

To invasively measure the volume of the wound cavity are applied two main methods: the saline method and the alginate method (Keast *et al.*, 2003).

- Saline method

This method, shown in Figure 2.7, consists of covering the wound with a transparent film and then, using a syringe, fill the wound cavity with a saline solution. The volume of the wound is obtained by the assumption that the volume of saline dispensed from the syringe into the wound is equivalent to the volume of the ulcer (Langemo *et al.*, 2008).

Figure 2.7- Usage of the saline method to quantify the volume of an ulcer (MAVIS II, 2006).

However, this method has limitations once it carries the risk of wound contamination, the wound might absorb the saline and the shape of the film might not be equivalent to the original healthy skin, affecting the precision of the measurement.

- Alginate method

The alginate method is a derivation of the first method described and the procedure consists of filling the cavity with an alginate or silicon based paste, which rapidly sets plastic and creates a mould (Figure 2.8). Once set, the material is still flexible enough to be easily extracted (Shai *et al.*, 2005; Hayward *et al.*, 1993; Pories *et al.*, 1966). The volume of the alginate cast can be obtained directly using the fluid displacement technique or by weighting the cast and dividing the weight by the density of the casting materials (Krouskop *et al.*, 2002).

This type of solution is well tolerated by wounds and granulating tissues, do not cause embarrassment to the patients and is capable of reproducing the irregularities of wounds.

Figure 2.8- The alginate method to quantify the volume of an ulcer (MAVIS II, 2006).

However, is mandatory the maintenance of a position by the patient to allow wound filling by the alginate based solution which may not be conceivable and can induce pain/discomfort to the patient (Shaw and Bell, 2011).

2.2.2.2 - Non-invasive methods

Diagnosis and follow-up of chronic wounds is one of the fields that can benefit from integrating image-based systems into the diagnostic process. The existing approaches are frequently invasive, subjective and time consuming. Therefore, fast, accurate and non-invasive instruments to achieve chronic wounds assessment are needed.

One application of imaging devices is to save the 3-D geometrical shape of the object surface in digital form which can be stored in any computer system, being useful for physicians and dermatologists.

- <u>Optical based techniques</u>

Optical based techniques allow assessment of CW with objectivity and non-invasiveness, avoiding all the resulting problems from physical contact to the wounds. However, these techniques are incapable of measuring not visible wound or lesions that extend around the extremity.

- Stereophotogrammetry (SPG)

This is a passive non-contact method in which a stereographical camera linked to a computer captures two photographs of the same wound from slightly different angles (Figure 2.9) then, the images are downloaded to the computer where they are reconstructed to produce a 3-D model of the wound for the purpose of tracing the wound perimeter. The re-projection of the images through

the same apparatus produces a full-scale three-dimensional image when viewed through polarising lenses. The plotting mechanism allows the operator to digitally record x, y, and z coordinates for computer analysis (Bulstrode *et al.*, 1986; Plassmann *et al.*, 1995; Langemo *et al.*, 1998).

The tracing is performed by moving the cursor on the monitor and the computer software then calculates the wound area, length and width from the recorded coordinates via several cross sections of the ulcer and fitted triangles on the ulcer surface (Bulstrode *et al.*, 1986; Plassmann *et al.*, 1995; Langemo *et al.*, 1998).

With this technique, the wound size can be measured in both in 2-D and 3-D (Bulstrode *et al.*, 1986; Plassmann *et al.*, 1995; Langemo *et al.*, 1998).

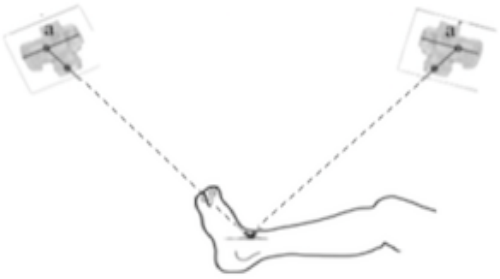

Figure 2.9- Diagram of the stereo camera in place over a leg where "a" are the cameras (Bulstrode *et al.*, 1986).

In the SPG technique from two different images a 3-D image is reconstructed via parallax/stereovision based on the fact that when an object is viewed along two different lines of sight, it apparent position is displaced similarly to what occurs with the visual perception of the human being. This is measured by the angle of inclination between these two lines. The parallax allows the measurement of the distance to the object. As shown in Figure 2.10, two objects, C (red) and D (blue), were placed in the Fields of View (FOVs) of both cameras A and B that ensure the epipolar rectification of the images (Lau, 2012).

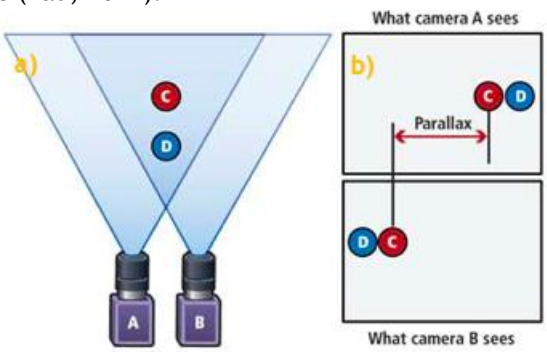

Figure 2.10- a) Camera A views the object in its right-hand FOV, while camera B views in its left. b) The blue object appears closer to the camera pair than the red object (Lau, 2012).

From camera A's perspective, the blue object is to the right of the red object, whereas from camera B's it is on the left. Due to the fact that the blue object has a larger parallax than the red one, it can be inferred that it is closer than the red object to the camera pair. Therefore, by making such parallax measurements on the objects in a scene, the distance from the cameras can be determined; next the 3D coordinates of the surface's points are calculated via triangulation and then a 3-D image of a scene can be reconstructed via pc (Lau, 2012; Peshko, 2005) through the cor-

respondence of points in the two images and computing the point depth based on the distance between corresponding points in the pair of images (Mohafez *et al.*, 2016).

The SPG method produces highly accurate and precise measurements. However, time consumption is still its main disadvantage, since photographs of the wound have to be taken first before a trained operator can make measurements from them after about 15 minutes (Plassmann *et al.*, 1995).

- Structured Light

The MAVIS (Measurement of Area and Volume Instrument system) (Plassmann and Jones, 1992; Plassman and Jones, 1998) shown in Figure 2.11 a), is an active method based on the structured light technique. In the structured light method, a projector illuminates the wound area with a set of 70 parallel stripes of light (Figure 2.11 b)) then, the wound is photographed at a known angle. From the known positions of the camera, the projector and the points of intersection of the stripes of light with the wound's surface, the computer produces a 3-D representation of the area and volume based on the captured images (Figure 2.11 c)) (Krouskop *et al.*, 2002; Plassman and Jones, 1998).

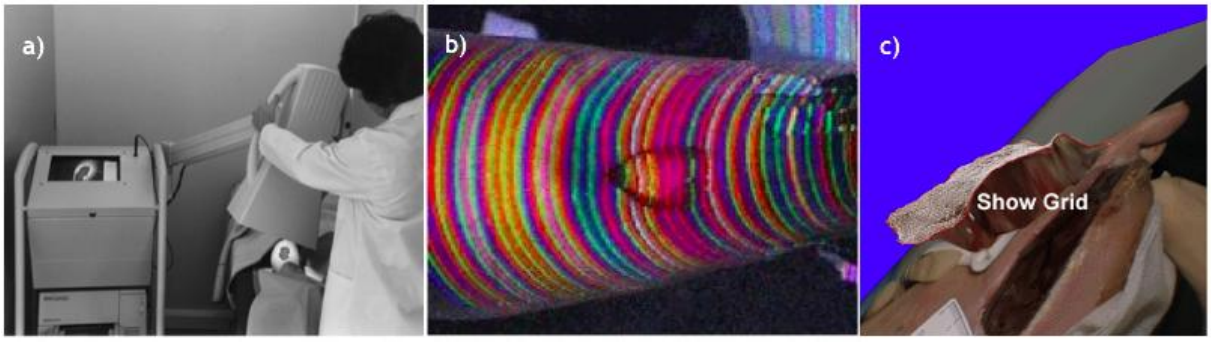

Figure 2.11- Structured Light a) The MAVIS b) The Structured Light method c) 3-D representation of the area and volume of the ulcer (Krouskop *et al.*, 2002; MAVIS II, 2006).

This 3-D representation of a wound can be obtained via active triangulation where every point illuminated is assumed to be the intersection point of two lines. The 1st line is formed by the ray originated in the light source and intersects the surface and the 2nd line is given by the reflected ray from the wound surface through the focal point of the imaging device to a point on the image plane.

Knowing the position and orientation of the light source and camera, the point on the surface can be computed through triangulation as shown in Figure 2.12, where (xc, yc, zc) are the coordinates of the centre of the camera, (xp, yp, zp) are the coordinates of the projector, (xpi, ypi) and (xci, yci) are the coordinates of the points of the projected and captured (deformed) images, respectively. (fc, fp) are the camera and projector focal lengths; α and ß are the angles of the basis with the project and the camera, respectively and (Xi, Yi, Zi) are the terrain coordinates of each point of the measured object (Buchón-Moragues *et al.*, 2016; Krouskop *et al.*, 2002; Peshko, 2005).

Then, the volume of a wound is sandwiched between two surfaces: the measured surface and the original, healthy skin surface which is created from undamaged parts of the skin surrounding the wound. Consequently, wound depth is the maximum distance between the measured and the reconstructed surface (Plassman and Jones, 1998).

Firstly, the outline of the wound is delineated by the operator tracing its edge in the image without stripes (this tracing is afterward used to calculate wound's area and circumference). Then Cubic splines are used to interpolate the original healthy skin, generating curves with minimum curvature which is thought to imitate the behaviour of normal skin being under tension from all sides (Plassman and Jones, 1998).

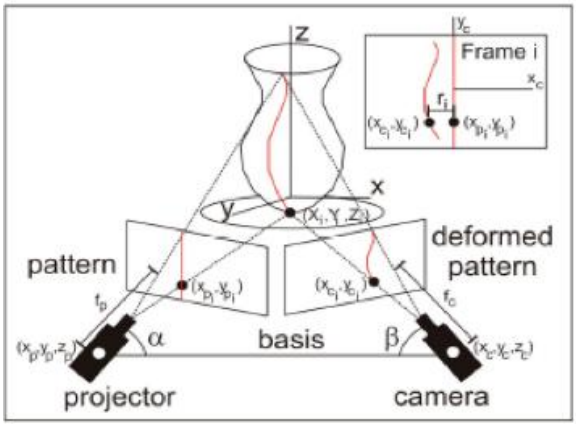

Figure 2.12- Acquisition of the 3-D surface of objects using the Structured Light method (Buchón-Moragues *et al.*, 2016).

The Structured Light method (Plassmann and Jones, 1992) does not need the production of intermediate slides since pictures of the wound are captured directly into a computer which does the subsequent image processing, so less user activity is required to operate the system which makes the method much easier to learn, less sensitive to operator introduced errors and faster than others systems (Plassmann and Jones, 1992).

The MAVIS (Plassmann and Jones, 1998) results are better than the traditional methods in repeatability of volume, area and depth measurements. Nevertheless, MAVIS has a big disadvantage, due to the optical principle of this instrument, it is incapable of measuring wounds that are undermined, being replaced by the MAVIS II (MAVIS II, 2006) and subsequent versions, which uses only a reflex digital camera equipped with special dual lens optics to record two half images from slightly different viewpoint.

- Combination of methods

In order to obtain the most accurate and objective assessment of chronic wounds, several methods have been proposed, however, when applied to all the different types of ulcers, the robustness of the existing instruments fail to achieve good characterisations.

For this reason, combinations of methods to increase the accuracy of the assessment have been tested. Barone *et al.* (Barone *et al.*, 2011) monitored the wound healing process based on a full combination of geometrical, thermal and chromatic data captured by a 3D optical scanner and an infrared (IR) detector. Colour and thermal images are segmented to support clinicians in extracting wound descriptors (i.e., colour and temperature), see Figure 2.13. The segmentation results are directly mapped onto 3D geometries of lesions creating a valuable multi-data tool, which allows real wound-bed evolutions to be monitored. This approach enables the acquisition of the main parame-

ters for monitoring chronic wounds: area, volume, colour and temperature, without necessitating physical contact with the patient (Barone *et al.*, 2011).

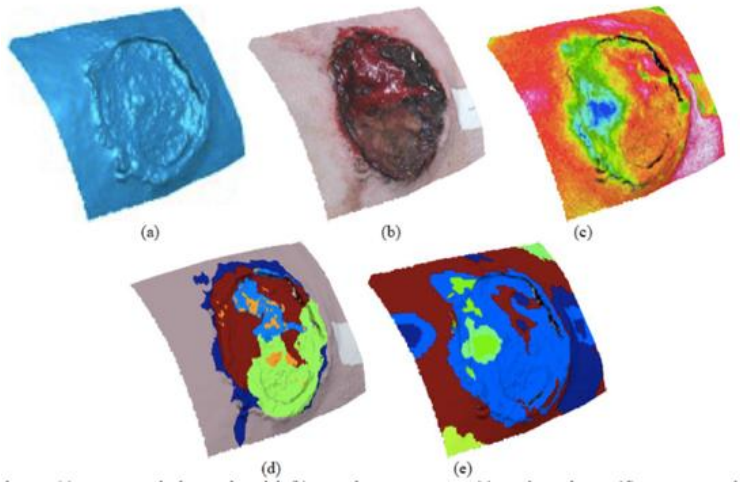

Figure 2.13- Results of the methodology created by (Barone *et al.*, 2011) where (a) 3D geometrical wound model, (b) 3D colour texture map, (c) 3D thermal map, (d) 3D segmented data using wound detection on the chromatic image, (e) 3D segmented data using wound detection on the thermal image.

The use of 3D temperature distribution represents a major advantage once it allows the objective monitoring of the healing process in complex chronic wounds, eliminating the dependence of good ambient lighting conditions to accurately assess wounds. However, the 3D thermo-scanner is a very expensive equipment, mainly due to the use of a thermal camera which translates in high initial investment (Barone *et al.*, 2011).

Leskovec *et al.* (Leskovec *et al.*, 2007) created a handheld laser-based 3D measuring device comprising a laser projector and a digital camera. While the wound is illuminated with light planes, the laser projector illuminates the wound and the camera photographs the wound from different angles (Figure 2.14). The images are then transferred to a computer and reconstructed into a 3D image (Sørensen *et al.*, 2015).

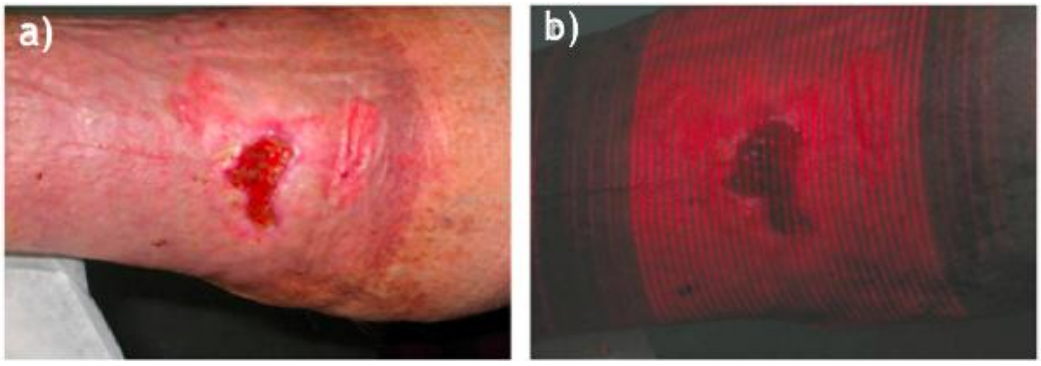

Figure 2.14- Methodology created by (Kecelj Leskovec *et al.*, 2007) a) Visual images captured by the camera and b) Wound being illuminated by light stripes.

Although the developed system was fast, easy to handle due to its small dimensions and did not required contact to obtain the measurements, tasks like the determination of wound edges and skin irregularities of the wound's neighbouring tissue were challenging (Sørensen *et al.*, 2015).

Still in the topic of combination of methods, Bowling *et al.* (Bowling *et al.*, 2011) created an optical system (Eukona®, Fuel 3D technologies, Oxford, UK) where a bespoke camera-like device, a computer software and single-use disposable optical targets were combined to obtain the 3D image of the reconstruction of diabetic foot wounds, see Figure 2.15 (Sørensen *et al.*, 2015).

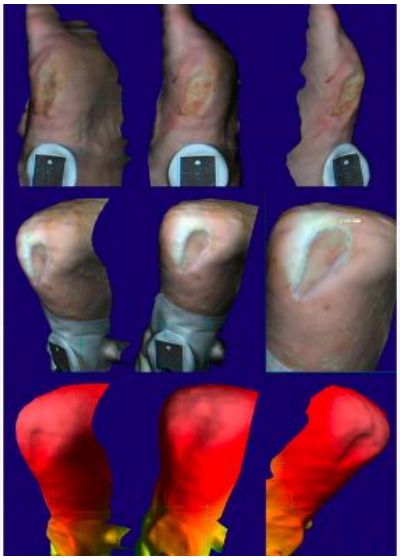

Figure 2.15- Methodology created by (Bowling *et al.*, 2011).

This system was defined as simple and easy to use, having a great potential to be implemented in a telemedical set-up. However, the small sample size used and the limited details given relative to the wound base were pointed as withdraws (Sørensen *et al.*, 2015).

None of the methods for wound measurement described in this document is close to perfection as shown by the information gathered in the Table 2.14. In summary, periodic quantitative assessment of chronic wounds over time is more accurate and able of providing a more trustworthy information if combined with a physician's experienced assessments.

Table 2.14 -Comparison of the advantages and disadvantages of the most used methods for quantitative wound characterisation (Plassmann *et al.*, 1995).

Measurement	Method	Advantages	Disadvantages
Depth	Depth gauge	Inexpensive Easy to use Fast	Highly invasive Operator dependent
Area	Ruler based	Highly correlated to more accurate methods. Fast Easy to learn and to use Inexpensive	High standard deviation of the measurements Measurements must be made under always the same conditions. Contact with the wound
	Transparency tracings	Fast Easy to learn Inexpensive Accurate Produces graphical record	Contact with the wound Time consuming
Volume	Ruler based	Fast Inexpensive Easy to learn	Inaccurate Invasive
	Casts	Inexpensive Moulds provide records Easy to learn	Invasive Source of errors
	Saline method	Inexpensive	Messy Inaccurate Wound absorbs saline Invasive
	Stereophotogrammetry	Very accurate Non-invasive Produces photographic records	Time consuming Expensive Trained operator required Limited field of view
	Structured Light	Accurate Non-invasive Produces photographic records Faster than SPG	Limited field of view Necessity of training Expensive Not practical to use in clinical environment

- Image processing and mobile applications

There are several issues with the actual practices for assessing objectively ulcers, as before mentioned. First, patients have to dislocate to their wound clinic on a regular basis to proceed to the assessment of their wounds by physicians. This regular clinical evaluation is inconvenient and time consuming for patients and physicians, it is associated to large health care costs (patients might necessitate exceptional transportation) and, as mentioned before, produces subjective meas-

urements and quantifiable parameters of the healing status (Wannous *et al.*, 2008) which makes the following of the wound healing process a problematic task.

The area of image analysis is a field of study that aims at the development of techniques that allow the extraction of maximum information from images, allowing to acquire a greater power of analysis, resulting in greater diagnostic support information (Gonzalez *et al.*, 2004).

The Figure 2.16 presents the different stages in image processing, it starts with the acquisition of the image, which contains the object of study, this acquisition can be performed by different devices that have a digital camera (Gonzalez *et al.*, 2004). After, is performed image quantisation which consists of mapping the image's continuous intensity range to a discrete number of intensity levels (Image Analysis and Computer Vision Laboratory, 2012). The image is then submitted to a pre-processing phase, which consists of several techniques (filtering, morphological operations, noise removal, etc.) used to increase the quality of images for future processing. After this, image segmentation is performed with the intention of partitioning an image into clusters according to a set of characteristics. The next phase is feature extraction/detection and classification which aims the extraction of the most important characteristics of the segmented components that are of interest to the study, being these characteristics used to train and test a classifier. In the final phase, registration, is performed the alignment or other operation between two or more images (Gonzalez *et al.*, 2004).

Computer software that automatically identifies the wound edge thus increasing accuracy and speed of measurement would be a major step forward (Sharifi *et al.*, 2002).

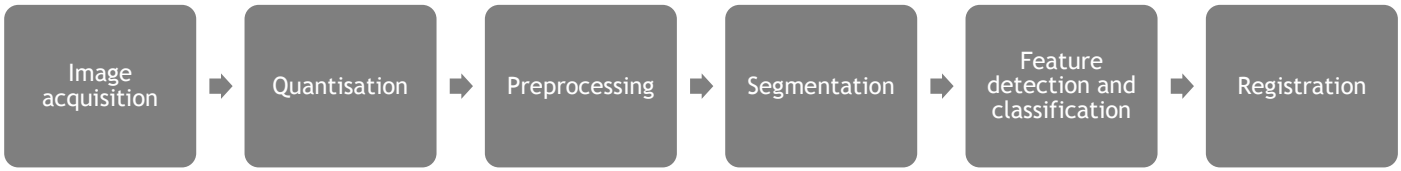

Figure 2.16- Block diagram of medical image processing and analysis.

There have been efforts to use image processing techniques for automatic and quantitative analysis of CW images, however, the distinction of the image background and the different types of tissue is a complex assignment. This is due to the fact that wounds have a non-uniform arrangement of red (granulation), yellow (slough) and black (necrotic) tissues conducing to colour ambiguity (Kolesnik and Fexa, 2005; Mukherjee *et al.*, 2014; Zheng *et al.*, 2004; Wannous *et al.*, 2007).

A developed methodology was based on the 3-D RGB colour histogram followed by a clustering technique to cluster the histogram bins and thus segment the different types of tissue in the wound. Lastly, the area of the segmented granulation tissue was used as a quantitative measure for wound healing assessment (Berriss and Sangwine, 1997). Even though the outcomes of this strategy were promising, the un-calibrated wound images used and the inadequate number of images disallowed the investigator from establishing colour reproducibility and generalise the proposed method. Furthermore, the low resolution of the RGB images, the criteria used for the selection of the seeds in the clustering algorithm and the order wherein the clusters were created limited the algorithm.

In another study, it was tested the segmentation and classification of the slough tissue in 30 PUs on the basis of the changes in the Hue, Saturation and Intensity (HSI) colour space after semi-automatic delineation of wounds by an adaptive spline method, then, the amount of slough was calculated via a quantitative measure during the wound healing assessment. When compared to the clinicians' decision to prove the accuracy of the colour characterisation obtained with this method-

ology, it was achieved 75% of agreement. Moreover, the uncontrolled lighting circumstance appeared as 10% shift in red patches of colour checker, jeopardising the consistency of the results once minor changes in hue were described (Hoppe *et al.*, 2001).

The same group of researchers using the same protocol, conducted another experiment, being the number of leg ulcers increased to 50. The results obtained, revealed that the colour shift of the red patches increased to 17%. Therefore, calibration of hue values previous to wound analysis was recommended (Oduncu *et al.*, 2004).

For classifying wound tissue, a study (Belem, 2004) was performed based on the support vector machine (SVM) using calibrated images. First, the wound was manually delineated and then was automatically segmented in CIE (Commission Internationale de l'Éclairage) L*u*v* (the L* component representing perceived lightness, while u* and v* represent chromatic components) (Mao, 2012) into smaller sections, with the purpose of distinguishing "healthy" from "non-healthy" tissues. After, parameters statistically extracted were imposed to a "brute force" method for selecting the most successful for following classification. Classification engines were employed such as: logistic regression, SVM and an artificial neural network that were compared against each other and the clinician's assessment by means of the Kappa agreement estimator. Results demonstrated that SVM was the best classifier, with more reliability in its decision than most of the healthcare professionals. Although, the outcomes of this study were promising, more evidence was vital to guarantee connection between actual wound inflammation status and classification as the infection is not necessarily the only cause of colour.

A multidimensional histogram sampling technique was applied in another study to automatically segment the wound region, which provided a set of feature vectors that served as an input for SVM classifier. The 3D colour histogram sampling produced more discriminatory set of features for SVM classifier than those of one dimensional histogram, enhancing the precision of the segmentation of the wound area by 20-30% (Kolesnik and Fexa, 2005). Though, this methodology unsuccessfully generated a contour as satisfactory as the one outlined by healthcare professionals.

In another research (Wannous *et al.*, 2007), before classification, an unsupervised segmentation method was applied to wound images increasing the robustness of tissue classification. Then, the colour and texture descriptors (standard deviation, average, skewness and kurtosis) were calculated in perceptually uniform colour spaces La*b* and LC*h* to create a SVM classifier with 88% consecutive overlying scores. To conclude, the unsupervised segmentation method was applied on test-samples, followed by the classification of the regions, being obtained a classification performance of 75% for granulation tissues and of 60% for slough tissues. Nevertheless, the characterisation error was superior to 50% for necrosis and the proposed methodology required initial manual selection of Region of Interest (ROI) (Veredas *et al.*, 2010).

With the purpose of classifying wound bed tissues in leg ulcers, Zheng *et al.* (Zheng *et al.*, 2004) proposed a new method with three 2-D histograms of RGB (Red, Green and Blue) pixel distribution values as an input for case-based recovery, K-Nearest Neighbours classifier. The outcomes verified that for binary classification, the accuracy went from 86.2 to 99.45%, whereas for multiclass segmentation was 87.2%, which is higher than the 77.6% obtained in the study performed by (Berriss and Sangwine, 1997).

Aiming the same as the study developed by (Zheng *et al.*, 2004), Galushka *et al.* (Galushka *et al.*, 2005) used as an input for case-based classifier, eighteen texture features from co-occurrence matrix of each RGB channel and eighteen RGB colour features. To evaluate the accuracy, two groups of experiments (one with three classes and other with six classes) were performed. From the achieved results, it was possible to state that the textural features were less efficient in multi-class

segmentation (58.3% of accuracy for 3-class and 54.4% of accuracy for 6-class), than the colour features (89.93% of accuracy for 3-class and 86.8% of accuracy for 6-class). This weakness is justified by the small size of the ROI which predictably reduced the classifier's accuracy.

Other approach for this problematic was the implementation of a hybrid design constituted by Bayesian classifiers and neural networks. A region-growing algorithm and a mean shift method were created to accomplish region segmentation. The texture and colour patterns served as inputs to train a set of k multilayer perceptrons, the outputs (tissue classes) were established by clinical experts. Finally, by training a Bayesian classifier for integrating the classifications of the k neural networks a Bayesian committee machine was designed. The results obtained for the binary cascade strategy were specificity = 94.7%, accuracy = 91.5%, and average sensitivity = 78.7% (Veredas *et al.*, 2010). It was concluded that with the exception of the granulation tissue, there were significant variances in sensitivity between the proposed methods to classify the remaining varieties of tissue.

For automatic tissue characterisation, a database with 74 different chronic wounds was imposed to Bayesian and SVM classifiers. Initially, it was performed the conversion of the wound images from RGB to the HSI colour space, next, the delimitation of the wound was realised through fuzzy-divergence-based thresholding. A set of colour and texture features were used as an input for the classifiers, in similarity with the previous described approaches. The obtained results demonstrated that the SVM exhibited higher accuracy for slough, granulation, and necrotic tissues of 90.47%, 86.94%, and 75.53%, respectively (Mukherjee *et al.*, 2014).

Medical applications for portable devices such as smartphones and tablets provide healthcare professionals, patients and the public a growing number of specialised tools and resources.

Several mobile applications appear every year relatively to CW with the purposes of promoting patient safety, improving patient outcomes, change the treatment used to a more satisfactory based on the evolution of the wound healing, enhancing financial and other efficiencies and facilitate the communication between multiple clinicians and healthcare centres, but most of them miss scientific documenting (Galushka *et al.*, 2005).

Next are described five highly related to CW characterisation mobile applications created over the years with the purpose of supporting patients and caregivers.

Mobile Wound Analyzer (MOWA) was created in 2011 (Healthpath, 2011) as non-invasive system to characterise wound tissue composition in PU (necrotic tissue, fibrinous tissue and granulation tissue), calculate the area of the wound and suggest treatments.

Firstly, the user (patient or caregiver) takes a photograph via the smartphone's camera, then designs a mask of the lesion and the segmentation of the ulcer is performed by the mobile application. Then, in order to obtain wound's area, the user must specify wound characteristics (exudate, infection, Haemorrhage, depth) and suggestions of treatments are displayed in the screen. The mobile application offers the option of saving the characterisation report, where it must be save or sent and with which format.

Although the provided characterisation by MOWA is very complete and accurate and it is available for Android and iOS devices, most of the parameters have to be added manually by the user (design of the mask, settings, and JPG and PDF reporting and posterior file sending through mail), the analysis takes up to 3 minutes, has to be purchased ($5.99 for android and $6.99 for iOS), does not allow physical comparison of the healing process of the wound throughout time, only evaluates pressure ulcers from Stage II forward (according to the EPUAP-NPUAP classification) and the identification of tissues in the wound bed is influenced by the quality of the photo.

In 2012 SmartWoundCare (Vivanco *et al.*, 2012; Friesen *et al.*, 2013) was created to satisfy three aims:

1. Promote and perform remote consultation (between facilities, practitioners, and/or remote communities);

2. Allow data organisation and analysis (automatically-generated text-based and graph-based wound histories and built-in alerts);

3. Provide user support for non-specialised caregivers with tutorials, simulation of patients and descriptions of specialised terminologies.

However, this mobile application, despite being free and available for android and iOS, it does not perform wound characterisation via image processing, only providing a system to store all patient's information, images of the lesions, treatments and assessments based on the PUSH and on the Braden scales.

In 2015, Varma *et al.* (Varma *et al.*,2016) created an Android application using Visual Studio with OpenCV with the aim of performing wound measurement in pixels and cm^2, identify pus regions and measure its percentage. This mobile application was created to be used by the patients due to its simplicity and facility of use thus, avoiding dislocations to healthcare centers.

This system performs wound segmentation by two processes: Otsu and Grab-Cut and the tissue classification is achieved by K-Means clustering using 3 regions (K = 3).

However, from the obtained results, it can conclude that the Otsu's method does not segment correctly low contrasting images, contrary to the grab-cut. Similar to the other documented mobile applications, this cannot provide information about wound volume or its three-dimensionality.

Lei Wang *et al.* (Wang *et al.*, 2015) created an application for smartphones which integrates wirelessly with the patient's personal glucose meter, tracks blood sugar levels, weight, exercise and other physical activities based on user input, generating specific messages to the user based on clinical information. This mobile application is oriented to patients with type 2 diabetes, therefore, and due to their mobility limitations, the image collection is performed via an image capture box by an optical system with a dual set of front surface mirrors, Light-Emitting Diode (LED) lighting and an inclined surface for the patients to put their foot.

The ulcer segmentation is performed by a mean-shift algorithm resulting in a segmentation of the input image into homogeneous regions with analogous colour features. After, an object recognition method based on three assumptions: the image includes irrelevant contextual data; the healthy skin on the sole of the foot has a uniform colour; outlines of the foot's edges do not contain foot ulcers, was implemented to understand the output of the segmentation and obtain the wound boundaries. Tissue colour classification is performed according to the RYB wound classification model via a K-means clustering methodology.

Although the image capture box guarantees consistent image collection conditions, i.e., illumination and object-camera distance, due to the direct contact with the wounded extremities, microbial contamination may occur in the box leading to wound contamination. Furthermore, misclassification of pixels during tissue classification was noticed and, since the data used is bi-dimensional, no measures of volume and depth are performed by this mobile application.

+WoundDesk was designed in 2015 by physicians with the aim of achieving a time saving and errorless characterisation of wound healing in both diabetic and pressure ulcers as well as burns/scars, being available for free in the basic version for Android devices. The assessment of the wounds is performed semi-automatically by the selection of a ROI by the user, providing measurements of wound area, severity/score and location. The output of the assessment includes registra-

tion of treatments and dressings, wound measurements and important clinical information about the patient.

However, the majority of the data present in the final report has to be manually included by the user thus, the mobile application does not establish connections between the wound measurements and its management by itself.

As presented in Table 2.15, the “perfect” mobile application for chronic wound assessment is far from being developed. None of the mobile applications found during the research for this project manage to completely characterise foot ulcers through visual image, i.e., none of the mobile applications automatically provides wound area, volume and texture as well as its 3-D representation combined with simplicity of use, mainly due to the lack of an ideal image processing methodology to automatically obtain wound area, volume and tissue classification.

Table 2.15- Mobile applications for characterisation of chronic ulcers (Healthpath, 2011; Vivanco *et al.*, 2012; Friesen *et al.*, 2013; Varma *et al.*,2016; Wang *et al.*, 2015; +Wounddesk, 2011).

Name of the mobile application	**MOWA**	**SmartWoundCare**	**Anudeep Varma *et al*. project**	**Sugar**	**+WoundDesk**
			Year		
	2011	2012	2015	2015	2015
			Aim		
	Support healthcare professionals in the analysis and treatment of pressure ulcers and provide an instrument for archiving photographs of pressure ulcers.	Improve the patient/caregiver communication, wound management and outcomes and facilitate patient engagement in their own care.	Enable the patients to analyse their wounds from their accommodations, reducing the overload on health care centres.	Reduce both the frequency and the number of wound clinic visits by analysing wound images of patients with type 2 diabetes suffering from foot ulceration.	Mobile time saving system for professional wound management that aims the reduction of errors and improves wound healing.
			Mobile operative system		
Android	● ($5.99)	● (free)	●	●	● (free)
IOS	● ($6.99)	● (free)			
			Type of chronic wound		
Burn		●	●	●	●
Pressure ulcer	●	●			●
Diabetic ulcer		●	●	●	●
			Features		
Image collection	●	●	●	●	●
Image analysis	●		●	●	●
Designed for patients	●	●	●	●	●
Designed for clinicians	●	●		●	●
Wound area calculation	●		●	●	●
Special features	Analyses tissues. Calculates wound area. Generates ideas for treatments. Creates an analysis report in PDF.	Re-assess wounds on patients using the PUSH and Braden Scale tool. Automatically creates wound histories in text, graph and image formats.	Measures wound area and pus area. The measured data is displayed both in pixels and in cm^2. Calculates the pixel area in cm^2 irrespective of	Captures images via an image capture box using an optical system with a dual set of front surface mirrors, integrated LED lighting and a slanted surface for placement of the	Uses a semi-automated and sterile wound measurement to calculate wound surface. Documents assessments. Generates severity scores.

			the height from which the image is captured.	patients' foot. Tracks the area and healing status of wounds and other relevant health parameters.	Registers treatments, wound recommendations and guidelines.
Limitations	Manual submission of several parameters by the user (design of the mask, settings and Jpg and pdf file sending via mail). Identification of tissues in the wound bed (necrotic, fibrin, granulation) is influenced by the quality of the photo.	Do not perform image analysis.	Do not measure the volume of the wound nor gives other information than wound area, pus area and pus percentage.	Lacks of information about wound texture.	Do not measure the volume of the wound Majority of the data needs to be include manually by the user. Only calculates wound surface semi-automatically.

2.3 - Wound care

The healing process of chronic wounds depends on intrinsic factors such as smoking, ischemia, foreign bodies, venous insufficiency, infection and cancer and on extrinsic factors like nutritional deficiencies, chronic renal failure, chemotherapeutic agents, distant malignancies, age, liver disease, steroids, drugs and heredity (Anderson and Hamm, 2012, Haug, 1999).

Extrinsic factors may be controlled by strict management of eating habits, social habits, medical therapy and local wound care (Haug, 1999).

2.3.1 -Dressings

In order to promote the right tissue granulation, wound closing and the decrease of wound colonisation by bacteria, some steps are obligatory after wound assessment: initially is mandatory to clean up the wound and perform its debridement and then, administrate treatments that promote cell migration and prevent desiccation (Buck and Galiano, 2013).

These treatments are defined based on the extent and nature of the exudate existing in the ulcer, determining the type of dressing to be applied (Buck and Galiano, 2013).

- Gauze

Gauze dressings usually consist of woven and non-woven fibres of cotton, rayon and polyesters (Boateng *et al.*, 2008) and are currently the "gold standard" treatment for non-specific wound care to which the Food and Drug Administration (FDA) compares most dressings, due to its low cost, prompt availability and the fact that it can be purchased impregnated with several substances (Buck and Galiano, 2013).

However, its usage can have a pro-inflammatory role leaving microfibers within the wound becoming a cause of possible infection and its removal can be painful leading to collateral damage of the adjacent healthy tissue (Buck and Galiano, 2013).

- Hydrogel Dressings

The aim of hydrogel dressings is to maintain the moist and rehydration of wounds via complex polysaccharides (e.g., starch) in order to enable healing via autolytic debridement. However, the application of this dressings, as others, can lead to the absorption of reasonable volumes of fluid from the lesion.

These dressings can take several physical forms: sheets, gels and impregnated into gauze, and since it does not adhere to the wound tissue, their removal does not cause major pain, still, its non-adherence leads to the obligation of including an extra dressing like gauzes (Buck and Galiano, 2013).

- Hydrocolloids

Hydrocolloids are gel-forming agents (gelatine, pectin or carboxymethyl cellulose), which constitutes a resistant barrier to gases and liquids and can take the form of powders, pastes or sheets (Buck and Galiano, 2013). Examples of this dressing are impermeable to bacteria, moisture and oxygen (Daley, 2017), providing a moist environment that stimulates cell migration and autolysis wound debridement. Due to their occlusive nature, they cannot be applied in severely bacteria's colonised wounds (Buck and Galiano, 2013).

- Foam Dressings

Foam dressings consist of a combination of non-adhering polyurethane and an occlusive cover. Although the outer layer forms a barrier against liquids via its hydrophobic properties, it allows exchanges of gases and water vapour (Ramos-e-Silva and Ribeiro de Castro, 2002). Since the polyurethane has a great absorption capacity, these dressings constitute a wick for wound fluids, being extremely advantageous for extremely exudative ulcers (Buck and Galiano, 2013), not requiring secondary dressings (Ramos-e-Silva and Ribeiro de Castro, 2002).

Nowadays, both adhesive and non-adhesive foams dressings exist (Ramos-e-Silva and Ribeiro de Castro, 2002).

- Alginates

Alginate dressings can take numerous forms and can absorb fluids up to nearly 20 times their dry weight being, therefore, extremely advantageous in the treatment of very exudative wound since they allow the elimination of fluids from the wound bed without requiring daily changes of the dressings (Buck and Galiano, 2013).

- Antimicrobials

Antimicrobial dressings consist of a broad group of dressings that comprise an antimicrobial agent. An example of these agents is silver to which are associated most of the advantages since it

is ionised in the moist environment of the wound, has biologic activity, has a wide range of bactericidal activity involving very resistant organisms and represents low toxicity to the cells of the human body (Buck and Galiano, 2013).

Another antimicrobial agent is cadexomer iodine, which consists of a slow-release arrangement of iodine that allows the achievement of constant bactericidal concentrations within the wound bed, without damaging the cells of the wound.

Other antimicrobials include preparations of sodium hypochlorite solution (Dakin's solution), mafenide acetate and silver sulfadiazine (Buck and Galiano, 2013).

- Semipermeable film

These dressings are acrylic adhesive films with little hydrating ability and no absorptive capacity, being mostly indicated for dry, clean ulcers with insignificant exudate or to hold in place an underlying absorptive dressing, to secure intravenous catheters and to shield high-friction parts and areas whose bandaging is a challenge (e.g., heels) (Daley, 2017).

- Hydrofiber

A hydrofiber is an absorptive textile fibber pad which, when combined with the exudate of the wound, produces a hydrophilic gel. Therefore, hydrofiber absorbent dressings have more advantages when applied in exudative wounds being covered with a secondary dressing (Daley, 2017).

In the table 2.16, a summary of the types of dressings more suitable for each wound type, examples of these dressings and their advantages and limitations are presented.

Table 2.16- Comparison of the different types of dressings and their application (Daley, 2017; Kannon and Garrett, 1995; Piacquadio and Nelson, 1992; Edgepark Surgical, 2005).

Type of dressing	Type of wound	Examples	Advantages	Limitations
Gauze	All wounds	Mesalt Curity gauze sponge Curity packing strip Xeroform Iodoform impregnated packing strips Vaseline gauze	Inexpensive accessible	Its removal can be painful Can lead to infection Demands change every 12-24 hours
Hydrogel	Wounds without eschar Wounds susceptible to desiccation Infected wounds	Aquasorb DuoDerm Intrasite Gel Granugel Normlgel Nu-Gel Purilon Gel KY Jelly	Retains moisture No traumatic removal Pain relief	Can lead to over hydration
Hydrocolloids	Wounds with moderate quantities of exudate	CombiDERM Comfeel DuoDerm Granuflex Tegasorb	Do not require change of dressing for 3 to 5 days Protects wound from contamination	Cannot be used in highly exudative wounds
Foam	Highly exudative wounds	Allevyn Lyofoam C 3M Adhesive Foam Allevyn hydrocellular	High capacity of absorbency Thermal insulation Occlusive	Cannot be used on non exudating or slightly exudating wounds Malodorous discharge
Alginates	Exudative wounds	AlgiSite Comfeel Curasorb Kaltostat Sorbsan Tegagel	Does not require daily dressing change or multiple dressing changes per day High capacity of absorbency	Lateral wicking
Antimicrobials	Infected/ contaminated wounds	Acticoat Aquacel Ag Iodosorb gel Silvasorb Inadine	High bactericidal activity Low toxicity to the human cells	May require secondary dressing Possible alteration of normal cutaneous flora
Semipermeable film	Clean, minimally exudative wounds Secondary dressing	OpSite Skintact Release Tegaderm Bioclusive	Protects wound from contamination Retains moisture Allow visual inspection	No absorption capacity Fluid trapping
Hydrofiber	Exudative wounds	Aquacel Aquacel-Ag Versiva	High capacity of absorbency	Fibrous debris

2.3.2 -Adjuncts to wound care

- Compression

Compression therapy is the most popular therapy to treat venous ulcers (Rojas and Phillips, 2001; Fletcher *et al.*, 1997; Cullum *et al.*, 2000), since by assisting the calf muscle pump and reducing distention in superficial veins leads to the relief of oedema and stasis (Rojas and Phillips, 2001) and stimulates the granulation of the healthy tissue (Cullum *et al.*, 2000). Compression can be administered through single-layer bandages, multilayer bandages, compression stockings or combinations of stockings and bandages, being classified by the level of compression applied to the extremity (compression stockings can give 35 mm Hg of pressure at the ankle, while compression bandages can give 60 mm Hg at the ankle) (Cullum *et al.*, 2000).

However, before applying the compression therapy, the patient should be consulted by vascular surgery to ascertain the presence of concomitant arterial insufficiency which, combined with compression can lead to gangrene, ulcer worsening and/or limb amputation (Callam *et al.,* 1987_a; Callam *et al.,* 1987_b).

- Topical negative pressure devices

Topical negative pressure (TNP) or vacuum-assisted closure (VAC) devices, comprise a fenestrated evacuation tube attached to a vacuum source and embedded in a foam dressing and covered with an airtight dressing. Through this device, is continuously or intermittently provided subatmospheric pressure (100-125 mm Hg) (Hess *et al.,* 2003) which allows the maintenance of a moist environment, exudate removal, reduction of bacteria, increase of local blood flow and formation of granulation tissue, accelerating the healing process of the wound (Hess *et al.,* 2003; Morykwas *et al.,* 1997; Saxena *et al.,* 2004; Shirakawa and Isseroff, 2005; Venturi *et al.,* 2005).

The TNP dressings are suited for venous, diabetic and pressure ulcers, however, they should not be applied to ischemic wounds since it can trigger necrosis of the wound boundaries (Venturi *et al.,* 2005; Clare *et al.,* 2002).

- Growth factors

Several essential cellular activities (cell division and migration, angiogenesis and synthesis of extracellular matrix constituents) comprised in the normal tissue repair process are controlled by growth factors, therefore, some suggest that a lack of them may happen in chronic wounds (Robson and Smith, 2001). Recombinant human platelet–derived growth factor isoform BB (rhPDGF-BB homodimer, becaplermin; Regranex; Johnson and Johnson) is the only topical growth factor approved by FDA for the treatment of chronic neuropathic lower limb diabetic ulcers. Becaplermin is used to treat pressure ulcers (Robson *et al.*, 1992; Mustoe *et al.*, 1994; Rees *et al.*, 1999) and has similar biologic activity to the PDGF-BB stimulating the chemotactic recruitment and proliferation of cells, leading to complete heal in less time (Steed, 1995; Ladin, 2000).

- Skin substitutes

Surgical skin grafting is recommended for recalcitrant ulcers. Grafting of split-thickness autologous skin is a well-known method of treating severe chronic venous leg ulcers, where allogenic and

synthetic skin substitutes are used to close longstanding wounds. These products allow the elimination of the requirement for a graft donor site, showing benefits when applied in venous and diabetic neuropathic ulcers (Gentzkow *et al.*, 1996; Falanga and Sabolinski, 1999; Veves *et al.*, 2001; Jones *et al.*, 2002; Marston *et al.*, 2003; Omar *et al.*, 2004).

- Hyperbaric oxygen therapy

Tissue hypoxia leads to the non-healing of several CW (Kranke *et al.*, 2004). For this reason, is applied the hyperbaric oxygen therapy, which consists of breathing 100% oxygen at supra-atmospheric pressures inside a compression chamber (Kranke *et al.*, 2004).

Hyperbaric oxygen therapy seems to decrease the rate of major amputation associated with diabetic foot ulcers and can increase the possibility of diabetic foot ulcer healing at one year (Berendt, 2006), however, it can introduce temporary myopia, oxygen toxicity to brain and lung, barotrauma to the ears, lungs and sinuses (Kranke *et al.*, 2004).

There is insufficient evidence to suggest benefits for venous, arterial, or pressure ulcers. In contrast, topical oxygen therapy (where the wounded extremity is introduced into an airtight bag and surrounding it with oxygen under slightly increased pressure), is thought to be clinically unsuccessful (Cronje, 2005).

2.4 - Summary

From this section, it can be understood the importance of wound assessment, since it provides information about its characterisation and the healing process allowing the adjustment of the treatments applied to the patients.

Qualitative assessment based on scales is widely used for its simplicity to create comparable semi-quantitative data (Wannous *et al.*, 2010) and promote better management of resources, however, it depends on visual inspection, being time consuming and susceptible to human errors, having its usefulness limited. In fact, most of the mentioned scales present several limitations, such as: not incorporating subjective symptoms such as pain or pruritus (Crowe *et al.*, 1998; Van der Wal *et al.*, 2012; Flanagan, 1993; Van Zuijlen *et al.*, 2002), not considering nutrition as a risk factor (Flanagan, 1997), not providing descriptions of their risk components (Norton, 1996) and the absence of recording the location of the ulcer and foot deformities. The patient self-assessments of CW can be affected by several aspects such as emotional influences, ulcer location (Martin *et al.*, 2003; Powers *et al.*, 1999), age (Singer *et al.*, 2000; Kearney *et al.*, 2001) and gender (Newton-Bishop *et al.*, 2004), thus, the assessment based on patient-related factors should also be included (Oyibo *et al.*, 2001). Furthermore, the resulting notes of the examination process are not always documented consistently and their storage constitute extra clinical work (Malian *et al.*, 2005; Veredas *et al.*, 2010). Additionally, there is not a *gold internationally adopted standard* scale for each type of wound and because the assessment is based on the observer and its experience, even in the same department of the same hospital, one scale can have its applicability adapted according to the observer perception.

The lack of fulfilment of some of the requirements, impelled the development of several different scales and modifications of the originals over the time, however the most critical unresolved issues remain: pre-requisite of training, need for clarity (Norton, 1996), predictive performance (Bick and Stephens, 2004; National Institute for Clinical Excellence, 2003; National Institute for Clinical Excellence, 2005) and definition of the critical threshold score (Clark and Farrar, 1992).

The quantitative visual assessment of CW based on the RYB system provides subjective and possibly inaccurate outcomes since red wounds can be healing (granulated), over-granulated or infected, which also applies to yellow wounds as they can contain slough or infected discharge (Cuzzel, 1988; Lorentzen *et al.,* 1999; Vermeulen *et al.,* 2007).

For obtaining a more accurate assessment than the one provided by scales, contact methods were further created based on manual techniques to acquire wound's shape, perimeter, area and depth. These methods are inexpensive and easy to learn and use in health centres, however, can lead to wound contamination, are extremely dependent on the health professional, can cause pain to the patient and are associated to high inaccuracy and variability, introducing errors in the resulting measurements (Flanagan, 2003; Majeske, 1992; Dealey, 1994; Goldman and Salcido, 2002; Rodgers *et al.*, 2010; Shaw and Bell, 2011; Griffin *et al.*, 1993).

The optical methods and their combinations can reconstruct the 3D shape of the wound with high precision, yet, their price, the requirement for training, time consumption and its problematic practicability in medical environment due to their great dimensions, are presented as limitations that restrict its availability in daily routine practice (Plassmann and Jones, 1992; Zhan and Miller, 2003). The non-invasive systems based on image processing techniques, although inexpensive and pain free, do not provide information of the 3D characteristics of wounds and the ones that do deliver this information, have its price enhanced due the combination of other technologies, shortening its clinical applicability.

Broad literature review revealed that there is an urgent necessity for automatic quantitative estimation of wound tissue within the wound bed, which might assist healthcare professionals to successfully monitor the wound healing rate.

Chapter 3

Methodology

The developed methodology can be resumed in three steps:

1. Selection of the technologies and programming languages to work with based on the problematic's nature.
2. Selection of the algorithms that better perform wound assessment.
3. Creation of an Android mobile application and incorporation of the algorithm previously created.

This chapter outlines the methodology used throughout this research work being described the necessary equipment for image acquisition and processing, the data collection, tested image processing techniques that did not succeed, the software and algorithms used to obtain the results, the design of the Android application and the analysis protocol used to evaluate the results of both methodologies.

3.1 - Equipment and Software

This project can be divided in two main phases:

1. Creation of an image processing methodology to characterise chronic ulcers using MATLAB.
2. Development of a mobile application using Android Studio and implementation of the methodology previously created, using OpenCV with a wrapper (JavaCV).

Therefore, to generate a dataset of 200 images to test the created methodologies, was used a standard digital camera in order to mimic the conditions and quality of the cameras of the current portable devices and the image processing methodology was implemented using MATLAB in a MacBook Air 13'' (Table 3.1 and 3.2).

Table 3.1- Equipment.

Quantity	Type	Model
1	Digital camera	Fujifilm Finepix L50 12mp
220	Calibration marker	2D White square adhesive with 2.5 x 2.5 cm^2
50	Calibration marker	3D White square adhesive with 1.0 x 1.0 x 0.5 cm^2
1	Portable Computer	MacBook Air 13'' 1.6 GHz Intel Core i5, 8GB 1600 MHz DDR3
1	Tablet	Asus Transformer Pad TF700T Wi-Fi - 32GB HDD 1GB RAM NVIDIA R Tegra R 3 quad-core 1.2 GHz

Table 3.2- Software.

Software	Type	Version
Android	Operative System	4.2.1 Jelly Bean
Mac OS X	Operative System	OS X 10.11.6 (15G31)
MATLAB	Mathematical computing software	2017a
Android Studio	Integrated development environment	2.3.0
OpenCV	Library	3.1.0
JavaCV	Library	1.3.2
iText	PDF Library	5.5.1
Microsoft Excel	Spreadsheet application	13.34

- MATLAB

MATLAB is a high-performance matrix-based language developed by MathWorks (Mathworks, 1984), which provides a vast range of libraries of prebuilt toolboxes with useful algorithms for tasks such as: image and signal processing, communications, machine learning, computational finance, computer vision, control design and robotics.

MATLAB's basic data element is an array that does not necessitate dimensioning therefore, this language allows the creation of solutions to technical computing problems that include matrix representations, with less coding and time spent writing code than it would take with languages like C

or C++, being chosen when the objective is to perform with ease and simplicity, image processing (Gonzalez *et al.*,2004; Gonzalez and Woods, 2002).

- Open Source Computer Vision Library (OpenCV)

Created initially by Intel Corporation in 1999, OpenCV is an open source computer vision and machine learning software library with more than 2500 optimised algorithms, offering a shared infrastructure for computer vision applications, being available for Windows, Linux and Mac OS as well as Android and iOS (OpenCV, 2012).

Although originally created to be implemented in C and C++, nowadays, this Library has interfaces ("wrappers") for Phyton and Java and is free for research use (OpenCV, 2012).

Although, MATLAB represents an easy and intuitive platform to perform image processing, OpenCV libraries are preferred when the aim is to create mobile applications since it increases ease of code conversion to Android java applications, magnifies the efficiency of it and reduces the time and complexity of running it on mobile platforms (Varma *et al.*,2016).

- Java Computer Vision Library (JavaCV)

JavaCV is a wrapper for OpenCV for the language Java, despite all of the actual computations being performed at a native level (C/ C++). The JavaCV library links the compiled functions, providing an interface to implementations using Java, being able to ultimately being incorporated in Android mobile applications, namely:

  - Android (Android)- Contains the classes that allow the conversion of OpenCV's variables Mat and Bitmap to the format used in Android.
  - Camera Calibration and 3D Reconstruction (Calib3d) - Include the classes related to the calibration of the camera and 3D reconstruction.
  - Core (Core)- Comprises basic OpenCV functionalities like Mat and Point.
  - 2D features (Feature2d): This module contains methods of extractors of keypoint descriptors represented as vectors in a multidimensional space.
  - Machine Learning (ml)- The Machine Learning module is a set of classes and utilities for statistical classification, regression and clustering of information.
  - Utilities (utils)- This module contains convertors for several types of variables and structures.
  - Object detection (objectdetect) – Contain methods like the Haar Feature-based Cascade Classifier for object detection.
  - Image processing (Imgcodecs and Imgproc)- The image filtering module allows geometric image transformations, image filtering and feature detection, histogram calculation and image writing.
  - Vídeo (video and videoio): The methods present in this Class, permit video capturing from video files, image sequences or cameras and video writing (OpenCV, 2012).

- iText

iText is an open source software developer toolkit that allows the incorporation of the PDF (Portable Document Format) functionalities in mobile applications, processes or products. (iText, 2000). The PDF format is widely used since it is effortlessly electronically exchanged and viewed and it is independent of software, hardware and operating system (Adobe, 1991).

3.2 - Data collection protocol

The image collection for the testing dataset was performed in the Diabetic Foot Clinic at *Centro Hospitalar do Porto*, after the Ethical Committee approval of the project (Appendix A). Following the normal procedures leading to the consultation, when a participant entered in the examination room, was suggested that he/she sited on the gurney, in order to elevate the oedematous extremities and off-load pressure points.

After, the dressings were removed by healthcare professionals (Figure 3.1 a)) and the wounded extremity was washed (Figure 3.1 b)). Next, the debridement of necrotic tissue, foreign bodies or devitalised tissue that act as a physical barrier to diffusion and the healing process, was performed. During these steps, the subject was informed about the purpose of the present study and asked if wanted to participate, if agreed, the term of agreement (Appendix B) was read and signed and then the questionnaire (Appendix C) was completed according to the date of realisation of the study, gender (male or female), age (in years), type of diabetes (type I, type II), type of diabetic foot ulcer (neuropathic, neuroischemic or ischemic), realisation of haemodialysis and the location of the lesion.

For the images collection, the camera was placed, perpendicular to the floor at one meter distance from the patient's foot and inclined according to the morphology of the site of the lesion, with a 90º angle to it, as shown in Figure 3.1 c), and a white disposable square adhesive marker (Figure 3.2 a) and b)) was included in the image, near the wound, as a calibration marker. Two images per diabetic foot ulcer were collected in order to assure the image processing of that ulcer despite one of the images being not focused, with bad illumination or shadows, etc.

After the collection, the image was then uploaded to a PC and its processing was performed in MATLAB (Figure 3.1 d)).

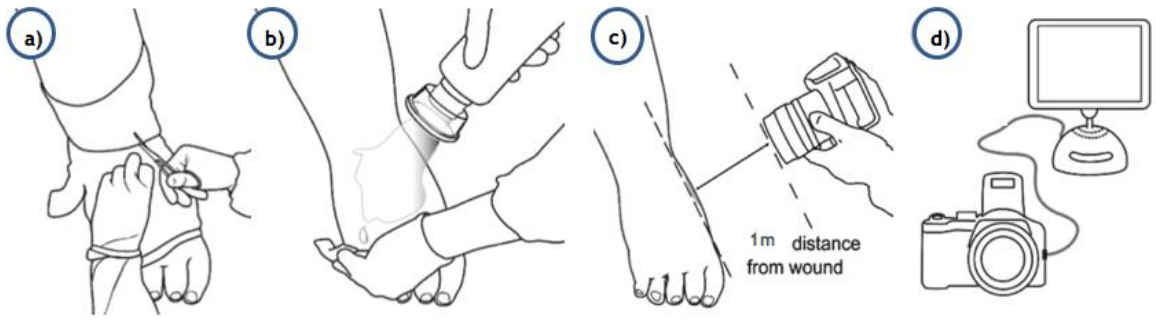

Figure 3.1 - Data collection protocol a) Wound exposure b) Washing of the wounded extremity c) Image capture of the ulcer d) Upload of the images to a PC where its processing was performed using MATLAB. Based on (Rennert *et al.*, 2009).

3.3 - Marker

During the image collection, two types of disposable markers were tested for wound area measurement purposes:

- 2D white square marker with length and width of 2.5 cm;
- 3D white square marker with length and width of 1.0 cm and height of 0.5 cm;

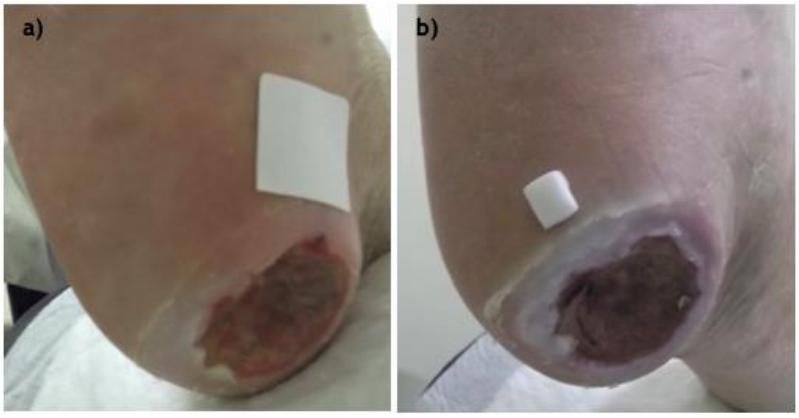

Figure 3.2 – Calibration markers a) 2D square marker (2.5 x 2.5 cm^2) b) 3D square marker (1.0 x 1.0 x 0.5 cm^2).

3.4 - Unsuccessful image processing techniques

During the research for this project, various techniques were implemented, however, not all of them worked for the aim of the study, not providing the most satisfactory results during image processing and wound and marker segmentation. From the referred list of methods, per phase, these are:

- Pre-processing

  - Gaussian filter

Gaussian filters are used in order to promote noise reduction, for that reason, during the pre-processing phase, it was tested the implementation of this filter using MATLAB's function *fspecial* with 'gaussian' as filter type, matrix size of 1/10 of the image size and a standard deviation of 1 (Gonzalez *et al.*, 2004; Gonzalez and Woods, 2002).

  - Bottom hat and Top hat filtering

The top-hat transform consists of the difference between the input image and its opening (i.e. the foreground pixels of an image that fit a certain structuring element). The bottom-hat transform is the difference between a closing operation (i.e. the group of background pixels of an image that fit a specific structuring element) of the original image and itself (Gonzalez *et al.*, 2004; Gonzalez and Woods, 2002). For this reason, the Bottom hat and Top hat operations were used in order to enhance image contrast using a structuring element of 1/10 of the size of the image with the shape 'disk' via MATLAB's function *imbothat* (Mathworks, 1984). Then, the original image was added to the top-hat filtered image, and to the result was subtracted the bottom-hat filtered image.

The contribution of the pre-processing tested techniques was further ascertain by calculating the Signal to Noise Ratio (SNR) in decibels of each output image individually according to equation 3.1 (Mathworks, 1984):

$$\mathrm{SNR} = 20 * \log_{10}(\frac{\mu_{signal}}{\sigma_{signal}}), \quad (3.1)$$

where the μ represents the average of the image values, i.e. the signal and the σ is the standard deviation of the image values, i.e. the noise.

- Ulcer and marker segmentation and tissue classification

  - Canny edge detector

Canny edge detector finds edges by searching for local maxima of the gradient. To achieve this, first it is applied a Gaussian filter to reduce noise and then the local gradient and edge direction are computed for every pixel of the image. Based on the gradient's peaks and where the derivative of the gradient function is zero, a non-Maximum suppression is performed. After, two thresholds (minimum and maximum) are used to detect weak and strong edges. The edges whose value is higher than the maximum threshold are considered strong real edges while the edges below the minimum threshold are only considered edges if they are 8-connected to strong edges (Gonzalez *et al.*, 2004; Gonzalez and Woods, 2002).

During the wound and marker segmentation process a Canny edge detector was implemented through MATLAB's function *edge* () to the image resultant from the histogram equalisation and median filtering.

  - Circle Hough transform (CHT)

A circle with radius R and centre (a, b) can be defined by the following two parametric equations (3.2 and 3.3):

$$x = a + R\cos(\theta) \quad (3.2)$$
$$y = b + R\sin(\theta). \quad (3.3)$$

When the angle θ reaches the full 360 degrees, visiting all of the range of points (x, y), the circle border is traced and the a and b are found. For this methodology, the CHT was applied, based on the approach created by Young (Young, 2016) where a neighbourhood-suppression method of peak finding is applied to ensure that the circles found are spatially apart. The input of this method was set to be the smoothed binary image of the bi-dimensional output of the pre-processing step (with application of a Gaussian filter followed by the Canny edge detector). The number of peaks to find was set to be 1 (i.e., one ulcer per image to be detected), the radii of the circle to be identified was set by a vector in which the possible radii values were set to be between 20 and 600 and the Hough score threshold was defined as being equal to the multiplication by 0.5 of the maximum value in the accumulator array that contains the number of votes for the circle centred at (a, b).

  - Gabor filtering

Another approach tested was the segmentation based on texture, which involves measurements in the spatial and the spatial-frequency domains. The Gabor filter(s) is a linear filter applied for tasks such as edge detection, having optimal joint localisation, or resolution, in both the spatial and

the spatial-frequency domains (Daugman, 1985). For this methodology, Gabor filtering was implemented based on the approach created by Jain and Farrokhnia (Jain and Farrokhnia, 1991) to perform texture segmentation, where an array of Gabor Filters with different frequencies and orientations was designed with the aim of identifying different frequency and orientation information in the input image (resultant from the pre-processing phase of the final methodology). For this, the samples orientations were defined to be between 0 and 150 degrees, incrementing in steps of 30 degrees. The minimum sample wavelength was set to be $4/\sqrt{2}$, up to the hypotenuse length of the input image.

The Gabor magnitude or Gabor Energy features (resultant from the application of different Gabor filters) were extracted from the input image and post processed with a Gaussian filter (with the quantity of smoothing applied to the Gabor magnitude responses being controlled by a smoothing term) in order to compensate for local variations. A map of spatial location information in both X and Y was further added, in order to allow the classifier to prefer sets of data spatially closer from one another. Finally, the features were normalised to be zero mean, unit variance (Mathworks, 1984).

- Watershed

The watershed transform finds "catchment basins" or "watershed ridge lines" present in an image by defining it as a topological surface where the values of each pixel are considered heights, and assuming that light pixels characterise high elevations and dark pixels signify low elevations.

The watershed was implemented (via *watershed* () function) in conjugation with the distance transform which represents the distance from every pixel to the nearest non-zero pixel implemented using *bwdist* (). This technique was tested for this project during ulcer segmentation and tissue classification phases.

- Region growing

Region growing is a clustering technique that performs image segmentation starting from initial seed points and growing its region based on properties (specific ranges of pixel brightness or colour) shared between the neighbour pixels and the seed(s), being the difference defined by a threshold (Gonzalez *et al.*, 2004; Gonzalez and Woods, 2002).

This method was implemented by using as input parameters the greyscale image resultant from the documented pre-processing, a set of 6 seed points selected manually by clicking the mouse and a threshold of the maximum intensity distance which was set to be 0.3.

- Active contour (Snakes)

A snake is a deformable curve that evolves from an initial position towards the contour of the object in an energy minimisation process of the functional energy, which is a weighted sum of the internal and the external energies (Kass *et al.*, 1988).

This type of active contour was implemented using the pre-processed image, a list of coordinates as seed points, chosen via click in the mouse by the user and a set of variables to control the snake's contour evolution from the initial points to the wound segmentation. This method was set to have 200 iterations and use an alpha value of 0.2 and a beta value of 0.6.

- Active contour ('Chan-Vese' method)

Contour based on the 'Chan-Vese' method is a special case of Mumford- Shah functional and, being of the same class as snakes, it also implements image segmentation based on an energy minimisation process. However, it differentiates from the other in the aspect that it is not edge depend-

ent, being extremely useful when the aim is to segment objects whose boundaries are not defined by a gradient (Jadav *et al.*, 2013).

When a methodology for ulcer segmentation was being designed, this method was implemented using as input a mask automatically created by some clicks on the mouse by the user with a number of iteration of 200 and using the function *activecontour* () with the type of active contour 'Chan-Vese'.

- Fuzzy-c-means

Fuzzy-c-means is a clustering technique that classifies the image by categorising analogous data points into clusters, which is achieved by iteratively minimising a cost function that is dependent on the distance of the pixels to the cluster centres in the feature domain.

This function cost is minimised when are given high membership values (probability that a pixel belongs to a certain cluster) to the pixels closer to the centroid of their clusters, and pixels whose data in more distant to the centroid are assigned low membership. The algorithm stops when the number of iterations is reached or when no changes in the membership function or in the cluster(s) centre(s) are noticed between two consecutive iterations. This method was implemented for this study with a maximum number of iterations of 100 and a number of centres equal to 4 in order to perform ulcer and marker segmentation as well as to characterise the tissues within the wound bed.

3.5 - Image processing methodology in MATLAB

Relatively to the first aim of this project, a methodology was created using MATLAB whose main phases can be divided in:

- Image acquisition;
- Image pre-processing;
- Ulcer and marker segmentation;
- Shape recognition;
- Ulcer area calculation;
- Tissue classification.

These main phases of the methodology include several operations (Figure 3.3) that led to the most accurate results:

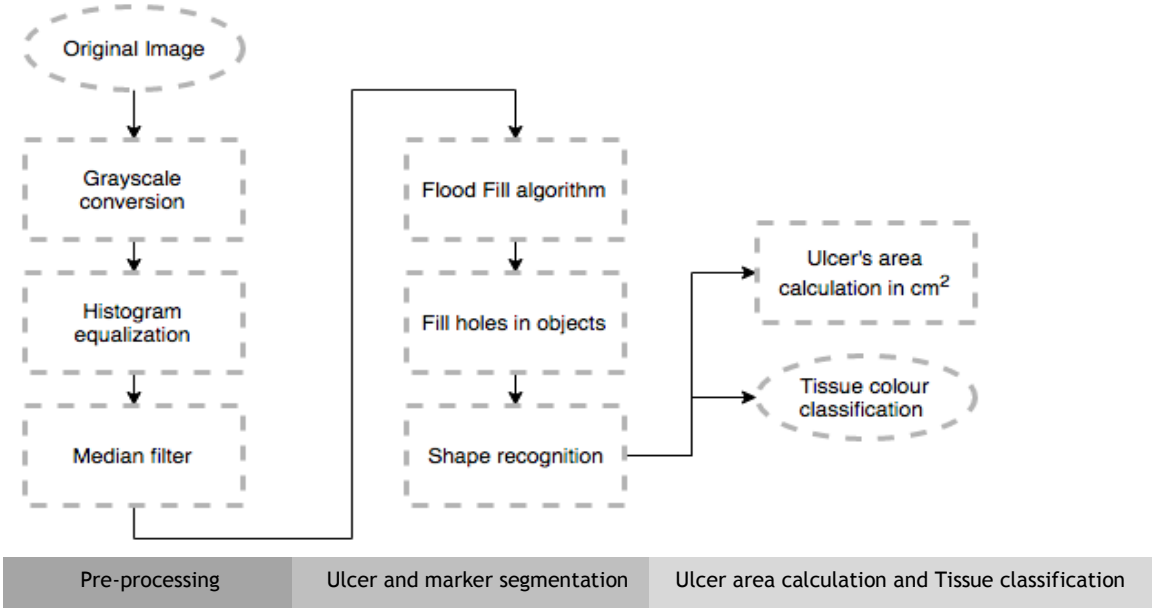

Figure 3.3- Methodology for image processing using MATLAB.

3.5.1 -Pre-processing

- Histogram equalisation

Histogram equalisation is an intensity transformation that corresponds to the redistribution of grey levels in order to get a histogram as uniform as possible, maximising the image information. Each pixel is replaced by the integral of the image histogram in that pixel. The net result of this intensity-level equalisation process is an image with increased dynamic range, which will tend to have higher contrast (Gonzalez *et al.*, 2004; Gonzalez and Woods, 2002). The implementation of this operation was achieved using MATLAB's function *histeq* () (Mathworks, 1984).

- Median filter

The median filter is a nonlinear operation that replaces the value of a pixel by the median of the intensity values of its neighbourhood pixels (the original value of the pixel is included in the computation of the median).

These types of filters are good at eliminating some types of random noise, as the "salt and pepper" noise, with considerably less blurring than linear smoothing filters of similar size, thus preserving edge information (Gonzalez *et al.*, 2004; Gonzalez and Woods, 2002).

For the referred methodology, it was applied a median filter with a structured element of 1/10 of the image size through the function *medfilt2*() (Mathworks, 1984).

3.5.2 -Ulcer segmentation

- Flood fill

To segment the ulcer in the foot, a flood-fill algorithm was designed where the intensity of the pixel chosen via click in the mouse by the user within the greyscale image resultant from the pre-processing phase, was the starting point to an iterative scan line search on the surrounding pixels with an empirical tolerance of 35 (Gonzalez *et al.,* 2004). The pixels considered part of the segmented object (ulcer and marker) are coloured in pink and the algorithm stops when there are no more pixels within the same range of brightness of the starting pixel.

- Filling holes

Chronic ulcers are characterised by their tissue heterogeneity, which signifies that the same ulcer can have several different tissue types with different colours. Therefore, to guarantee that all the pixels within the boundaries of the obtained ulcers and markers are considered as belonging to them, an operation of filling with the option "holes" using MATLAB's *imfill* (image, "holes") (Mathworks, 1984) was performed on the flood fill's resultant binary image containing both the marker and the ulcer.

3.5.3 -Shape recognition and ulcer area calculation

After the hole filling operation, was obtained a binary image with the marker and the ulcer segmented. To perform ulcer's area calculation, the objects of the binary image were labelled using MATLAB's *bwlabel ()* (Mathworks, 1984) from which were obtained both the pixel's list and the number of objects. Then, properties as "Area" in pixels, "Extent", "Centroid", "Perimeter", "Equivalent diameter", "Major axis length", "Minor axis length" and "Eccentricity" of both objects were obtained via *regionprops ()* (Mathworks, 1984).

To calculate the ulcer area in cm^2, it was mandatory that first, the two objects in the binary image were automatically identified as "ulcer" or "marker". This shape recognition was performed via two observed conditions:

- Chronic wounds (Diabetic foot ulcers) are mostly circular and the marker used is a square.
- Circular shapes have higher circularity (Equation 3.4) and eccentricity (given by regionprops) or higher circularity and lower eccentricity than square shapes.

$$\text{Circularity} = \frac{4 * \pi * \text{area}}{\text{perimeter}^2}\ , \tag{3.4}$$

where π is a mathematical constant (π=3.14159).

Ulcer's real area calculation in the bibliography is generally performed by using known distances from the camera to the lesion (Varma *et al.*, 2016). However, since with the daily use of the mobile application and the variation of user, would be of great difficulty predict the distance or maintain it, for this project a calibration marker was designed and implemented during the image collection. This adhesive marker allowed the calculation of the area in cm^2 of the segmented lesion by multiplying the number of pixels within the ulcer (given by *regionprops()*) by the real area of the marker (which is $6.25cm^2$ or $1cm^2$), divided by the total number of pixels of the marker (given by *regionprops()*) according to the Equation 3.5.

$$\text{Ulcer's area} = \frac{\text{area of the ulcer in pixels} * \text{area of the marker in cm}^2}{\text{area of the marker in pixels}} \quad (3.5)$$

3.5.4 -Tissue classification

The final goal of the methodology was to classify wound tissue, which was performed on the basis of the Red-Yellow-Black (RYB) wound colour classification by Hellgren and Vincent (Hellgren and Vincent, 1986) mentioned in Chapter 2 section 2.2.1 Visual characterisation of wounds, as well as the knowledge transmitted by the healthcare professionals at *Centro Hospitalar do Porto*.

After intersecting the original image with the image resultant from the shape recognition step, an image with RGB values on the pixels of the ulcer and black background was obtained.

Tissue classification based on colour was achieved by thresholding the range of pixels within the ulcer image based on their R, G an B histograms:

- Red tissue was classified by two thresholds: one for the healthy granulating tissue which is represented by light red pixels and one for the dark red pixels which characterise unhealthy granulating tissue. All the threshold values used were obtained empirically. The dark pixels were classified by thresholding the red channel to have values between 40 and 90 and allowing the blue and green channels to have values equal or lower than 50. The light pixels were obtained by thresholding the red channel to values equal or higher than 90 and the green and blue channels were thresholded to values equal or lower than 50.
- For the classification of the black tissues, all of the 3 RGB channels of the image were thresholded to values equal or lower than 40.
- In order to obtain the pixels relative to white/yellow tissues, the implemented thresholds suppressed values equal or lower than 90 for the red and green channels and equal or higher than 70 for the blue channel.

With the characterisation algorithm created were obtained 4 images corresponding to each tissue type and their percentages (by dividing the number of each tissue's pixels by the total number of pixels of the wound).

3.6 - Android mobile application

The final objective of this project is to create an easy, simple, fast and efficient Android application capable of:

1. Capturing images of chronic ulcers using the device's camera and access to images in the internal memory of the device;
2. Perform wound characterisation based on its area and tissue colour and provide important information of the ulcer characterisation into a PDF report.

In order to perform these tasks, the mobile application needs to satisfy some essential functional and non-functional requirements, however, their fulfilment has costs and risks as shown in Table 3.3.

Table 3.3- Mobile application requirements.

	Requirements	Priority	Cost	Risk
Functional requirements	The application must take a picture and store it sequentially in both the camera roll and in an independent directory.	High	High	Low
	The system must calculate and display the ulcer's area in cm^2 and $inches^2$.	High	Low	Low
	The application must perform tissue colour classification (RGB).	High	High	Low
	The application must generate a dataset of the characterisation of the wound.	High	High	Average
Non-functional requirements	The application must run in all android tablets with back camera.	High	Average	Low
	The application must run in all android tablets with minimum API of 15.	High	Average	Average
	The application must run in all android tablets with OpenCV installed.	High	Average	Average
	The application must not take more than 120 seconds to display the results.	High	High	High/Average
	The application must have a simple, easy and unequivocal use.	High	Average	Low
	The system must store at least 1000 images without replacing themselves.	Average	High	Average

3.6.1 -External libraries incorporation

The incorporation of the OpenCV with a "wrapper" (JavaCV) and the iText library in the Android Studio was a fundamental step of this project in order to allow image processing and documentation with ease. This was achieved by adding the OpenCV library as a module dependency to the application after downloaded from the OpenCV's official web page (http://www.opencv.org/) with the minimum SDK version being set to be 8 and the target SDK and API versions were set to be 23 and Android 6.0 (Marshmallow), respectively.

The iText was added as a .jar dependency of the project in the "Project structure" section of the Android Studio.

For it to be possible to access the camera of the device, store, access and write images and save the PDF report file in the device's memory, three permissions were added in the Extensible Markup Language (XML) file of the mobile application's manifest:

- android.permission.CAMERA;
- android.permission.READ_EXTERNAL_STORAGE;
- android.permission.WRITE_EXTERNAL_STORAGE;

3.6.2 -Graphic interface

During the design of the graphic interfaces, the simplicity and ease of use of the mobile application were preferred in order for it to be practical during its implementation in clinical environment. Therefore, the main activity of the application i.e., the activity that first is presented to the user was chosen to be a menu where the user selects the origin of the image containing the ulcer to be characterised: the gallery application or the device's camera (Figure 3.4).

The mobile application default language is set to be Portuguese however, all the activities give the user the option of clicking on the button at the end of every screen to instantly translate the text in the screen to English. In the translated activity, the same button will appear with the Portugal's flag which allows the return to the default language.

Figure 3.4- Preview of the main activity of the mobile application.

If the user selects the option of picking an already existent image to process, the mobile application shows the directories from which the user can choose the image. After selected, the image is displayed and the user approval to start the characterisation is required (see Figure 3.6).

Otherwise, the camera view opens with a 1280 x 960 frame (dimensions that provide the perfect equilibrium between the quality of the captured image and its size in memory), shown in Figure 3.5, with a button to capture the image.

Though the remaining activities can be seen and operated in both "Portrait" and "Landscape" modes, the camera activity can only perform correctly in "Landscape" mode due to the incorporation of OpenCV (which causes changes in the orientation of the camera view).

Figure 3.5- Live feed activity.

After collecting an image, a third activity is shown (Figure 3.6) where the user can preview the image and determine if wants to proceed to the characterisation and/or return to the previous activity (to capture or to re-select another image).

When the button "Caracterizar" is pressed, another activity starts and the image is stored (if captured in real time) and pre-processed.

In this activity, the user should also specify the real area (in cm^2 for the Portuguese users or in $inches^2$ for the foreign English speaking users) of the square marker incorporated during image collection.

Figure 3.6- Preview of the confirmation.

Wound segmentation starts with two transitory input activities that were created in order for the user to choose a seed pixel for both the ulcer (Figure 3.7 a)) and the marker (Figure 3.7 b)) to start the characterisation.

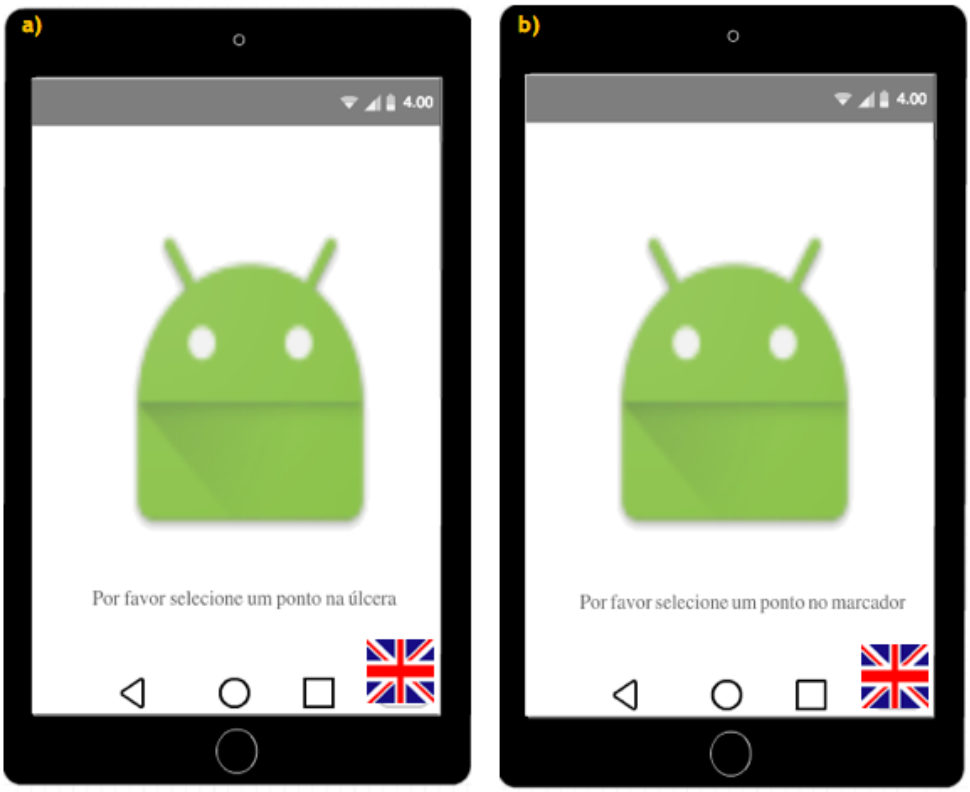

Figure 3.7- Touch interface of seed point selection a) ulcer b) marker.

The wound's segmentation result and the outputs of the ulcer characterisation (area in cm^2 and in $inches^2$, and dark red, light red, black and white/yellow tissues percentages) are displayed in the screen according to Figure 3.8.

The home button in the upper right corner of this screen can be pressed to return to the home activity of the mobile application (menu to choose the source of the image to be processed).

Figure 3.8- Preview of the result of the wound characterisation.

The PDF report of the resultant ulcer classification is then stored in a directory with a serial numeric name. In this report, it can be consulted the date and time of the characterisation, the properties already displayed in the mobile application as a result of the ulcer characterisation (ulcer area in cm^2 and $inches^2$, percentage of healthy and unhealthy granulating tissues, white/yellow tissue and necrotic tissue) as well as the images representative of every tissue type classification (Figure 3.9).

Figure 3.9- Structure of the PDF report with the result of the wound characterisation.

3.6.3 -Android mobile application overview

The developed mobile application was designed as shown in Figure 3.10.

First, the source of the image to be processed is selected: device's internal memory or camera. If the first option is selected, the directories in the device's internal memory are listed and an already existent image is chosen from there (JPEG, JPG or PNG formats).

If the second option is preferred, an image is collected from the device's own camera.

Then, if the user decides to proceed to characterisation, the image is stored (only if captured by the camera) in the camera roll and in a directory named "Pé diabético" in the internal storage of the device with a PNG format and a unique numeric name for future reference of the state of the lesion otherwise, the user returns to the menu of selection of the image origin.

Next, the pre-processing of the collected image is performed and then, the user is invited to choose two seed points for the flood fill algorithm in order to start the ulcer and marker segmentation phase.

After isolating the ulcer in the image, the area of the lesion is calculated and its tissue composition is characterised based on its colour by means of a RGB histogram thresholding methodology.

Finally, the results of the ulcer characterisation are displayed on the device's screen and a PDF report with the results achieved is stored in a directory within the one previously created in the device's internal storage for future reference of the characterisation.

If no more characterisations are to be performed, the android application can be closed, otherwise, the user can return to the starting menu.

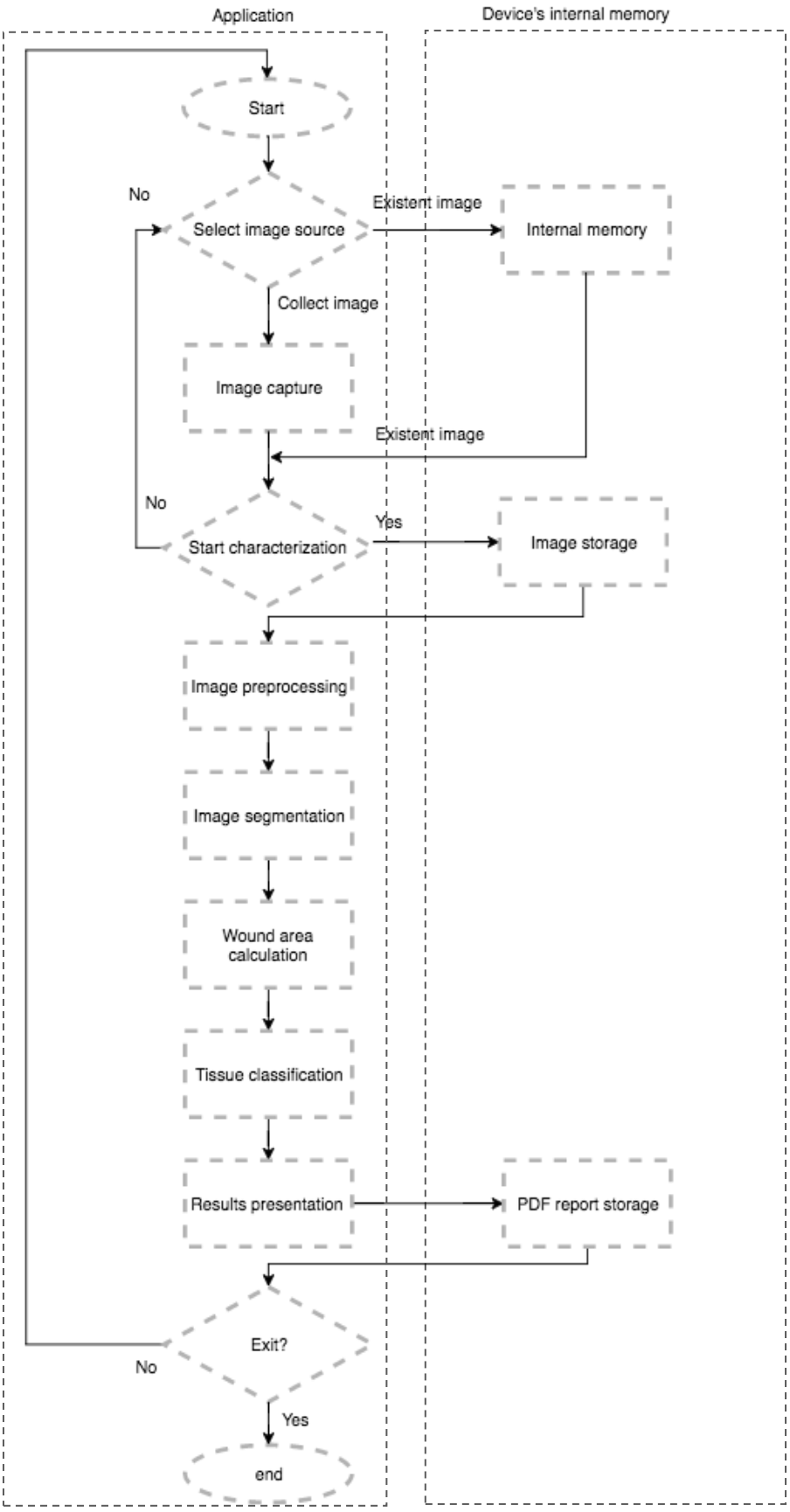

Figure 3.10- Mobile application design using Android Studio.

3.6.4 -Pre-processing

After captured, the image is compressed to the PNG format with a compression factor of 80 (factor that provided the best balance between quality and storage space) and converted to Mat to allow its processing.

Then the colour space of the original image was changed from BGRA (OpenCV predefined colour space) to RGB and from RGB to GRAY using the OpenCV class *Imgproc* and the pre-built function cvtColor which has three parameters: the source image, the destiny image and a colour code which for the first conversion was *Imgproc.COLOR*_BGRA2RGB and for the second conversion was used *Imgproc.COLOR_RGB2GRAY*.

To the greyscale image was then applied a histogram equalisation using OpenCV's function *equalizeHist* of the *Imgproc* library and a median filter using a kernel with 1/10 of the image size by means of the *medianBlur* method present in the same library which has as parameters the source image, the destiny image and the size of the structuring element to perform the filtering.

3.6.5 -Segmentation

For the ulcer and marker segmentation, was implemented a flood fill algorithm via the OpenCV's pre-built method *floodFill* from the class *Imgproc*. This function has 8 parameters:

- An input image which was the resultant greyscale image of the histogram equalisation and the median filtering operations;
- An output image that consisted of a one-channel image filled with zeros with the same length of the original image plus 2 and width equals to the original image's width plus 2 (condition obligatory in OpenCV for this function for computation purposes) created using the function zeros of the class Mat;
- A seed point whose coordinates were given by the user via a click in the screen of the portable device in which the mobile application is running;
- The colour to which the flood filled pixels appear in the output image (was chosen white);
- A rectangle from which the search is performed according to the connectivity.
- The lower and upper parameters for tolerance purposes which was set to be 40 for both thresholds.
- Flags consisting of the pixels connectivity used to perform the operation being set to 8-connectivity.

This algorithm was applied to both the marker and the ulcer being obtained two binary images of the segmentation of both. After, to eliminate black pixels within the boundaries of each object, a morphological operation of closing (a dilation followed by an erosion with the same structuring element) was performed in both images with a kernel of 1/10 of the size of the input image, created using the function *getStructuringElement* of the *Imgproc* class with the parameters: kernel shape (was selected an elliptical shape using *Imgproc.MORPH_ELLIPSE* method) and the kernel size.

The closing operation was implemented through the *morphologyEx* method of the *Imgproc* library using each binary image as input, selecting the type of operation to closing via *Imgproc.MORPH_CLOSE* and the kernel created.

3.6.6 -Ulcer area calculation

The shape recognition was not necessary in the methodology implemented in the Android application since the area in pixels of each object (ulcer and marker) was obtained using a method of the *Core* class named *countNonZero* which devolves the number of pixels different from zero. Then, to calculate the ulcer's real area in cm^2 the same formulae from the MATLAB's methodology was applied (Equation 3.5) where the real area of the marker was multiplied by the number of pixels of the ulcer and then divided by the number of pixels of the marker. For the mobile application, an additional measurement unity to describe wound area was added: $inches^2$, which was obtained by multiplying the obtained cm^2 area by a conversion factor of 0.155, since 1 cm^2 = 0.155 in^2 (Whitaker, 2000).

3.6.7 -Tissue classification

To perform tissue colour classification was created a RGB image through the intersection of the flood fill's result with the original image.

Wound tissue classification was achieved based on the Red-Yellow-Black (RYB) wound colour classification by Hellgren and Vincent (Hellgren and Vincent, 1986) mentioned in Chapter 2 section 2.2.1 Visual characterisation of wounds and the knowledge transmitted by the healthcare professionals at the Diabetic Foot Clinic.

Therefore, a histogram thresholding methodology was implemented using the *inRange (input_image, low_threshold, high_threshold, output_image)* method from the *Core* class with the criteria:

- Similar to the MATLAB methodology, in the mobile application, red tissue was classified using two thresholds (clinically, light red tissue is associated with healthy granulating tissue and dark red tissue exemplifies unhealthy granulating tissue). Again, all the threshold values used were obtained empirically. Therefore, the dark red pixels were assessed by thresholding the red channel to have values between 45 and 95 and the green and blue channels were selected to have values equal or lower than 55. Healthy granulating tissue was obtained by thresholding the red channel to have values equal or higher than 95 while the blue and green channels were limited to have lower or equal values than 55.
- To segment the black tissues were considered pixels values equal and/or bigger than 10 for the 3 channels of the image and pixels equal and/or smaller than 45 for the R, the G and the B channels;

- White/yellow tissue was obtained by considering pixels with RGB pixel values equal or higher than 95 and equal or lower than 255 for the red and blue channels and for the green one minimal and maximal values of 75 and 255, respectively.

The percentage of each tissue was obtained by multiplying per 100 the division of the number of pixels of each tissue type in each image resultant from the tissue classification step by the total number of pixels of the ulcer area (both given by *Core*'s method *countNonZero*).

The characterisation is compiled into a PDF file by means of incorporation of the iText Library as a dependency in Android Studio and it is stored.

3.7 - Assessment evaluation

The clinical evaluation of the MATLAB methodology's and the mobile application's ulcer characterisation results and the testing of the mobile application, was performed by 7 healthcare professionals (5 physicians and 2 podiatrists), who were asked to characterise the chronic ulcers of the dataset and to capture and analyse other 15 ulcers in real time with the prototype designed. The Android application's evaluation was performed according to the questionnaire in Appendix F, where five global questions about the mobile application performance were asked to the professionals with possible scores between 1 and 5 (being 1 the worst score and 5 the best score):

1. How do you evaluate the provided ulcer area?
2. How do you evaluate the provided ulcer tissue characterisation?
3. The mobile application is applicable in clinical environment?
4. The mobile application usage is simple, easy and unequivocal?
5. Global score?

The professionals were also asked which method, in their judgement, performed ulcer segmentation and tissue classification with more accuracy: the MATLAB methodology or the Android mobile application.

The resemblance of the results obtained with both methodologies was further ascertained by correlating their outcomes using Pearson correlation, using Microsoft Excel, and by correlating them with the health professionals' assessment of the ulcers.

Chapter 4

Results

At this chapter, the main results of this study are presented. Initially, the characterisation of three different diabetic foot ulcers is shown in the respective subsections (pre-processing, ulcer segmentation and tissue classification) as well as ulcer area calculations and tissue percentages from both the image processing methodology in MATLAB and the mobile application.

Then, the obtained results and the mobile application's performance evaluation are accomplished according to the opinion of 7 healthcare professionals from the Diabetic Foot Clinic at *Centro Hospitalar do Porto*. This opinion is based on their quantitative assessment of the ulcers which it is the most common approach of wound characterisation being used as a ground truth for this study.

4.1 - Marker segmentation

For wound calculation purposes, a calibration marker was designed and implemented during image collection. To allow the wound collection with simplicity and ease and eliminate the obligation of a second person holding the marker next to the wound during the collection as most seen in other researches, were designed two white square adhesive markers: 3-dimensional (1 cm length, 1 cm width and 0.5 cm thick) and 2-dimentional (2.5 cm length by 2.5 cm width). During the testing of the created methodologies was found that 2.5% of the markers (5 out of 200) were not correctly segmented presenting an area error of more than 0.1 cm^2.

The area returned from the segmentation of the maker present in the Figure 4.1 resulted in an 0.35 cm^2 error relatively to its real area.

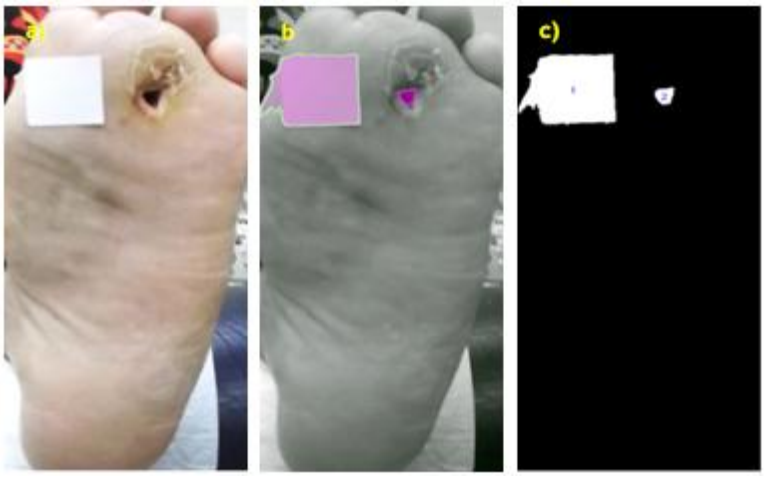

Figure 4.1- Unsuccessful 2D marker segmentation a) Original image b) Result of the flood fill c) Erroneous marker segmentation.

The maker segmentation of Figure 4.2 returned, for the biggest object representing the marker, an 0.15cm^2 error relatively to its real area.

Figure 4.2- Unsuccessful 3D marker segmentation a) Original image b) Result of the flood fill c) Four labels detected during shape recognition instead of two.

With the segmentation of the makers in the Figure 4.3 was obtained, for the Figure 4.3 a) a deviation of 0.20 cm^2 relatively to the marker's real area whereas for both the Figure 4.3 b) and the Figure 4.3 c) was found an error of 0.15 cm^2.

Figure 4.3- Marker a) Marker not totally adherent to the skin b) Marker appears bended c) Marker shape modification due to the capture angle of the image.

4.2 - Unsuccessful image processing techniques

During this research project, in order to obtain the image processing techniques that provided the most satisfactory results, several methods were tested to pre-process the images as shown in Figure 4.4.

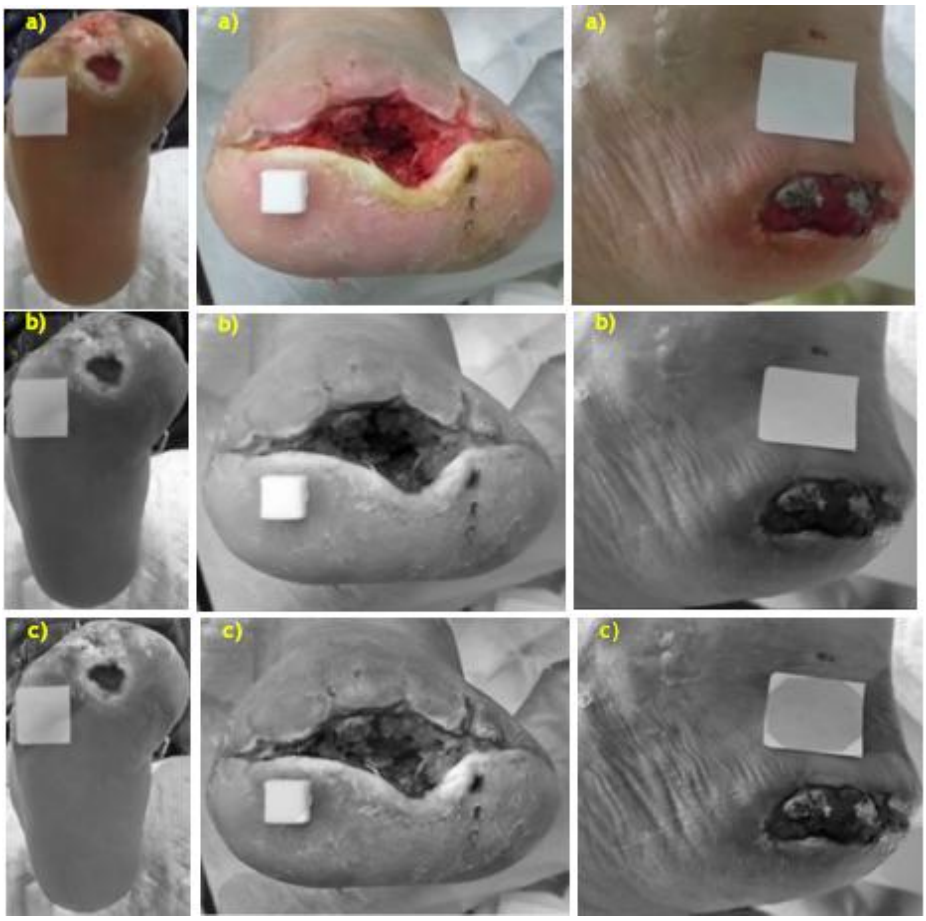

Figure 4.4- Techniques tested for image pre-processing a) Original image b) Gaussian filtering c) Bottom-hat and Top-hat operations.

The SNR calculations performed to ascertain the contribution of the tested pre-processing operations revealed for the Figure 4.4. a) left, a value of 13.02 dB. The resulting image of the designed pre-processing methodology returned a value of 13.15 dB. The application of the gaussian filtering resulted in a SNR of 12.05 dB, whereas for the resulting image of the Bottom-hat and Top-hat operations was obtained a SNR of 10.68 dB.

Relatively to the Figure 4.4 a) centre, the calculations returned, for this image, a SNR value of 15.40 dB. The output image of the designed pre-processing methodology presented a SNR of 15.49 dB however, the application of the gaussian filtering resulted in a SNR ratio of 12.25 dB and for the resulting image of the Bottom-hat and Top-hat operation was achieved a SNR of 10.58 dB.

Lastly, for the Figure 4.4 a) right, a value of 16.20 dB was returned. The output image of the implementation of the histogram equalisation and the median filtering achieved a SNR of 16.26 dB.

The image resultant from the gaussian filtering returned 11.23 dB for the SNR calculations, while for the resulting image of the Bottom-hat and Top-hat operations was achieved a SNR of 10.70 dB.

Furthermore, after designing the pre-processing methodology to be followed, several segmentation strategies were applied to the image in order to perform wound and marker segmentation and tissue classification, illustrated by Figure 4.5 and Figure 4.6.

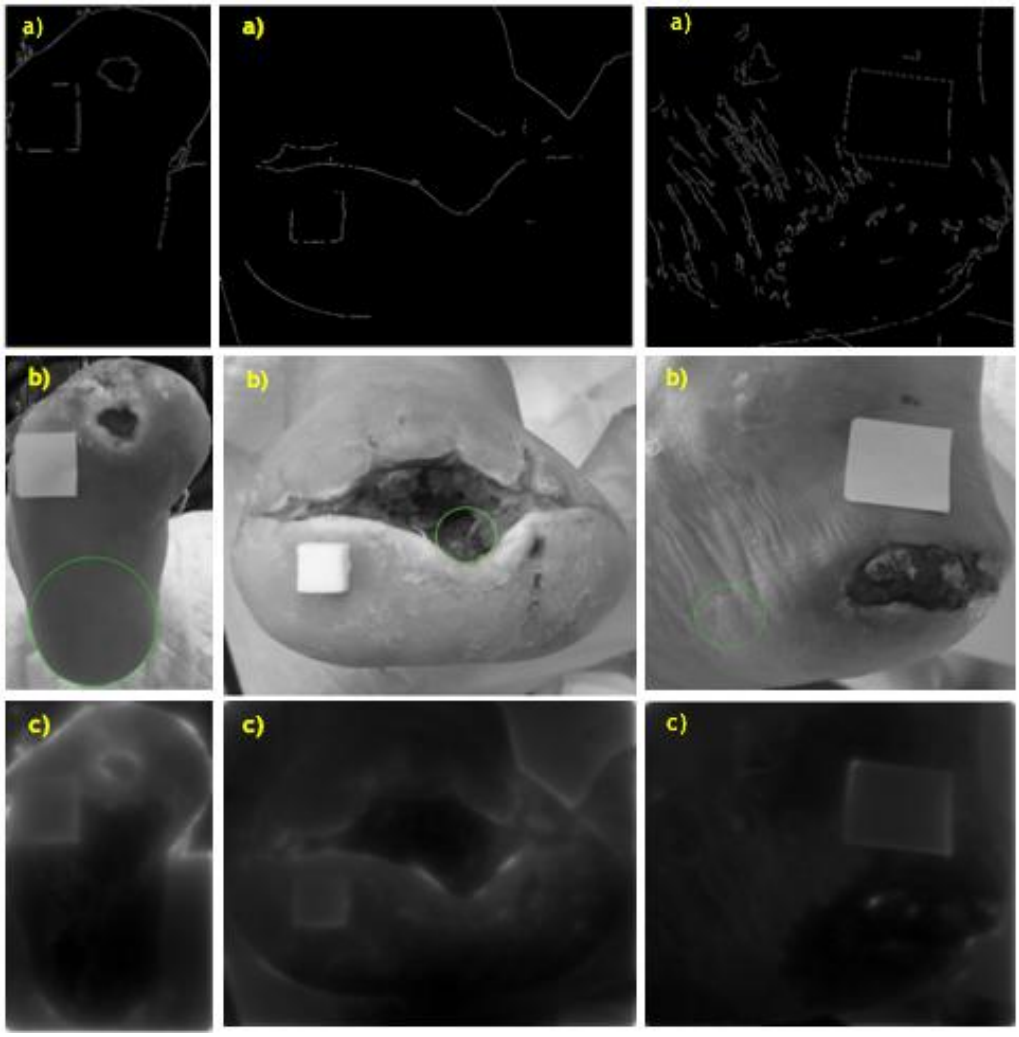

Figure 4.5- Techniques tested for wound and maker segmentation whose results were not satisfactory a) Canny edge detector b) Circle Hough transform c) Gabor filtering.

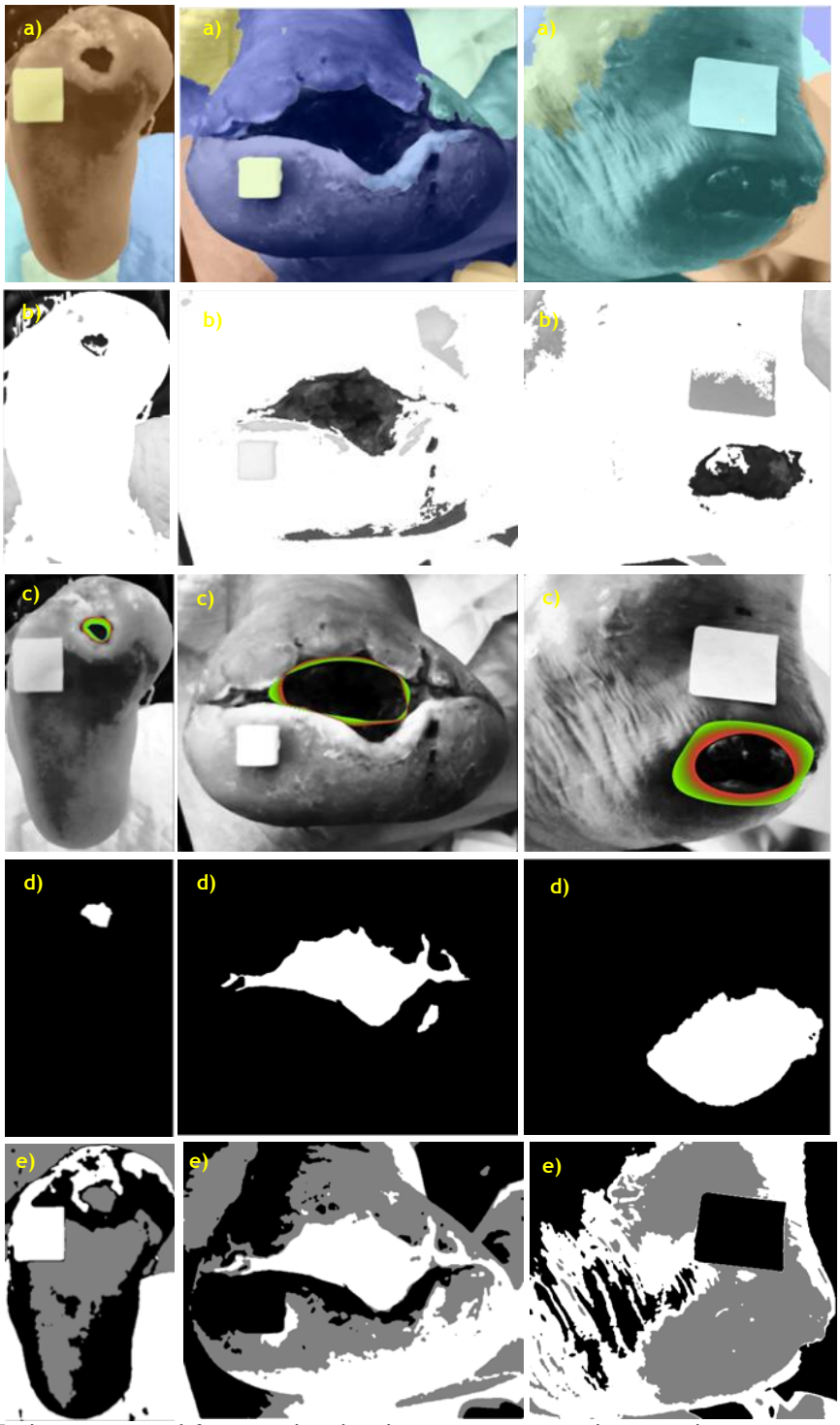

Figure 4.6- Techniques tested for wound and maker segmentation whose results were not satisfactory a) Watershed algorithm b) Region Growing algorithm c) Active contour with snakes d) Active contour ('Chan-Vese' method) e) Fuzzy-c-means Clustering.

4.3 - Image processing methodology in MATLAB

4.3.1 -Pre-processing

In order to fully evaluate the performance results of both the MATLAB and the mobile application methodologies, three images representative of the main tissue compositions in diabetic ulcers (mostly with red tissue, combination of red and black tissues and combination of red and white/yellow tissues) were selected from all of the collected images.

According to the Figure 4.7, representative of ulcers with combination of red and white/yellow tissues, i.e. ulcers with both granulating tissue and devitalised tissue, infection (pus) or with a visible anatomic structure (bone, tendon), one can see the results of the median filter and the histogram equalisation operations compared to the original image.

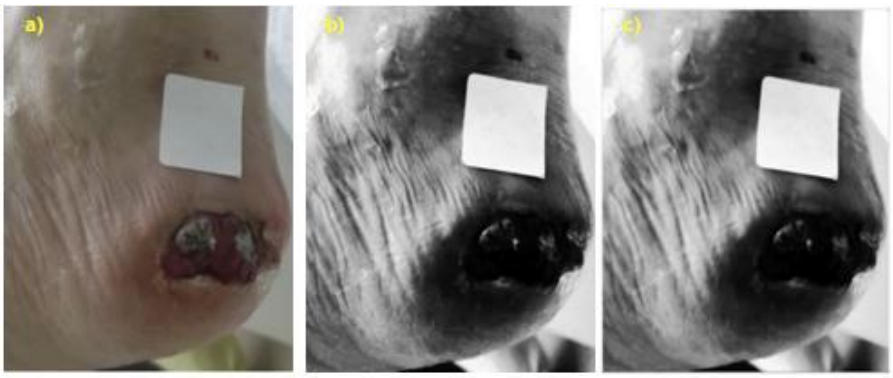

Figure 4.7- Pre-processing using MATLAB of the ulcer with white/yellow tissue a) Original image b) Histogram equalisation c) Median filtering.

Likewise, the Figure 4.8 shows the results of the designed pre-processing methodology applied to the ulcer with combination of red and black pixels representative of ulcers with granulating and necrotic tissues.

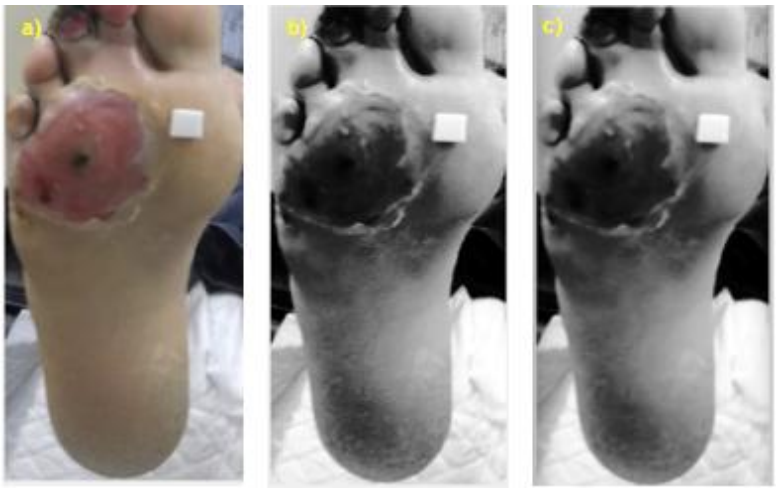

Figure 4.8- Pre-processing using MATLAB of the ulcer with necrotic tissue a) Original image b) Histogram equalisation c) Median filtering.

At the final study case, is shown the ulcer with mostly red pixels, i.e. a predominantly granulating ulcer, present in Figure 4.9 a), the resultant image of the histogram equalisation operation (Figure 4.9 b)) and the result of the application of the median filtering (Figure 4.9 c)).

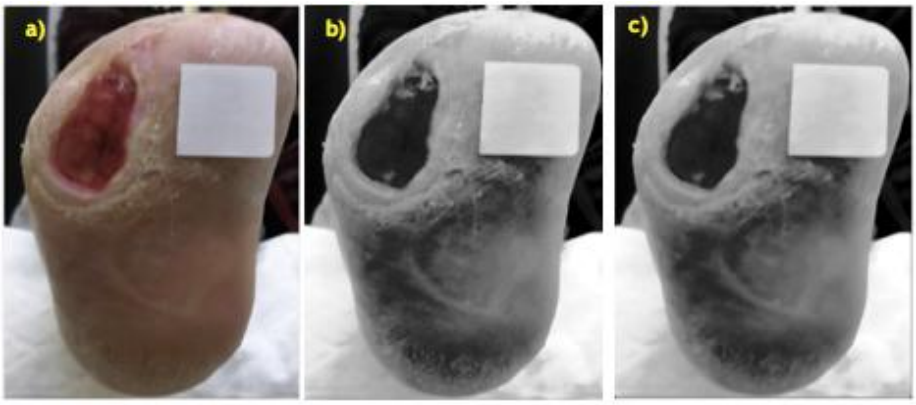

Figure 4.9- Pre-processing using MATLAB of the ulcer with mostly granulating tissue a) Original image b) Histogram equalisation c) Median filtering.

4.3.2 -Ulcer segmentation

- Successful cases

The tolerance for the flood fill algorithm was empirically set to be 35 for the image processing methodology in MATLAB and 40 for the Android application. In Figure 4.10 is represented the process of selecting the algorithm's search tolerance for the image processing methodology in MATLAB, in order to achieve a satisfactory ulcer segmentation. The same process was elaborated in order to select the tolerance that led to the achievement of the most acceptable results for the Android application.

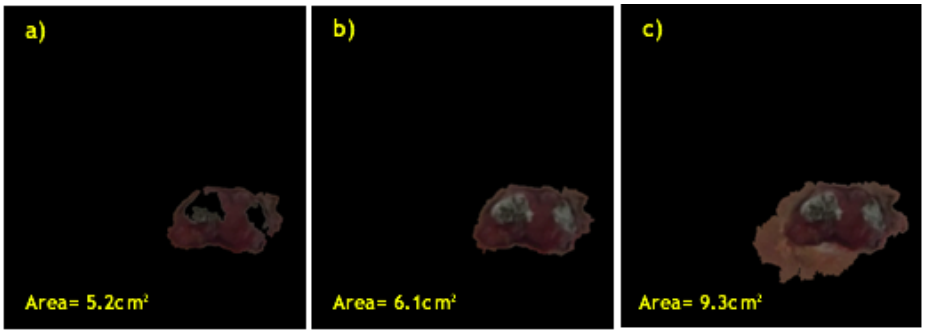

Figure 4.10- Segmentation process of the ulcer with white/yellow tissue using MATLAB a) Result of the implementation of the flood fill algorithm with a tolerance of 30 b) Result of the implementation of the flood fill algorithm with a tolerance of 35 c) Result of the implementation of the flood fill algorithm with a tolerance of 40.

Since the flood fill method is colour based, to guarantee better results for ulcers with great tissue heterogeneity, a hole filling operation was performed.

In the Figure 4.11 a) the raw result of the flood fill is shown, followed by the results of the hole filling operation (Figure 4.11 b)) and the final ulcer segmentation result in Figure 4.11 c) obtained from the intersection of the original image with the flood fill's binary output.

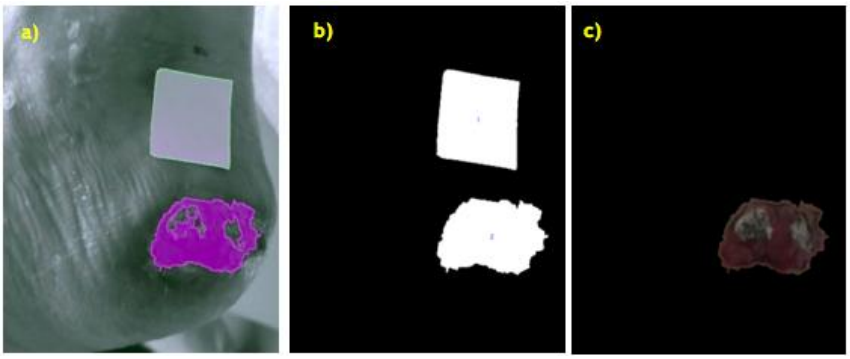

Figure 4.11- Segmentation process of the ulcer with white/yellow tissue using MATLAB a) Result of the implementation of the flood fill algorithm b) Binary image resultant of the filling holes and object labelling operations c) Final segmentation result.

The segmentation of ulcers with necrotic composition was also achieved with great efficacy as shown in Figure 4.12.

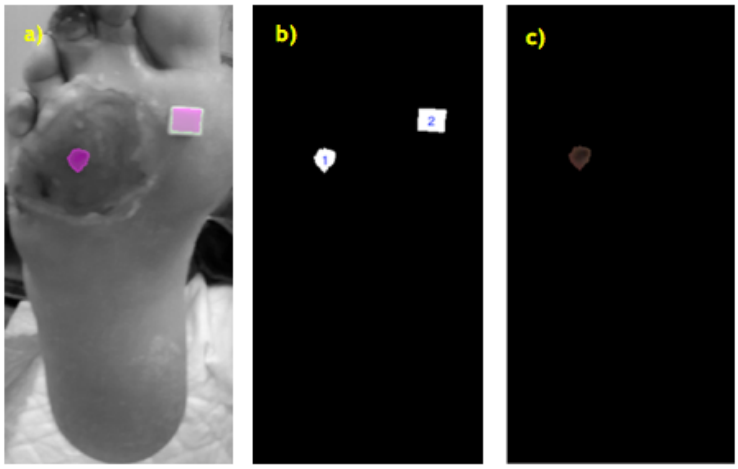

Figure 4.12- Segmentation process of the ulcer with necrotic tissue using MATLAB a) Result of the implementation of the flood fill algorithm b) Binary image resultant of the filling holes and object labelling operations c) Final segmentation result.

In Figure 4.13 a), the result of the segmentation of the mostly granulating wound is shown as well as the outcomes of the hole filling operation (Figure 4.13 b)) and the final result of the full segmentation of the CW (Figure 4.13 c)).

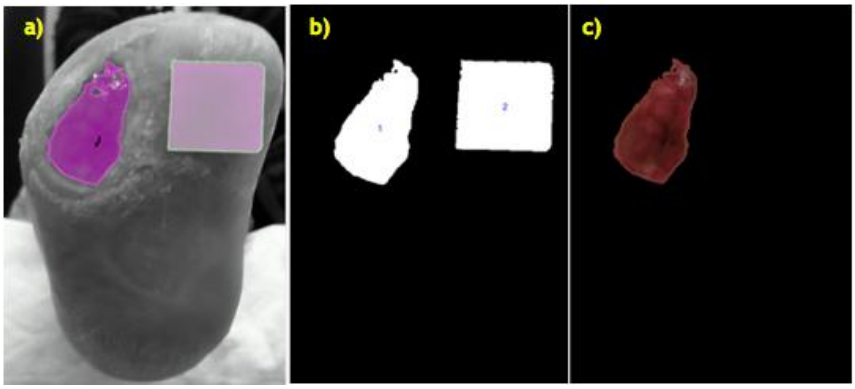

Figure 4.13- Segmentation process of ulcer with mostly granulating tissue using MATLAB a) Result of the implementation of the flood fill algorithm b) Binary image resultant of the filling holes and object labelling operations c) Final segmentation result.

- Unsuccessful cases

Cases where the ulcers were not successfully segmented by the flood fill algorithm were also found, being registered a 3% of failure, i.e., 6 of the 200 images with ulcers that constitute the dataset. These ulcers are shown in Figure 4.14.

Figure 4.14- Examples of ulcers that were not segmented by the flood fill.

4.3.3 -Tissue classification

Tissue classification was achieved through RGB histogram thresholding of the image obtained from the intersection of the flood fill result and the original image.

The results of the thresholdings applied are next displayed for the ulcer with white/yellow tissue. In the Figure 4.15 a) the representation of the tissue classified as necrotic is performed by the blue colour, the classification of the devitalised tissue or infection or visible anatomic structure is present in Figure 4.15 b) and granulating tissues (healthy and unhealthy) within the ulcer are shown both separately in Figure 4.15 c) and d), respectively. Finally, in the Figure 4.15 e), the combination of the ulcer segmentation image with the results of the tissue classification process is displayed.

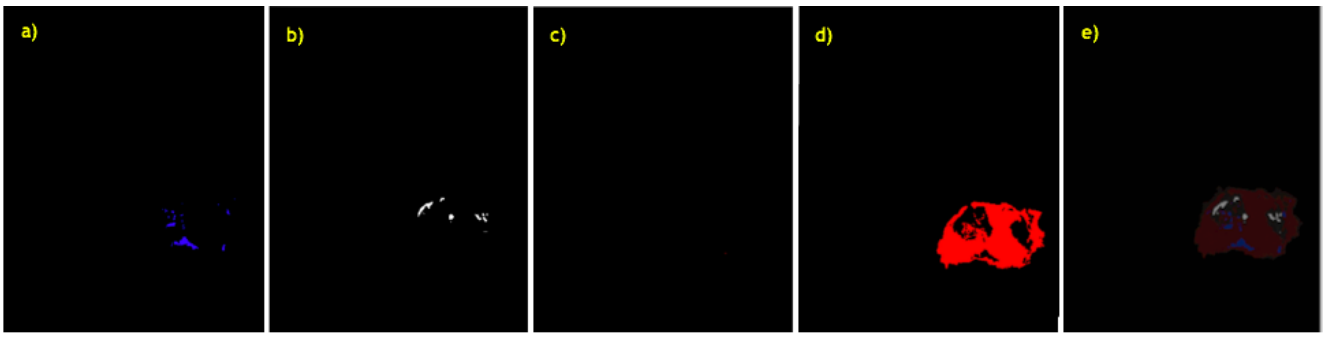

Figure 4.15- Tissue classification of the ulcer with white/yellow tissue using MATLAB a) Representation of the black pixels b) Representation of the white pixels c) Representation of the light red pixels d) Representation of the dark red pixels e) Tissue classification of wound.

The tissue classification's outcomes for the ulcer with granulating and necrotic tissues are presented in Figure 4.16 a) for the necrotic tissue, in the Figure 4.16 b) is shown the classification of the white/yellow tissue, the Figure 4.16 c) and d) represents the classification of healthy and un-

healthy granulating tissue and the Figure 4.16 e) combines all of the tissue characterisations, respectively.

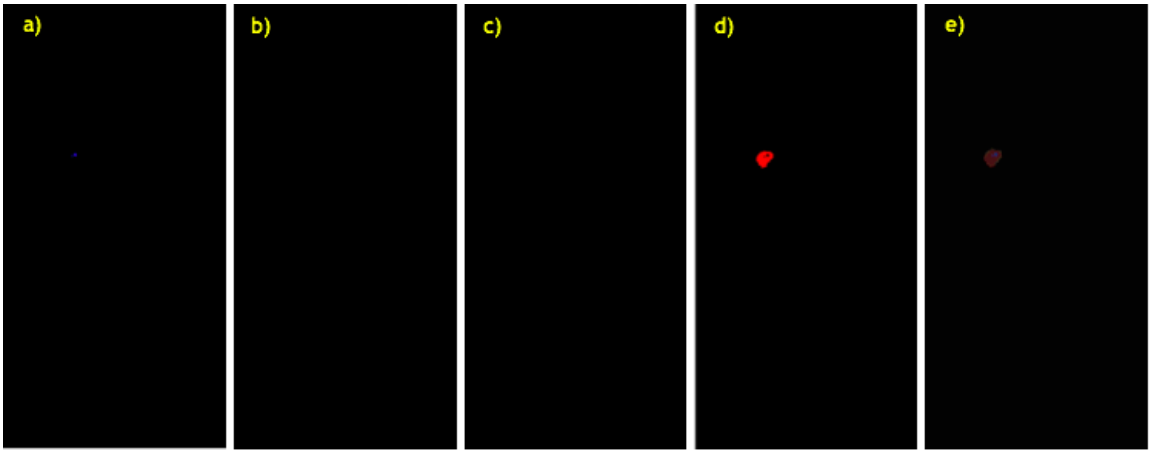

Figure 4.16- Tissue classification of the ulcer with necrotic tissue using MATLAB a) Representation of the black pixels b) Representation of the white pixels c) Representation of the light red pixels d) Representation of the dark red pixels e) Tissue classification of wound.

For the ulcer with mostly granulating tissue, the returned necrotic tissue classification is shown in Figure 4.17 a), the white pixels representative of the white/yellow tissue classification are presented in Figure 4.17 b), in the Figures 4.17 c) and d) the classification of the light and dark red pixels within the ulcer boundaries are displayed and in the Figure 4.17 e) the global tissue classification of the wound is presented.

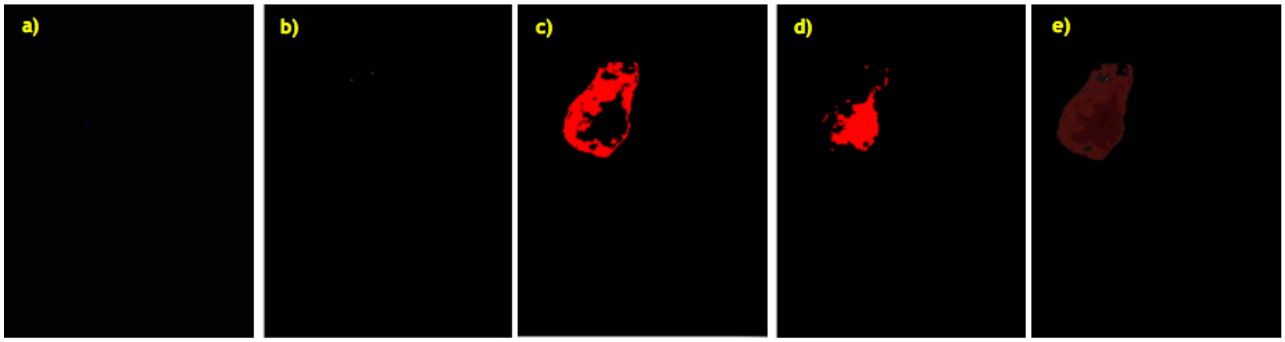

Figure 4.17- Tissue classification of the ulcer with mostly granulating tissue using MATLAB a) Representation of the black pixels b) Representation of the white pixels c) Representation of the light red pixels d) Representation of the dark red pixels e) Tissue classification of wound.

Analysing the Table 4.1, where the characterisation outputs are organised according to features, the characterisation of the ulcer with white tissue revealed that it has the biggest area (6.1 cm^2 or 0.95 $inches^2$) in comparison with the other two presented cases, for the ulcer manly composed by granulating tissue was obtained an area of 4.8 cm^2 (0.74 $inches^2$) and the ulcer with both granulating and necrotic tissues presented 0.57 cm^2 or 0.09 $inches^2$ of area.

Likewise, the tissue characterisation returned, for the ulcer representative of lesions with mainly granulating tissue, 33.30% of dark granulation tissue and 54.90% of light granulation tissue and percentages lower than 1% for both necrotic and white/yellow tissues. Similarly, for the ulcers with combination of granulating and necrotic and granulating and white/yellow tissues, it was found that the first case was classified has having 81.40% of dark granulating tissue, while the second re-

turned a percentage of 67.50% for the dark granulating tissue however, both presented 0% of healthy granulating tissue. Relatively to black tissue percentages, the ulcer with necrotic tissue returned the higher percentage of black pixels (8.60%) when compared with the ulcer with white/yellow tissue and the ulcer with granulating tissue (8.20% and 0.05%, respectively). From the three wounds, the one with lower percentage of white/yellow tissue is the ulcer with necrotic tissue (0.00%), followed by the ulcer with manly granulating tissue (0.51%) and the ulcer with combination of granulating and white/yellow tissues (2.00%).

Table 4.1- Results of the wound characterisation using MATLAB.

Properties	Ulcer with white/yellow tissue	Ulcer with necrotic tissue	Ulcer with granulating tissue
Ulcer area (cm^2)	6.10	0.57	4.80
Ulcer area ($inches^2$)	0.95	0.09	0.74
Percentage of dark red tissue	67.50	81.40	33.30
Percentage of light red tissue	0.00	0.00	54.90
Percentage of black tissue	8.20	8.60	0.05
Percentage of white/yellow tissue	2.00	0.00	0.51

4.4 - Android mobile application

4.4.1 -Pre-processing

Identical to the system of presenting the results of the MATLAB methodology, to investigate about the obtained outputs of the mobile application, three images are next shown to represent its performance on the most common diabetic foot ulcers types (mostly granulating, combination of granulating and necrotic and combination of granulating and white/yellow tissues).

The representative image of the ulcers with combination of granulating and white/yellow tissues (devitalised tissue, infection or with a visible anatomic structure), is shown in Figure 4.18 a) and the pre-processing outcomes of the histogram equalisation and the median filtering operations are presented in the Figures 4.18 b) and c), respectively.

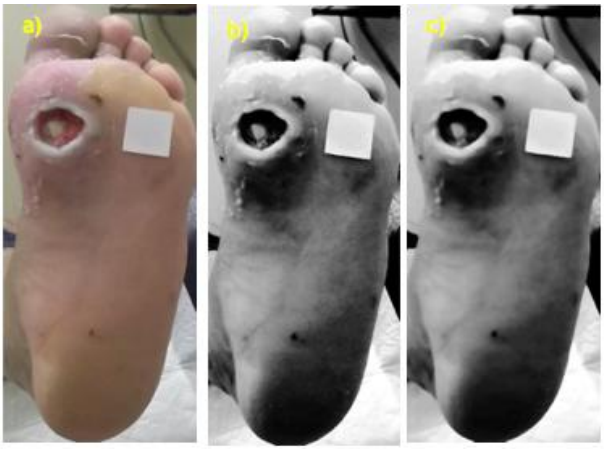

Figure 4.18- Pre-processing using the Android application of the ulcer with white/yellow tissue a) Original image b) Histogram equalisation c) Median filtering.

The original image of the ulcer with combination of granulating and necrotic tissues is shown in Figure 4.19 a), the result of the histogram equalisation appears on the Figure 4.19 b) and the median filter operation outcome is presented by Figure 4.19 c).

Figure 4.19- Pre-processing using the Android application of the ulcer with necrotic tissue a) Original image b) Histogram equalisation c) Median filtering.

Lastly, the outcomes of each phase of the image pre-processing step for the ulcer with mostly granulating tissue can be conferred in Figure 4.20.

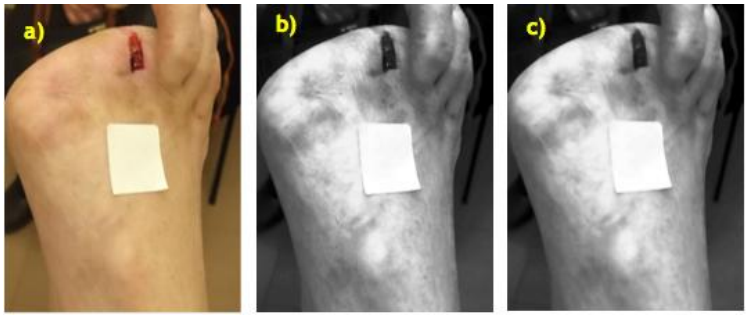

Figure 4.20- Pre-processing using the Android application of the ulcer with mostly granulating tissue a) Original image b) Histogram equalisation c) Median filtering.

4.4.2 -Ulcer segmentation

- Successful cases

In figure 4.21 a) is represented the result of the ulcer segmentation phase for the ulcer with white/yellow tissue using the Android application. The outcomes of the hole filling operation for the ulcer and the marker are presented in Figures 4.21 b) and c), respectively. The final result of the ulcer segmentation, given by the intersection of the hole filling operation with the original image can be seen in Figure 4.21 d).

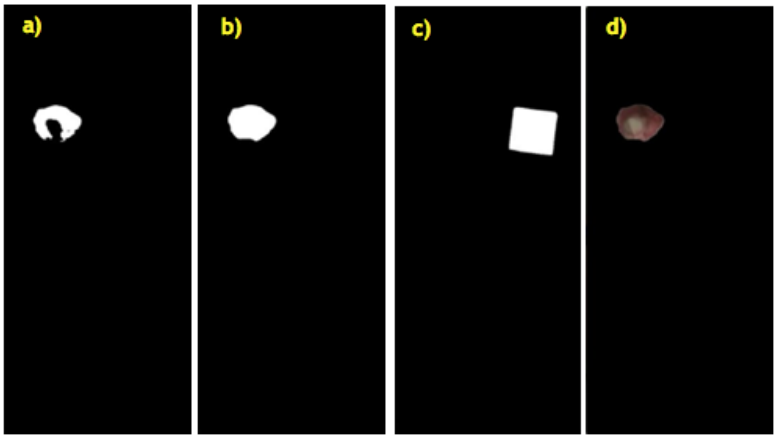

Figure 4.21- Segmentation process of the ulcer with white/yellow tissue using the Android application a) Binary ulcer image resultant of the implementation of the flood fill algorithm b) Binary image of the ulcer resultant of the closing operation c) Binary image of the marker resultant of the closing operation d) Final segmentation result.

The segmentation methodology performed on the ulcer with combination of granulating and necrotic tissues can be observed in the Figure 4.22.

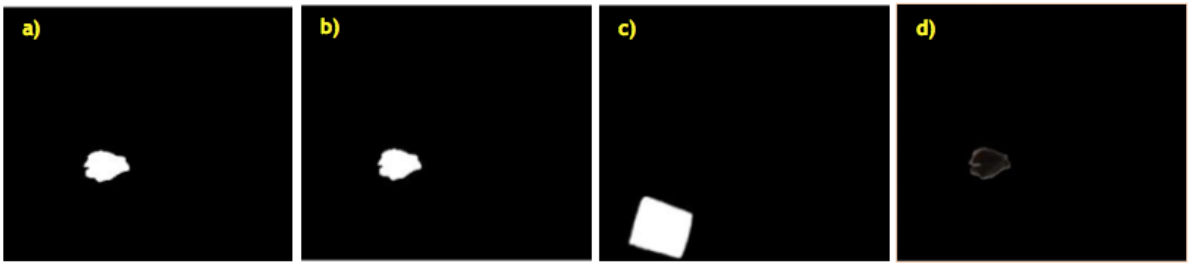

Figure 4.22- Segmentation process of the ulcer with necrotic tissue using the Android application a) Binary ulcer image resultant of the implementation of the flood fill algorithm b) Binary image of the ulcer resultant of the closing operation c) Binary image of the marker resultant of the closing operation d) Final segmentation result.

The first step of the ulcer segmentation methodology for the mostly granulating ulcer can be consulted in Figure 4.23 a), whereas the outcomes of the hole filling operation on the ulcer image as well as on the marker image are displayed in Figure 4.23 b) and c), respectively. In Figure 4.23 d), can be conferred the final result of the ulcer segmentation methodology.

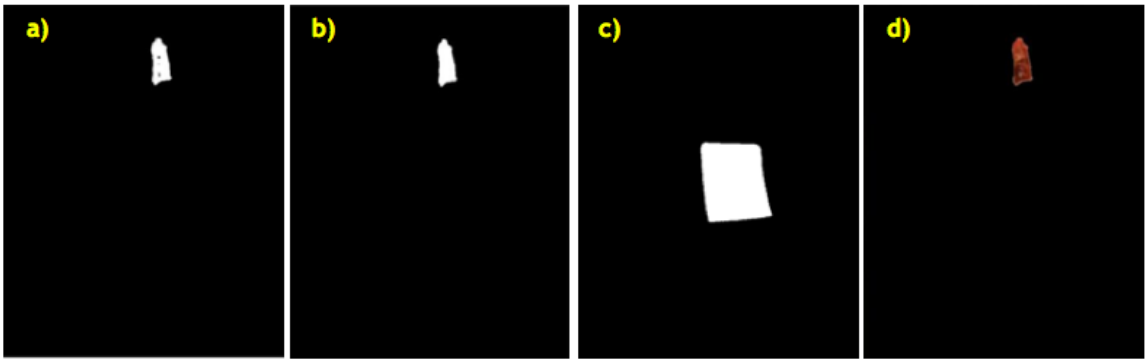

Figure 4.23- Segmentation process of the ulcer with mostly granulating tissue using the Android application a) Binary ulcer image resultant of the implementation of the flood fill algorithm b) Binary image of the ulcer resultant of the closing operation c) Binary image of the marker resultant of the closing operation d) Final segmentation result.

- Unsuccessful cases

During the segmentation phase was observed that the same 6 images (Figure 4.14) that were not segmented during the same step in the MATLAB methodology were not segmented by the Android application and thus, the same 3% of unsuccessful segmentation was achieved with the mobile application.

4.4.3 -Tissue classification

The tissue classification achieved with the RGB thresholding of the tissue composition of the ulcer with combination of granulating and white/yellow tissues, is shown in Figure 4.24.

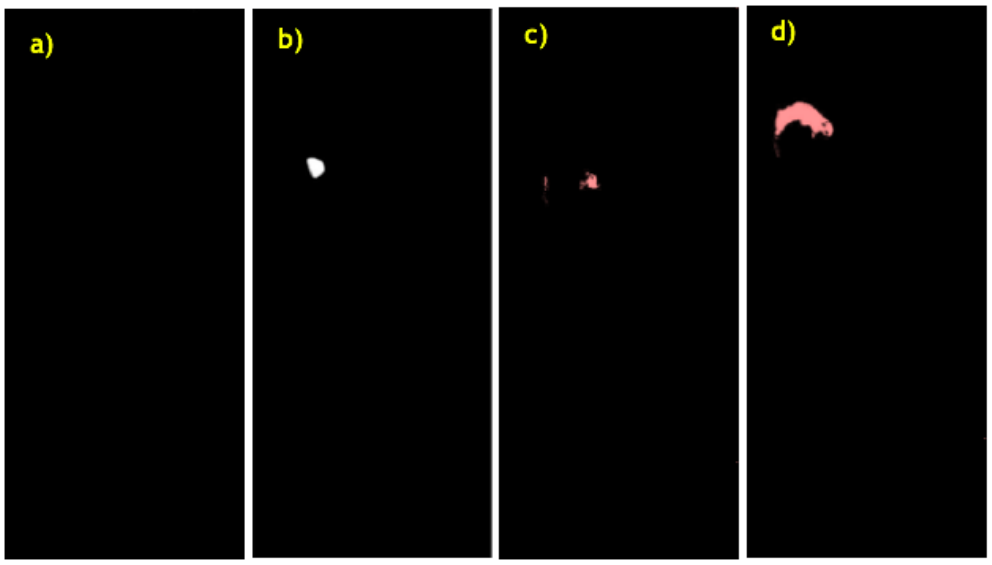

Figure 4.24- Tissue classification of the ulcer with white/yellow tissue using the Android application a) Representation of the black pixels b) Representation of the white pixels c) Representation of the light red pixels d) Representation of the dark red pixels.

The classification of the necrotic tissue of the ulcer with combination of granulating and necrotic tissues can be seen in Figure 4.25 a). The classification of the white/yellow, the healthy granulating and the unhealthy granulating tissues area shown in Figure 4.25 b), c) and d), respectively. Both Figure 4.25 b) and c) are all black due to no white/yellow and light red pixels found during the characterisation.

Figure 4.25- Tissue classification of the ulcer with necrotic tissue using the Android application a) Representation of the black pixels b) Representation of the white pixels c) Representation of the light red pixels d) Representation of the dark red pixels.

For the ulcer with mostly granulating tissue, the tissue classification approach returned no black tissue as shown by Figure 4.26 a) and a few white/yellow tissue (Figure 4.26 b)). The outcomes of the classification of the healthy and unhealthy granulating tissue are shown on the Figure 4.26 c) and d), respectively.

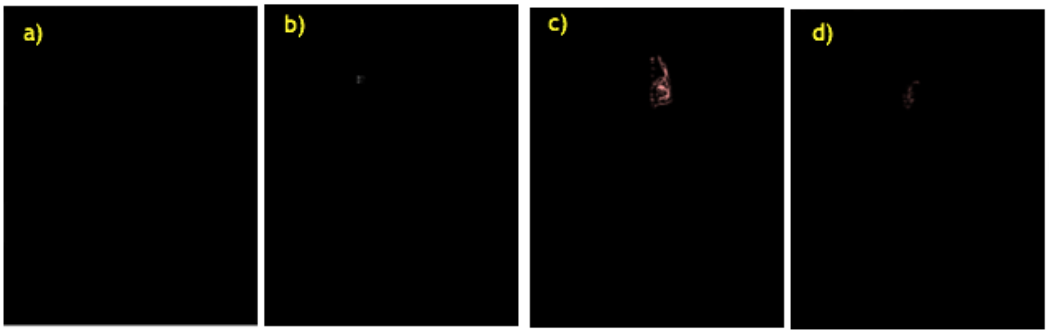

Figure 4.26- Tissue classification of the ulcer with mostly granulating tissue the Android application a) Representation of the black pixels b) Representation of the white pixels c) Representation of the light red pixels d) Representation of the dark red pixels.

At Table 4.2 there are reunited the outputs of the wound characterisation performed by the mobile application. From the area results, the ulcer with bigger squared area is the ulcer with granulating and white/yellow tissues with 4.51 cm^2 or 0.70 $inches^2$, followed by the ulcer with necrotic tissue with 2.86 cm^2 or 0.44 $inches^2$ and the smaller ulcer, classified as having an area of 0.80 cm^2 or 0.12 $inches^2$ was the ulcer with only granulating tissue.

From the achieved tissue percentages, the ulcer considered as mostly granulating presents the higher percentage of healthy granulating tissue (31.82%) relatively to the remaining ulcers (13.96% and 0% for the ulcer with white/yellow tissue and for the ulcer with necrotic tissue, respectively) and lower percentages of black (0%) and white/yellow tissue (3.10%) as well. Moreover, the tissue classification of the necrotic wound returned the highest percentage of necrotic tissue (45.04%) and the lowest healthy and white/yellow tissues percentage (0% for both) of all the three ulcers. The ulcer with combination of granulating and white/yellow tissues returned the highest percentage of white/yellow tissue (15.63%) and unhealthy granulating tissue (35.27%).

Table 4.2- Results of the wound characterisation using the mobile application.

Properties	Ulcer with white/yellow tissue	Ulcer with necrotic tissue	Ulcer with granulating tissue
Ulcer area (cm^2)	4.51	2.86	0.80
Ulcer area ($inches^2$)	0.70	0.44	0.12
Percentage of dark red tissue	35.27	35.04	16.50
Percentage of light red tissue	13.96	0.00	31.82
Percentage of black tissue	0.00	45.04	0.00
Percentage of white/yellow tissue	15.63	0.00	3.10

4.5 - Assessment evaluation

The performed clinical analysis by the 7 healthcare professionals of the Diabetic foot clinic at *Centro Hospitalar do Porto* regarding the mobile application performance returned, as shown in Figure 4.27, a median score of 4.30 relatively to the evaluation of the ulcer area measurements obtained. The performed ulcer tissue characterisation was evaluated with a mean score of 4. Higher scores were given by the healthcare professionals to the applicability of the application in clinical environment (4.71) as well as to its simplicity, ease and clarity during its usage (5).

Globally, an overall score of 4 out of 5 was given to the mobile application by the health professionals.

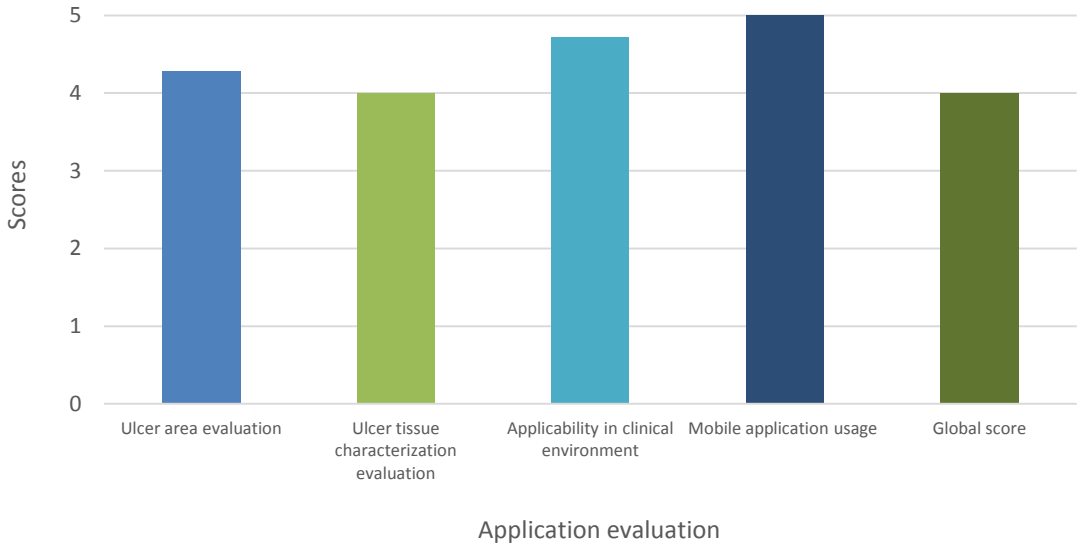

Figure 4.27- Healthcare professionals' evaluation of the mobile application (n=7).

When asked to compare their evaluation of the ulcers with the assessment performed by the MATLAB methodology and the mobile application, all of the results were classified as clinically acceptable and, as according to Figure 4.28, 71.43% of the healthcare professionals (i.e. 5) have chosen the Android application's results over the MATLAB methodology's.

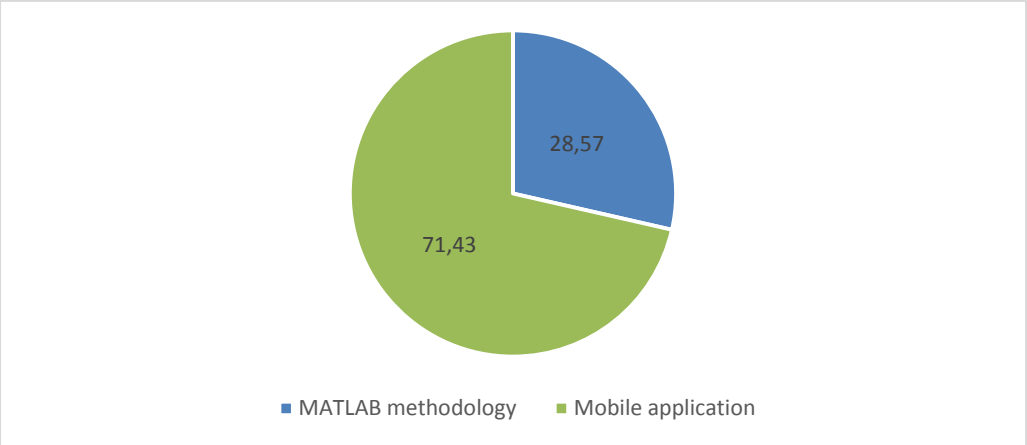

Figure 4.28- Healthcare professionals' opinion on the two methodologies (n=7).

The resemblance of the obtained results with both methodologies was evaluated and correlations higher than 0.95 were achieved:

Correlating the areas provided by both the MATLAB's methodology and the Android mobile application in cm^2 was obtained a 0.998 correlation between the results, as shown by Figure 4.29.

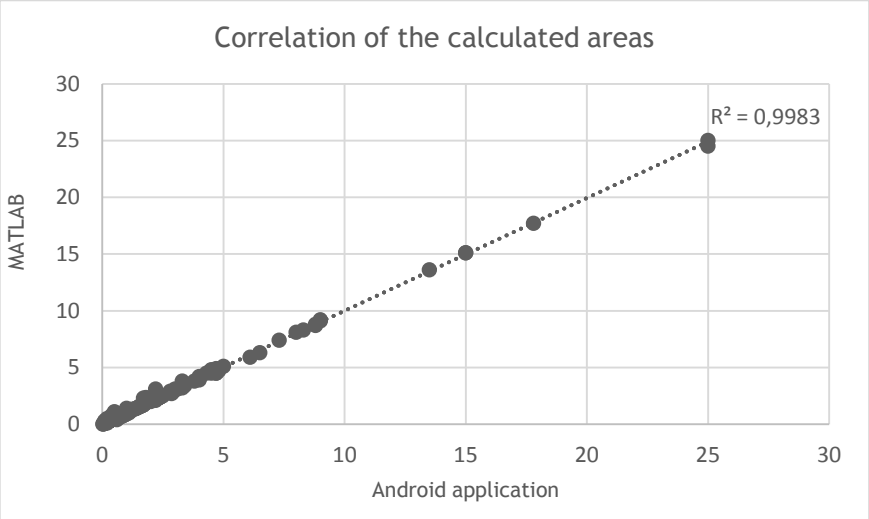

Figure 4.29- Correlation of the areas obtained with both methodologies.

Further, the correlation of the areas provided by the MATLAB methodology, the Android application and the healthcare professional's assessment gave a R^2 value of 0.999 for the Android application and 0.998 for the image processing methodology with MATLAB as it can be seen in Figure 4.30.

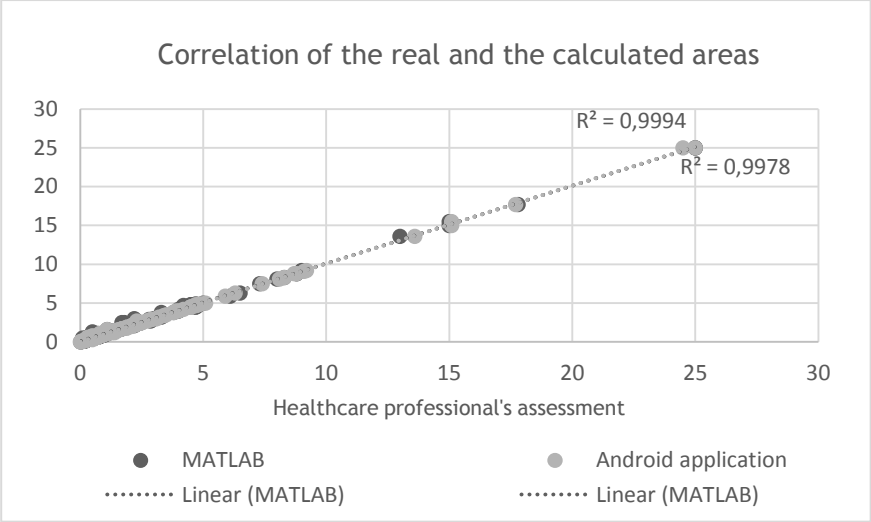

Figure 4.30- Correlation of the real area of the lesions provided by healthcare professionals and the areas obtained with both methodologies.

The correlation of the percentages of dark red tissue, i.e., unhealthy granulating tissue, of both methodologies revealed a 0.998 probability of relationship between the measurements as shown by Figure 4.31.

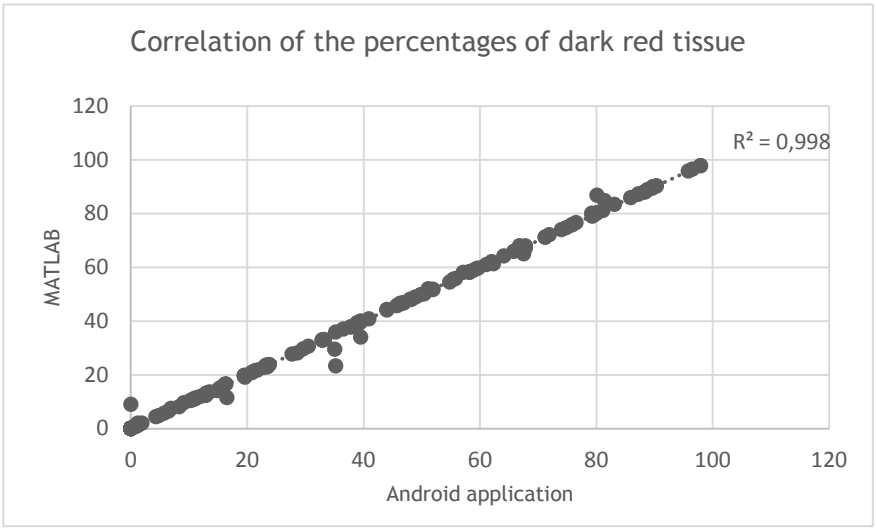

Figure 4.31- Correlation of the dark red tissue's percentages obtained with both methodologies.

The comparison of the percentages of light red tissue, i.e., healthy granulating tissue, of both methodologies (Figure 4.32) revealed a 0.961 probability of correlation between the measurements.

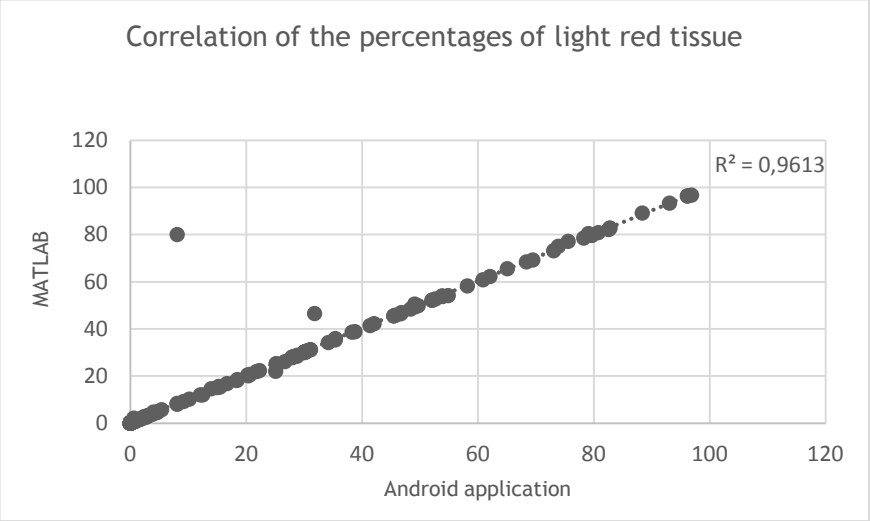

Figure 4.32- Correlation of the light red tissue's percentages obtained with both methodologies.

The statistical analysis performed between the percentages of necrotic tissue provided by both methodologies revealed a 0.995 probability of correlation between the measurements as it can be seen by Figure 4.33.

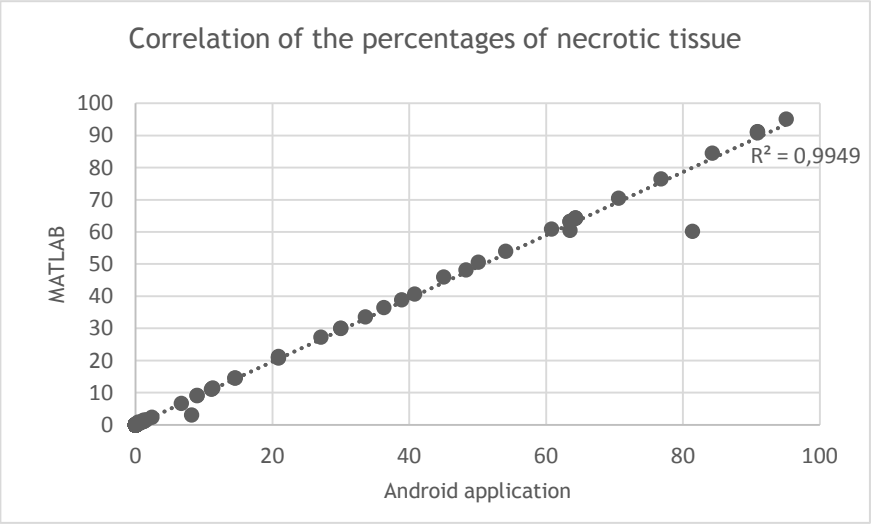

Figure 4.33- Correlation of the necrotic tissue's percentages obtained with both methodologies.

The last correlation calculated was performed by comparing the percentages of white tissue given by both the methodologies. A value of 0.998 of probability of correspondence between these measurements was found as shown in Figure 4.34.

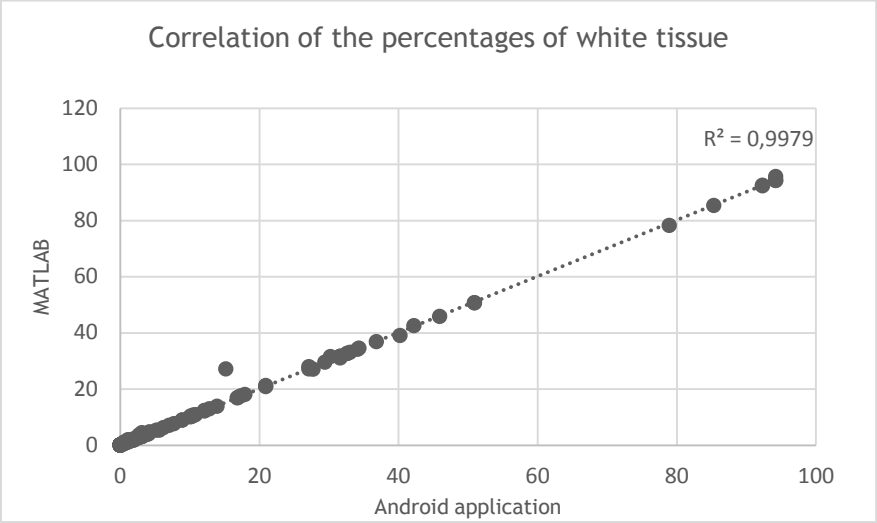

Figure 4.34- Correlation of the white tissue's percentages obtained with both methodologies.

4.6 - Summary

The results of the MATLAB and the Android mobile application methodologies were presented relatively to the performance of marker segmentation, pre-processing, ulcer segmentation and area calculation and tissue characterisation as well as the outcomes of the previously documented image processing techniques whose results were unsatisfactory.

The results reported the same percentage and cases of ulcer and marker segmentation failure for both methodologies.

The statistical analysis performed on the results obtained with both methodologies returned high probability of correlation between both methodologies, however, when the obtained area measurements were compared to the ones resultant from the clinical assessment, the mobile application achieved a slightly higher correlation than the MATLAB approach.

The image collection protocol, the addiction of a calibration marker during the image collection and the image processing approach designed and incorporated in both the MATLAB methodology and the Android mobile application resulted in a fully segmentation of 97% of the ulcers and 97.5% of the markers present in the 200 collected images.

According to the judgement of 7 healthcare professionals, the results were classified as clinically adequate and acceptable.

Moreover, the healthcare professionals' evaluation resulted in a preference of the results obtained with the Android mobile application.

Chapter 5

Discussion

In this section, the performance of the methodologies created during this project relatively to the initial objectives is discussed. First, some considerations are performed relatively to the features that affected the marker segmentation process and some improvements are recommended. Then, the ulcer segmentation performed by both methodologies is examined and considerations about its accuracy are presented. Further, conclusions about the implementation of the image processing techniques defined in subchapter "3.4- Unsuccessful image processing techniques" and why their employment did not achieve the most acceptable results can be consulted.

The ulcer area calculation and tissue characterisation is further evaluated during the section "5.4 - Assessment evaluation" where the results of these steps and their comparison with the healthcare professionals' assessment are performed. This chapter ends with a summary of the main conclusions of the discussion.

5.1 - Marker segmentation

For wound area calculation purposes, two experimental types of calibration markers were designed and implemented throughout image collection. During the image collection and processing, it was noticed that the choice of a disposable adhesive marker was a positive aspect since it allowed a fast image collection without disturbing the normal functioning of the clinic nor promoting wound contamination or discomfort to the patient. However, a few negative aspects regarding the markers' features were noticed:

- Colour

One of the many complications of Diabetes is vascular disease which, in some cases, can lead to a poorer irrigation of the lower extremities due to the absence of palpable arterial pulses causing an ischemic foot. Visually, poorer irrigation in the lower extremity results in whiter skin when the foot is elevated. During the image processing, it was verified that the choice of white markers caused that, in some cases where the patient had an aggravated ischemic foot, the segmentation of the marker represented a difficult task (Figure 4.1), being hard to distinguish which were the marker's pixels and the foot skin's pixels. This drawback could be attenuated by using another colour for the marker.

- Dimensionality

Comparing the 2-D 2.5 x 2.5 cm^2 marker with the 3-D 1.0 x 1.0 x 0.5 cm^2 marker was also noticed that the second one was more challenging to recognise in images. This can be explained by the fact that sometimes the surface of the 3D marker was omitted and/or appeared different in the collected images due to the angle of the image collection (Figure 4.2).

An erroneous segmentation of the marker leads, in this project, to a wrong ulcer area calculation and characterisation, therefore, 2D makers are more recommended for this task.

- Size

Globally, from the 200 collected images it can be concluded that the 2.5 x 2.5 cm^2 marker was sometimes too big to implement is certain sites once, besides all the efforts during the image capture, due to the intrinsic irregularities of a diabetic foot, were verified situations where the marker was not captured totally or its shape was changed in the image considering the best angle to capture the wound (Figure 4.3 a) b)).

Thus, for future reference, a smaller 2D square adhesive with maximum length and width of 2 cm would be a wiser solution.

5.2 - Unsuccessful image processing techniques

In the Methodology chapter image processing techniques were defined that due to the intrinsic complexity of the diabetic foot ulcers, did not succeed.

The application of the low pass Gaussian filter, besides reducing notoriously image noise, it also led to loss of edge information which is essential to obtain a good ulcer and maker segmentation.

Further processing after the Bottom hat and Top hat filtering shown that its contribution was not as notorious as expected in the segmentation step and "Shadowing" effects (Figure 4.4 c) right) were noticed namely in the marker possibly due to the size and type of structuring element used.

According to the formulae of SNR, images with low noise will have a higher SNR and, equally, the images with a higher level of noise will present a lower SNR. Therefore, the designed pre-processing methodology led to a reduction of noise and an enhancement of the image contrast, which resulted in the achievement of most satisfactory segmentation outcomes than the remaining techniques. This is supported by the results of SNR calculations, where the designed pre-processing methodology achieved a higher SNR ratio than the other techniques tested for the same purpose.

The results of the application of the Canny edge detector to segment the ulcers and the marker, due to the tissue and shape complexity of the lesions, made obvious that this method did not identi-

fied all of the wound's edges so, to successfully segment the lesion, a more tangled method had to be designed.

The CHT did not succeed returning substantial false positive cases of ulcer segmentation. This erroneous segmentation can be explained by analysing the output of the canny edge detector, used to create the binary input of the transform, where the ulcer edges information is not well defined, especially when the ulcer is located in the outlines of the foot. Moreover, the most returned result was the identification of the heel (when intact) of the patients' foot due to its intrinsic circularity. This method was very time consuming specially for extensive ulcers.

One of the attempts to automatically perform wound segmentation was made based on texture using Gabor filters. Despite of the first results being promising as shown in Figure 4.5 c), further processing and classification of the information did not lead to successful ulcer or maker segmentation, especially for bigger and more complex ulcers. Furthermore, during the testing of this approach, it was observed that it was very time consuming.

Although the Watershed method, for most of the cases, achieved good segmentation of the maker, it revealed poor capacity in segmenting the ulcer in the foot classifying it as being part of the same label as some of the healthy skin in the foot. Furthermore, tissue classification with this technique did not provide successful results relatively to the distinction of the two different granulating tissues.

With the Region growing approach, the majority of the tissue of the wound was segmented however, different tissues with different properties within the ulcer were not fully considered. Further, from the consecutive tests performed, it was observed that the results remained too dependent of the initial seed points and less than 6 starting pixels did not provide good results.

Active contour (Snakes) did not achieve great results since, for more irregular ulcers, the 200 iterations were not sufficient to segment the whole lesion (Figure 4.6 c) centre) and with the increasing of the number of iterations and the alpha and beta values adjustment to obtain more satisfactory results, the method became computationally very demanding and time consuming which is not desirable to incorporate in a mobile application. Was also observed that the results were too dependent on the inputs.

The segmentation achieved with the Active contour ('Chan-Vese' method) methodology was not perfect even for "simple" ulcers, providing irregular contours and for the "more complex" lesions, the algorithm revealed over segmentation returning more than one object for the ulcer segmentation (Figure 4.6 d) centre).

The use of the Fuzzy-c-means clustering technique did not provide a good segmentation of the ulcer since pixels within the ulcer were categorised as being in the same cluster as pixels of the image's background or as being in the same cluster as pixels belonging to healthy skin in the foot. Furthermore, this technique when applied to characterise the tissues within the ulcer bed, returned unsatisfactory results relatively to the differentiation between healthy and non-healthy granulating tissues.

5.3 - Ulcer segmentation

The implemented flood fill methodology showed better results than most of the other techniques tried as presented in the previous point, however, since it performs a search based on pixel "colour", due to the heterogeneity of tissue types and colours present in some ulcers, occasionally the first result of the segmentation phase was not ideal, especially when white (devitalised tissue or

visible anatomic structure) and yellow (pus) tissues are present within the ulcer bed. This weakness of the methodology, was overcome by means of a hole filling (methodology in MATLAB) or a morphological closing (methodology incorporated in the mobile application) operations which led to the fully segmentation of 97% of the 200 ulcers. The empirical selection of the 35 and 40 tolerances for the flood fill in the MATLAB methodology and the Android mobile application, respectively, provided the most successful ulcer and marker segmentation when compared to other tolerances tested for both the methodologies and to the clinical assessment (see Figure 4.10).

Cases where the ulcers where not successfully segmented by the flood fill algorithm were also found, which can be justified by the lack of colour difference between the tissues within the ulcer's bed and its boundaries/surrounding tissue or the lack of well-defined edges thus hindering the stopping condition of the flood fill algorithm.

5.4 - Assessment evaluation

The first evaluation of the methodologies created was performed by healthcare professionals. The results of both methodologies, ulcer area and tissue characterisation were classified as clinically acceptable however, and as expectable, the outcomes of the Android application were preferred over the MATLAB methodology ones by the majority of the professionals' due to some sub segmentation and sub tissue classification observed in the MATLAB methodology.

During the design and creation of the Android application an attempt of keeping it easy, simple, unequivocal to use and applicable in clinical environment was made. This was reinforced by the maximum classifications given by the health professionals to its simplicity and to its applicability in healthcare centres. Although globally, the Android application was classified as a "4" and complemented relatively to its helpful input in the health professionals assessment, the tissue characterisation performed achieved the lowest classification relatively to the other parameters evaluated, greatly because of the subjectivity associated to the clinical assessment, where was observed that some identified higher presence of unhealthy granulating tissue and white tissue when compared to other professionals and to what the mobile application returned.

The second evaluation of the achieved results was accomplished by performing a Pearson correlation analysis. Good correlation (higher than 0.95) was achieved by comparing the results of both methodologies as well as comparing them with the results provided by the healthcare professionals. However, the correlation between the ulcer areas acquired with the Android application and the areas provided by the health professionals achieved a higher correlation than with the areas obtained with the MATLAB methodology, which indicates a higher probability of relation between the real measurements and the outcomes of the mobile application.

5.5 - Summary

Wound assessment is a complex task that is predominantly performed by clinical observation and invasive assessment, being subjective and possibly leading to wound contamination and discomfort to the patient.

Wound characterisation was achieved in this project, by first developing a methodology in MATLAB divided in image acquisition, image pre-processing, ulcer segmentation, shape recognition, area calculation and tissue classification. This methodology served as a foundation for the creation of an image processing algorithm that was then incorporated in an Android application.

The two methodologies shown good correlation and although some unsuccessful cases of chronic wounds' segmentation were detected (3%), 7 healthcare professionals considered the outcomes of both of the methodologies clinically acceptable and the features provided, pertinent and helpful, being preferred the results obtained with the Android application over the ones provided by the MATLAB methodology. The handling of the mobile application demonstrated its simplicity and ease of use as well as the good applicability in clinical environment.

Chapter 6

Conclusion

Chronic wounds are a debilitating disease that directly affects patients and global economy. Image processing, in particular associated with mobile applications have been used as an alternative to accurately characterise ulcers easily, being non-invasive and observer independent, thus producing better diagnosis and follow up of the healing process of the ulcers.

During this project, an Android application incorporating a methodology that was able to characterise chronic ulcers relatively to its area and tissue colour was developed and assessed. This was a very complex task due to the impossibility of controlling some environmental variables (such as illumination, noise, patient movement, etc.).

The mobile application created allowed fully segmentation of 97% of the 200 ulcers analysed and presented good correlation when compared with the healthcare professionals' assessment, being fast (analysis process takes less than 2 minutes), easy and unequivocal to use, improving the quality of assistance, helping to identify and measure ulcer tissues, improving the follow up of the therapies, automating the clinical documentation, improving the communication and collaboration, easing the monitoring of new products, reducing the use of ineffective products and supports home care assistance and telemedicine, and thus leading to a considerable reduction of the associated costs with this health condition.

6.1 - Future work

For further work, the following suggestions would contribute to the enhancement of the current results:

- Test the mobile application in other chronic wounds.
- Incorporate more facilities to the mobile application as control of the glycaemic values, registration of medication and patients' personal data in order to follow up the healing process.
- Send the final characterisation report to the personal historic of the patient via email or to the healthcare software.
- Use a local and/or remote database to store all examinations and be able to evaluate treatments monitoring.
- Adopt a system of two simultaneous cameras, attached infrared camera, capturing an image of the wound to achieve 3/4-dimensional wound characterisation.

Appendix A – Ethical approval of the project by the *Centro Hospitalar do Porto*

centro hospitalar
do Porto

Hospital Santo António | Hospital Maria Pia | Maternidade Júlio Dinis | Hospital Joaquim Urbano

Largo Prof. Abel Salazar
4099-001 PORTO
www.hgsa.pt

Exma. Sra. Rita Frade

Aluna da Faculdade de Engenharia da UP

ASSUNTO: Trabalho Académico - Mestrado - **"Classificação automática de úlceras por imagem visual" - N/ REF.ª 2016.192(162-DEFI/151-CES)**

O Conselho de Administração do CHP **autoriza** a realização do estudo de investigação acima mencionado nesta Instituição, na Clínica do Pé Diabético, sendo Investigadora Principal a aluna Rita Frade.

O estudo de investigação foi previamente analisado pela Comissão de Ética para a Saúde, pelo Gabinete Coordenador de Investigação do Departamento de Ensino, Formação e Investigação do CHP, bem como pela Direção do Departamento de Ensino, Formação e Investigação, tendo obtido Parecer Favorável.

Cumprimentos,

CONSELHO DE ADMINISTRAÇÃO
04/04/14 14 JAN. 2017

Dr. PAULO BARBOSA — Presidente
Dr.ª ÉLIA GOMES — Vogal Executiva
Prof. Doutor JOSÉ BARROS — Diretor Clínico
Dr. RUI PEDROSO — Vogal Executivo
Enf.º EDUARDO ALVES — Enfermeiro Diretor

* Em todas as eventuais comunicações posteriores sobre este estudo é indispensável indicar a nossa ref.ª.

centro hospitalar do Porto

Hospital de Santo António · Maternidade Júlio Dinis · Hospital Maria Pia

Largo Professor Abel Salazar
4099-001 PORTO
www.hgsa.pt

APRECIAÇÃO E PARECER PARA A REALIZAÇÃO DE **TRABALHO ACADÉMICO – MESTRADO**

Título: **"Classificação automática de úlceras por imagem visual"**		Ref.ª: **2016.192(162-DEFI/151-CES)**
		Investigador: **Rita Frade** **Aluna da Faculdade de Engenharia da UP**

DIREÇÃO DE ENFERMAGEM:	**PRESIDENTE DO CONSELHO DE ADMINISTRAÇÃO:**
☐ **PARECER FAVORÁVEL**	☒ **PARECER FAVORÁVEL**
☐ **PARECER NÃO FAVORÁVEL**	☐ **PARECER NÃO FAVORÁVEL**
Data:	Data: 03/07/017 **DR. PAULO BARBOSA** Presidente do Conselho de Administração do CHP

Em conformidade, Pode ser autorizado
Prof.ª Doutora Luísa Lobato
Diretora do DEFI

Prof.ª Doutora Luísa Lobato
Diretora do DEFI

centro hospitalar
do Porto

Hospital de Santo António Maternidade Júlio Dinis Hospital Maria Pia

Largo Professor Abel Salazar
4099-001 PORTO
www.hgsa.pt

COMISSÃO DE ÉTICA PARA A SAÚDE

APRECIAÇÃO E VOTAÇÃO DO PARECER

Deliberação	Data: 14.12.2016	Órgão: Reunião Plenária

Título: **"Classificação automática de úlceras por imagem visual"**		Ref.ª: **2016.192(162-DEFI/151-CES)**
Protocolo/Versão: **TA - Mestrado**	Promotor: **o(a) próprio(a)**	Investigador: **Rita Frade** **Aluna do 2º Ano do Mestrado em Engenharia Biomédica da FEUP**

A Comissão de Ética para a Saúde – CES do CHP, ao abrigo do disposto no Decreto-Lei n.º 97/95, de 10 de Maio, em reunião realizada nesta data, apreciou a fundamentação do relator sobre o pedido de parecer para a realização de **TA - Mestrado** acima referenciado:

Ouvido o Relator, o processo foi votado pelos Membros da CES presentes:

Presidente: Dr.ª Luisa Bernardo
Vice-Presidente: Dr.ª Paulina Aguiar

Dr.ª Fernanda Manuela, Enf.ª Paula Duarte, Prof.ª Doutora Carla Teixeira, Prof.ª Doutora Maria Manuel Araújo Jorge, Dr. Gonçalo Senhorães Senra.
Resultado da votação:

PARECER FAVORÁVEL

Parecer Favorável

A deliberação foi aprovada por unanimidade.

Pelo que se submete à consideração superior.

3/11/16
DR. SEVERO TORRES

Data 14.12.2016

A Presidente da CES

Dr.ª Luisa Bernardo

Imp. 10/2009

Appendix B- Informed consent

TERMO DE CONSENTIMENTO INFORMADO

Título do estudo de investigação: Classificação automática de úlceras por imagem visual

Eu, abaixo-assinado _____, fui informado de que o Estudo de Investigação acima mencionado se destina a caracterizar automaticamente a úlcera.

Sei que neste estudo está prevista a realização de recolha de imagem visual e dados demográficos tendo-me sido explicado em que consistem.
Foi-me garantido que todos os dados relativos à identificação dos Participantes neste estudo são confidenciais e que será mantido o anonimato.
Sei que posso recusar-me a autorizar a participação ou interromper a qualquer momento a participação no estudo, sem nenhum tipo de penalização por este facto.
Compreendi a informação que me foi dada, tive oportunidade de fazer perguntas e as minhas dúvidas foram esclarecidas.
Aceito participar de livre vontade no estudo acima mencionado ou Autorizo de livre vontade a participação daquele que legalmente represento no estudo acima mencionado.
Também autorizo a divulgação dos resultados obtidos no meio científico, garantindo o anonimato.

Nome do Participante no estudo	Data
_____	____/____/_____

Nome do Investigador Responsável	Data
_____	____/____/_____

Appendix C- Questionaire

U.PORTO FEUP FACULDADE DE ENGENHARIA UNIVERSIDADE DO PORTO

DEFI centro hospitalar do Porto DEPARTAMENTO DE ENSINO, FORMAÇÃO E INVESTIGAÇÃO

Classificação automática de úlceras por imagem visual

Data de realização do inquérito: _____/_____/_____

Género: ☐ Masculino ☐ Feminino

Idade: ___ (anos)

1. **Tipo de diabetes:**

☐ Diabetes tipo I ☐ Diabetes tipo 2 (☐ Insulino-tratado ☐ Não Insulino-tratado)

2. **Tipo de pé diabético:**

☐ Pé neuropático ☐ Pé neuroisquémico ☐ Pé isquémico

3. **Realiza hemodiálise:**

☐ Sim ☐ Não

4. **Local da lesão:**

Appendix D- Image collection protocol

U.PORTO
FEUP FACULDADE DE ENGENHARIA UNIVERSIDADE DO PORTO

DEFI centro hospitalar do Porto
DEPARTAMENTO DE ENSINO, FORMAÇÃO E INVESTIGAÇÃO

CLASSIFICAÇÃO AUTOMÁTICA DE ÚLCERAS POR IMAGEM VISUAL

PROTOCOLO DE CAPTURA

1. Equipamento necessário

- O equipamento necessário para a recolha de dados será:
- Camara digital standard;
- Objeto padronizado (com a função de escala visual);

2. Captura de imagens

Aquando da captura das imagens visuais o investigador principal manter-se-á com a camara a uma distância de 0,7 metros (mínima) a 1 metro (máxima) encontrando-se esta paralela à localização da úlcera.

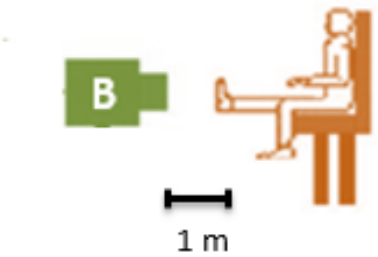

Figure 1 - Esquema do Sistema de captura das imagens das ulceras no ambiente controlado. B é a camara digital standard.

Appendix E- Wound characterisation protocol

CLASSIFICAÇÃO AUTOMÁTICA DE ÚLCERAS POR IMAGEM VISUAL

PROTOCOLO DE CARACTERIZAÇÃO

A classificação das úlceras é feita com base na conjugação dos seguintes parâmetros:

- Tamanho da úlcera
- Profundidade da úlcera
- Contornos
- Loca
- Tipo de tecido necrosado
- Quantidade de tecido necrosado
- Tipo de exsudado
- Quantidade de exsudado
- Cor da pele circundante da ferida
- Edema de tecido periférico
- Indução tecidular periférica
- Tecido de granulação
- Epitelização

Appendix F- Mobile application clinical evaluation

Após ter manuseado a aplicação criada no âmbito da dissertação "Caracterização automática de úlceras por imagem visual" para obtenção do grau Mestre em Engenharia Biomédica pela Faculdade de Engenharia, Universidade do Porto, que visa fornecer um método prático e fidedigno para caracterizar úlceras crónicas, pede-se que preencha o seguinte questionário anónimo colocando um **X** na coluna da tabela correspondente à pontuação que considera mais correta para cada uma das afirmações apresentadas. **(1 representa "Muito mau" e 5 representa "Muito Bom").**

Obrigada pela colaboração.

	1	2	3	4	5
Relativamente aos resultados obtidos durante a utilização da aplicação:					
Como avalia a área da lesão mostrada.					
Como avalia a caracterização tecidular obtida.					
Relativamente ao uso desta aplicação:					
A aplicação é aplicável em meio clinico.					
O seu uso é simples, fácil e inequívoco.					
Pontuação global.					

Data de preenchimento: ____/___/___.

References

+Wounddesk. (2011). Mobile enhanced Wound Management. Retrieved November 2, 2016, from https://wounddesk.com/.

Adobe (1991). Adobe. Retrieved May 14, 2017, from https://acrobat.adobe.com.

Agrawal, K., & Chauhan, N. (2012). Pressure ulcers: Back to the basics. *Indian J Plast Surg*, 45(2), 244-254.

Ahn, C., & Salcido, R.S. (2008). Advances in wound photography and assessment methods. *Adv Skin Wound Care*, 21(2), 85–93.

Anderson, K., & Hamm, R. L. (2012). Factors That Impair Wound Healing. *J Am Coll Clin Wound Spec*, 4(4), 84–91.

Apelqvist, J., Larsson, J., & Agardh, C.D. (1993). Long-term prognosis for diabetic patients with foot ulcers. *J Intern Med*, 233(6), 485–491.

Ballerini L., Li X., Fisher R.B., & Rees J. (2010). *A Query-by-Example Content-Based Image Retrieval System of Non-melanoma Skin Lesions*. In: Caputo B., Müller H., Syeda-Mahmood T., Duncan J.S., Wang F., Kalpathy-Cramer J. (eds) *Medical Content-Based Retrieval for Clinical Decision Support*. MCBR-CDS 2009. Lecture Notes in Computer Science, 5853. Berlin, Heidelberg: Springer.

BaranoskI, S., & Ayello, E. (2004). *O essencial sobre o tratamento de feridas: Princípios práticos*. Trad. João Gouveia. Loures: Lusodidata.

Barone, S., Paoli, A., & Razionale, A.V. (2011). Assessment of chronic wounds by three-dimensional optical imaging based on integrating geometrical, chromatic and thermal data. *Proc IMechE, Part H: J Eng Med*, 225(2), 181–193.

Bayat, A., McGrouther, D.A., & Ferguson, M.W. (2003). Skin Scarring. *BMJ*, 326(7380), 88-92.

Beausang, E., Floyd, H., Dunn, K.W., Orton, C.I., & Ferguson, M.W. (1998). A new quantitative scale for clinical scar assessment. *Plast Reconstr Surg*, 102(6), 1954–1961.

Beeckman, D., Schoonhoven, L., Fletcher, J., Furtado, K., Gunningberg, L., Heyman, H., & Defloor, T. (2007). EPUAP classification system for pressure ulcers: european reliability study. *J Adv Nurs*, 60(6), 682-91.

Belem, B. (2004). Non-invasive wound assessment by image analysis. PhD thesis, University of Glamorgan, Wales, U.K.

Bell, J. (2005). Are pressure ulcer grading and risk assessment tools useful? *Wounds*, 1(2), 62-69.

Benbow, M. (2006). Guidelines for the prevention and treatment of pressure ulcers. *Nurs Stand*, 20(52), 42–44.

Benotmane, A., Mohammedi, F., Ayad, F., Kadi, K., & Azzouz, A. (2000). Diabetic foot lesions: etiologic and prognostic factors. *Diabetes Metab*, 26(2), 113–117.

Berardesca, E., Elsner, P., & Wilhelm, K.P., Maibach, H.I. (1995). *Bioengineering of the skin: methods and instrumentation*. Boca Raton, FL: CRC Press.

Berendt, A.R. (2006). Counterpoint: hyperbaric oxygen for diabetic foot wounds is not effective. *Clin Infect Dis*, 43(2), 193-198.

Bergstrom, N., Braden, B.J., Laguzza, A., & Holman, V. (1987). The Braden Scale for Predicting Pressure Sore Risk. *Nurs Res*, 36(4), 205-210.

Berlowitz, D.R., Brandeis, G.H., Anderson, J., & Brand, H.K. (1997). Predictors of pressure ulcer healing among long-term care residents. *J Am Geriatr Soc*, 45(1), 30–34.

Berriss, W.P., & Sangwine, S.J. (1997). A colour histogram clustering technique for tissue analysis of healing skin wounds. *IET Conference Proceedings*, 443(1), 693-697.

Bick, D., & Stephens, F. (2004). *Pressure ulcer risk assessment and prevention: report of a national audit pilot project*. London: Royal College of Nursing.

Boateng, J.S., Matthews, K.H., Stevens, H.N., & Eccleston, G.M. (2008). Wound healing dressings and drug delivery systems: a review. *J Pharm Sci*, 97(8), 2892-2923.

Bolton, L. (2007). Which pressure ulcer risk assessment scales are valid for use in the clinical setting? *J Wound Ostomy Continence Nurs*, 34(4), 368–381.

Bose, K. (1979). A surgical approach for the infected diabetic foot. *Int Orthops*, 3(3), 177–181.

Boulton, A.J., Vileikyte, L., Ragnarson-Tennvall, G., & Apelqvist, J. (2005). The global burden of diabetic foot disease. *Lancet*, 366(9498), 1719–1724.

Bowling, F. L., King, L., Paterson, J. A., & Boulton, A. J. (2011). Remote assessment of diabetic foot ulcers using a novel wound imaging system. *Wound Repair Regen*, 19(1), 25-30.

Brusselaers, N., Pirayesh, A., Hoeksema, H., Verbelen, J., Blot, S., & Monstrey, S. (2010). Burn Scar Assessment: A Systematic Review of Different Scar Scales. *J Surg Res*, 164(1), 115–123.

Buchón-Moragues, F., Bravo, J.M, Ferri, M., Redondo, J., & Sánchez-Pérez, J. V. (2016). Application of Structured Light System Technique for Authentication of Wooden Panel Paintings. *Sensors*, 16(6), 881.

Buck, D.W., & Galiano, R. D. (2013). Plastic surgery, Part I - Principles, techniques, and basic science. Chapter 3 Wound Care. Retrieved February 17, 2017, from http://doctorlib.info/surgery/plastic/3.html.

Bulstrode, C. J., Goode, A.W., & Scott P.J. (1986). Stereophotogrammetry for measuring rates of cutaneous healing: a comparison with conventional techniques. *Clin Sci*, 71(4), 437-443.

Callam, M.J., Harper, D.R., Dale, J.J., & Ruckley, C.V. (1987a). Arterial disease in chronic leg ulceration: an underestimated hazard? Lothian and Forth Valley leg ulcer study. *Br Med J (Clin Res Ed)*, 294(6577), 929–931.

Callam, M.J., Ruckley, C.V., Dale, J.J., & Harper, D.R. (1987b). Hazards of compression treatment of the leg: an estimate from Scottish surgeons. *Br Med J (Clin Res Ed)*, 295(6610), 1382-1428.

Callieri, M., Cignoni, P., Pingi, P., Scopigno, R., Coluccia, M., Gaggio, G., & Romanelli, M. N. (2003, November). Derma: monitoring the evolution of skin lesions with a 3D system. In *VMV*, 167-174, Germany, Munich, November 19–21.

Capobianco, M.L., & McDonald, D.P. (1996). Factors affecting the predictive validity of the Braden Scale. *Adv Wound Care*, 9(6), 32–36.

Cheng, S., Chan, A., Fong, S., Lam, M., Leung, A., Lee, P., & Wu, A. (1996). Outcome studies for burn patients in Hong Kong: Patients' satisfaction. *Burns,* 22(8):623-626.

Clare, M.P., Fitzgibbons, T.C., McMullen, S.T., Stice, R.C., Hayes, D.F., & Henkel, L. (2002). Experience with the vacuum assisted closure negative pressure technique in the treatment of non-healing diabetic and dysvascular wounds. *Foot Ankle Int*, 23(10), 896–901.

Clark, M., & Farrar, S. (1992). *Comparison of pressure sore risk calculators*. In: Harding, K.G., Leaper, D.L., Turner, T.D. (eds), Proceedings of the First International Conferences of Advances in Wound Management. London: Macmillan, 158–161.

Collier, M. (2003). The elements of wound assessment. 99(13), 48. Retrieved January 1, 2017, from https://www.nursingtimes.net/clinical-archive/wound-care/the-elements-of-wound-assessment/205546.article.

Cronje, F.J. (2005). Oxygen therapy and wound healing—topical oxygen is not hyberbaric oxygen therapy. *S Afr Med J*, 95(11), 840.

Crowe, J.M., Simpson, K., Johnson, W., & Allen, J. (1998). Reliability of photographic analysis in determining change in scar appearance. *J Burn Care Rehabil*, 19(2), 183-186.

Cuddigan, J. (1997). Pressure ulcer classification: What do we have? What do we need? *Adv Wound Care*, 10(5), 13-15.

Cullum, N., Nelson, E.A., Fletcher, A.W., & Sheldon, T.A. (2001). Compression bandages and stockings for venous leg ulcers. *Cochrane Database Syst Rev*, (2), CD000265.

Cuzzel, L J. Z. (1988). The New RYB Color Code. *Am J Nurs*, 88(10), 1342-1346.

Daley, B. J. (2017). Wound Care Treatment & Management: Medical Care, Surgical Care, Future and Controversies. Retrieved February May 13, 2017, from http://emedicine.medscape.com/article/194018-treatment.

Dargaville, T. R., Farrugia, B.L., Broadbent, J.A., Pace, S., Upton, Z., & Voelcker, N.H. (2013). Sensors and imaging for wound healing: A review. *Biosens Bioelectron*, 41(0), 30-42.

Daugman, J.G. (1985). Uncertainty Relation for Resolution in Space, Spatial-Frequency, and Orientation Optimized by two-dimensional Visual Cortical Filters. *J Opt Soc Am*, 2(7), 1160-1169.

Dealey, C. (1994). *The Care of Wounds*. Oxford, Boston: Blackwell Scientific Publications (1st Ed).

Defloor, T., Schoonhoven, L., Clark, M., Halfens, R., & Nixon, J. (2001). A draft EPUAP position statement on risk assessment in pressure ulcer prevention and management. *EPUAP Review*, 3(2), 46–52.

DGS (1997). Direcção Geral de Saúde. Retrieved June 20, 2017, from https://www.dgs.pt/.

DiPietro, L.A., Burdick, M., Low, Q. E., Kunkel, S. L., & Strieteri, R. M. (1998). MIP-1alpha as a critical macrophage chemoattractant in murine wound repair. *J Clin Invest*, 101(8), 1693–1698.

Dorileo, E. A. G., Frade, M. A. C., & Rangayyan, R. M. (2010). Segmentation and analysis of the tissue composition of dermatological ulcers. Proceedings of the Symposium of the IEEE Canadian Conference on Electrical and Computer Engineering, 1, 1–4, Calgary, Canada, May.

Draaijers, L.J., Tempelman, F.R., & Botman, Y.A. (2004). The patient and observer scar assessment scale: A reliable and feasible tool for scar evaluation. *Plast Reconstr Surg*, 113(7), 1966-7.

Edgepark Surgical, (2005). *Catalog*. Ohio, Twinsburg.

Edmonds, M.E., Roberts, V.C., & Watkins, P.J. (1982). Blood flow in the diabetic neuropathic foot. *Diabetologica*, 22(1), 9–15.

Edwards, M., (1995). The levels of reliability and validity of the Waterlow pressure sore risk calculator. *J Wound Care*, 4(8), 373-378.

European Pressure Ulcer Advisory Panel, (2003). The EPUAP Guide to Pressure Ulcer Grading. Retrieved April 21, 2016, from http://www.epuap. org/grading.html.

European Pressure Ulcer Advisory Panel, (1999). Guidelines on treatment of pressure ulcers. *EPUAP Review*, 1(2), 31–33.

Falanga, V. (2005). Wound healing and its impairment in the diabetic foot. *Lancet*, 366(9498), 1736–1743.

Falanga, V., & Sabolinski, M. (1999). A bilayered living skin construct (Apligraf) accelerates complete closure of hard-to-heal venous ulcers. *Wound Repair Regen*, 7(4), 201–207.

Fearmonti, R., Bond, J., & Erdmann, D. (2010). A Review of Scar Scales and Scar Measuring Devices. *Eplasty*, 10, e43.

Ferrell, B.A., Josephson, K., Norvid, P., & Alcorn, H. (2000). Pressure ulcers among patients admitted to home care. *J Am Geriatr Soc*, 48(9), 1042–1047.

Flanagan, M. (1993). Pressure sore risk assessment scales. *J Wound Care*, 2(3), 162–167.

Flanagan, M. (1997). Choosing pressure sore risk assessment tools. *Professional Nurse Supplement*, 12(6), 3–7.

Flanagan, M. (2003). Wound Measurement: can it help us to monitor progression to healing? *J Wound Care*, 12(5), 189-194.

Fletcher, A., Cullum, N., & Sheldon, T.A. (1997). A systematic review of compression treatment for venous leg ulcers. *BMJ*, 315(7108), 576–580.

Friesen, M. R., Hamel, C., & McLeod, R. D. (2013). A mHealth application for chronic wound care: Findings of a user trial. *Int J Environ Res Public Health*, 10(11), 6199–6214.

Frykberg, R.G. (1991). *The High Risk Foot in Diabetes Mellitus*, New York, NY: Churchill Livingstone.

Fung, Y. C. (2001). A proposal to the National science Foundation for An Engineering Research Centre at USCD. *Center for the Engineering of Living Tissues. UCSD, 865023*, 2001.

Galushka, M., Zheng, H., Patterson, D., & Bradley, L. (2005). Case-based tissue classification for monitoring leg ulcer healing. In 18th IEEE Symposium on Computer-Based Medical Systems. *IEEE*, 353-358, Ireland, Dublin, June 23-24.

Gardner, S., Frantz, R., Bergquist, S., & Shin, C. (2005). A prospective study of the pressure ulcer scale for healing. *J Gerontol A Biol Sci Med Sci*, 60(1), 93-97.

Gelfand, J.M., Hoffstad, O., & Margolis, D.J. (2002). Surrogate endpoints for the treatment of venous leg ulcers. *J Invest Dermatol*, 119(6), 1420–1425.

Gentzkow, G.D., Iwasaki, S.D., Hershon, K.S., Mengel, M., Prendergast, J.J., Ricotta, J.J. et al. (1996). Use of dermagraft, a cultured human dermis, to treat diabetic foot ulcers. *Diabetes Care*, 19(4), 350–354.

Goldman, R.J., & Salcido, R. (2002). More than one way to measure a wound: an overview of tools and techniques. *Adv Skin Wound Care*, 15(5), 236-243.

Gonzalez, R. C., & Woods, R. E. (2002). *Digital Image Processing*. Upper Saddle River, NJ: Prentice Hall (2nd Ed).

Gonzalez, R. C., Woods, R. E., & Eddins, S. L. (2004). *Digital Image Processing Using MATLAB*. Upper Saddle River, NJ: Pearson Education (2nd Ed).

Griffin, J.W., Tolley, E.A., Tooms, R.E., Reyes, R.A., & Clifft, J.K. (1993). A comparison of photographic and transparency-based methods for measuring wound surface area. *Phys Ther*, 73(2), 117-122.

Harrist, T.J., et al. (1999). *The skin*. In: Rubin E, Farber JL (ed) Pathology Philadelphia, Lippincott-Raven, 1236–1299.

Haug, R.H. (1999). Chronic problem wounds. *J Oral Maxillofac Surg Med Pathol*, 57(2), 213-218.

Hayward, P.G., Hillman, G.R., Quast, M.J., & Robson, M.C., (1993). Surface area measurement of pressure sores using wound molds and computerized imaging. *J Am Geriatrics Society*, 41(3), 238–240.

Healthpath (2011). Mowa - Mobile Wound Analyzer for Iphone, Ipad And Android- Healthpath. Retrieved November 2, 2016, from http://www.Healthpath.It/Imowa.Html.

Hellgren, L., & Vincent, J. (1986). A classification of dressings and preparations for the treatment of wounds by second intention based on stages in the healing process. *Care sci pract*, 4, 13-17.

Herndon, D.N., LeMaster, J., Beard, S., Bernstein, N., Lewis, S.R., Rutan, T.C., & Gore, D. (1986). The quality of life after major thermal injury in children: An analysis of 12 survivors with greater than or equal to 80% total body, 70% third-degree burns. *J Trauma*, 26(7), 609-619.

Hess, C.L., Howard, M.A., & Attinger, C.E. (2003). A review of mechanical adjuncts in wound healing: hydrotherapy, ultrasound, negative pressure therapy, hyperbaric oxygen, and electrostimulation. *Ann Plast Surg*, 51(2), 210–218.

Hon, J., Lagden, K., Mclaren, A.M., O'sullivan, D., Orr, L., Houghton, P.E., & Woodbury, M.G. (2010). A prospective, multicenter study to validate use of the PUSH in patients with diabetic, venous, and pressure ulcers. *Ostomy Wound Management*, 56(2), 26–36.

Hop, M.J., Polinder, S., Vlies, C.H., Middelkoop, E., & Baar, M.E. (2014). Costs of burn care: a systematic review. *Wound Repair Regen*, 22(4), 436-450.

Hoppe, A., Wertheim, D., Melhuish, J., Morris, H., Harding, K.G., & Williams, R.J. (2001). Computer assisted assessment of wound appearance using digital imaging In: Proceedings of the 23rd Annual International Conference of the IEEE Engineering in Medicine and Biology Society, Istanbul, Turkey, October 25-28.

Hunt, T.K., Knighton, D.R., Thakral, K.K., Goodson, W.H., & Andrews, W.S. (1984). Studies on inflammation and wound healing: angiogenesis and collagen synthesis stimulated in vivo by resident and activated wound macrophages. *Surgery*, 96(1), 48–54.

Hyunjoo, K., Junhyung, K., Jaehoon, C., & Woonhyuk, J. (2015). The Usefulness of Leukosan SkinLink for Simple Facial Laceration Repair in the Emergency Department. *Archives Plastic Surg*, 42(4), 431-437.

Image Analysis and Computer Vision Laboratory 2° Practical Exercise, (2012) -Requantization of the pixel intensities. Retrieved November 22, 2016, from http://www.vision.ee.ethz.ch/~cvcourse/solutions/1_sol.pdf.

iText (2000). iText library. Retrieved May 10, 2017, from http://itextpdf.com/.

Jadav, R. A., Patel, S. S., & Joshi, D. C. (2013). Image segmentation Based on Chan-Vese Active Contours using Finite Difference Scheme. *IJSRD*, 1(6), 2321-0613.

Jain, A. K. C. (2012). A new classification of diabetic foot complications: a simple and effective teaching tool. *J Diabetes Complications*, 4(1), 1-5.

Jain, A. K., & Farrokhnia, F. (1991). Unsupervised Texture Segmentation Using Gabor Filters. *Pattern Recognition*, 24(12), 1167-1186.

Jeffcoate, W.J. & Van Houtum, W.H. (2004). Amputation as a marker of the quality of foot care in diabetes. *Diabetologia*, 47(12), 2051–2058.

Jones, E.W., Peacock, I., McLain, S., & Fletcher E. (1987). A clinico-pathological study of diabetic foot ulcers. *Diabetic Med*, 4(5), 475–479.

Jones, I., Currie, L., & Martin, R. (2002). A guide to biological skin substitutes. *Br J Plast Surg*, 55(3), 185–193.

Kannon, G.A., & Garrett, A.B. (1995). Moist wound healing with occlusive dressings: a clinical review. *Dermatol Surg*, 21(7), 583–590.

Kantor, J., & Margolis, D.J. (2000). A multicentre study of percentage change in venous leg ulcer area as a prognostic index of healing at 24 weeks. *Br J Dermatol*, 142(5), 960–964.

Kass, M., Witkin, A., & Terzepoulos, D. (1988). Snakes: Active Contour Models. *Int J Comp Vision*, 1(4), 321-331.

Kaufman, J., Breeding, L., & Rosenberg, N. (1987). Anatomical location of acute diabetic foot infection: its influence on the outcome of treatment. *Am Surg*, 53(2), 109–112.

Kearney, C.R., Holme, S.A., Burden, A.D., & McHenry, P. (2001). Long-term patient satisfaction with cosmetic outcome of minor cutaneous surgery. *Australas J Dermatol*, 42(2), 102-105.

Keast, D.H., Bowering, K., Burrows, C., & D'Souza, L. (2003). New techniques in assessing non-healing ulcers— measuring up. Ninth Annual Conference, Canadian Association of Wound Care, Toronto, ON, Nov 6–9.

Kolesnik, M., & Fexa, A. (2005). *Multi-dimensional Color Histograms for Segmentation of Wounds in Images*. In: Kamel M., Campilho A. (eds) Image Analysis and Recognition. ICIAR 2005. Lecture Notes in Computer Science, 3656, 1014-1022, Berlin, Heidelberg: Springer.

Kranke, P., Bennett, M., Roeckl-Wiedmann, I., & Debus, S. (2004). Hyperbaric oxygen therapy for chronic wounds. *Cochrane Database Syst Rev*, 1(2), CD004123.

Krouskop, T. A., Baker, R., & Wilson, M. S. (2002). A noncontact wound measurement system. *JRRD*, 39(3), 337–346.

Kundin, J.I. (1985). Designing and developing a new measuring instrument. *Perioper Nurs Q*, 1(4), 40-45.

Kundin, J.I. (1989). A new way to size up wounds. *Am J Nurs*, 89(2), 206-207.

Ladin, D. (2000). Becaplermin gel (PDGF-BB) as topical wound therapy. *Plast Reconstr Surg*, 105(3), 1230–1231.

Langemo, D., Anderson, J., &nHanson, D. (2008). Measuring Wound Length, Width, and Area: Which Technique? *Adv Skin Wound Care*, 21(1), 42-45.

Langemo, D.K. (2005). Quality of life and pressure ulcers: What is the impact? *Wounds*, 17(1), 3–7.

Langemo, D.K., Melland, H., Hanson, D., Olson, B., Hunter, S., & Henly, S.J. (1998). Two-dimensional wound measurement: comparison of 4 techniques. *Adv Skin Wound Care*, 11(7), 337-343.

Langemo, D.K., Melland, H., Olson, B., Hanson, D., Hunter, S., Henly, S.J., & Thompson, P. (2001). Comparison of two wound volume measurement methods. *Adv Skin Wound Care*, 14(4), 190-196.

Langer, R., & Vacanti, J. P. (1993). Tissue engineering. *Science*, 260 (5110), 920–926.

Lanza, R., Langer, R., & Vacanti, J. (2007). *Future Perspectives*. In: Lanza, R. (ed.). *Principles of tissue engineering*. Academic Press (3rd Ed).

Larsson, J., Apelqvist, J., Castenfors, J., Agardh, C.D., & Stenstrom, A. (1993). Distal blood pressure as a predictor for the level of amputation in diabetic patients with foot ulcer. *Foot Ankle*, 14(5), 247–253.

Lau, D. (2012). Leading edge views: 3-D Imaging Advances Capabilities of Machine Vision: Part I. Retrieved December 1, 2016, from http://www.vision-systems.com/articles/print/volume-17/issue-4/departments/leading-edge-views/3-d-imaging-advances-capabilities-of-machine-vision-part-i.html.

Lavery, L.A., Armstrong, D.G., & Harkless, L.B. (1996). Classification of diabetic foot wounds. *J Foot Ankle Surg*, 35(6), 528–531.

Leskovec, N. K., Jezeršek, M., Mozina, J., & Lunder, T. (2007). Measurement of venous leg ulcers with a laser-based three-dimensional method: Comparison to computer planimetry with photography. *Wound Repair Regen*, 15(5), 767-171.

Levin, M. (1993). Diabetic foot ulcers: pathogenesis and management. *JET Nurs*, 20(5), 191–198.

Levin, M.E. (1998). Classification of Diabetic Foot Wounds. *Diabetes Care*, 21(5), 681-682.

Lorentzen, H. F., Holstein, P., & Gottrup, F. (1999). Inter-observer variation in the Red-Yellow-Black wound classification system. *Ugeskr Laeger*, 161(44), 6045-6048.

Kolesnik, M., & Fexa, A. (2005). Multi-dimensional color histograms for segmentation of wounds in images. In Proc. of Image Analysis and Recognition, *LNCS*, 3656, 1014-1022.

Mackelbust, J. (1997). PUSH tool reality check: Audience response. *Adv Wound Care*, 10(5), 102-106.

Majeske, C. (1992). Reliability of wound surface area measurements. *Phys Ther*, 72(2), 138-141.

Malian, A., Azizi, A., Van den Heuvel, F.A., & Zolfaghari, M. (2005). Development of a robust photogrammetric metrology system for monitoring the healing of bedscores. *Photogrammetric Record*, 20(111), 241-273.

Mani, R. (1999). Science of measurements in wound healing. *Wound Repair Regen*, 7(5), 330–334.

Mao, X. (2012). Evaluation of Chronic Wounds by Raman Spectroscopy and Image Processing, PhD Thesis, Faculty of Drexel University.

Margolis, D.J., Bilker, W., Knauss, J., Baumgarten, M., & Strom, B.L. (2002). The incidence and prevalence of pressure ulcers among Elderly patients in General Medical Practice. *Ann Epidemiol*, 12(5), 321–325.

Margolis, D.J., Hoffstad, O., Gelfand, J.M., & Berlin, J.A. (2003). Surrogate end points for the treatment of diabetic neuropathic foot ulcers. *Diabetes Care*, 26(6), 1696-1700.

Mark, A.K., & Warren, S.J. (2007). Update of treatment of diabetic foot infections. *Clin Podiatr Med Surg*, 24, 383-396.

Marston, W.A., Hanft, J., Norwood, P., & Pollak, R. (2003). The efficacy and safety of Dermagraft in improving the healing of chronic diabetic foot ulcers: results of a prospective randomized trial. *Diabetes Care*, 26(6), 1701–1705.

Martin, D., Umraw, N., Gomez, M., & Cartotto, R. (2003). Changes in subjective vs objective burn scar assessment over time: does the patient agree with what we think? *J Burn Care Rehabil*, 24(4), 239–244.

Martin, P. (1997). Wound healing—aiming for perfect skin regeneration. *Science*, 276(5309), 75–81.

Martin, P., & Parkhurst, S.M. (2004). Parallels between tissue repair and embryo morphogenesis. *Development*, 131(13), 3021–3034.

Mathworks, (1984). Mathworks. Retrieved April 28, 2017, from https://www.mathworks.com/.

MAVIS II (2006). MAVIS II: 3D Wound Instrument Measurement. Retrieved November 21, 2016, from https://at-web1.comp.glam.ac.uk/staff/pplassma/MedImaging/Projects/index.html.

Mayfield, J.A., Reiber, G.E., Sanders, L.J., Janisse, D., & Pogach, L.M. (1998). Preventive foot care in people with diabetes. *Diabetes Care*, 21(12), 2161–77.

Mayrovitz, H.N. (1997). Shape and area measurement considerations in the assessment of diabetic plantar ulcers. *Wounds*, 9(1), 21-28.

Mayrovitz, H.N., & Soontupe, L.B. (2009). Wound areas by computerized planimetry of digital images: accuracy and reliability. *Adv Skin Wound Care*, 22(5), 222-229.

Mazharinia, N., Aghaei, S., & Shayan, Z. (2007). Dermatology Life Quality Index (DLQI) scores in burn victims after revival. *J Burn Care Res*, 28(2):312-317.

McHorney, C.A., & Tarlov, A.R. (1995). Individual-patient monitoring in clinical practice: are available health status surveys adequate? *Quality Life Research*, 4(4), 293–307.

Mohafez, H., Ahmad, S. A., Roohi, S. A., & Hadizadeh, M. (2016). Wound Healing Assessment Using Digital Photography: A Review. *JBEMI*, 3(5), 1-13.

Morykwas, M.J., Argenta, L.C., Shelton-Brown, E.L., & McGuirt, W. (1997). Vacuum-assisted closure: a new method for wound control and treatment: animal studies and basic foundation. *Ann Plast Surg*, 38(6), 553–562.

Mukherjee, R., Manohar, D. D., Das, D K., Achar, A., Mitra, A., & Chakraborty, C. (2014). Automated tissue classification framework for reproducible chronic wound assessment. *BioMed Research Int*, 2014, 1-9.

Mustoe, T.A., Cutler, N.R., Allman, R.M., Goode, P.S., Deuel, T.F., & Prause, J.A. (1994). A phase II study to evaluate recombinant platelet-derived growth factor-BB in the treatment of stage 3 and 4 pressure ulcers. *Arch Surg*, 129(2), 213–219.

National Institute for Clinical Excellence (2003). Pressure ulcer prevention. Pressure Ulcer Risk Assessment and Prevention, Including the Use of Pressure-relieving Devices (beds, mattresses and overlays) for the Prevention of Pressure Ulcers in Primary and Secondary Care. Retrieved June 2, 2017, from https://www.nice.org.uk/guidance/cg7.

National Institute for Clinical Excellence (2005). The management of pressure ulcers in primary and secondary care. Retrieved November 2, 2016, from http://www.nice.org.uk/page.aspx?o=CG029.

Nedelec, B., Shankowsky, A., & Tredgett E.E. (2000). Rating the resolving hypertrophic scar: comparison of the Vancouver Scar Scale and scar volume. *J Burn Care Rehabil*, 21(3), 205–212.

Newton-Bishop, J.A., Nolan, C., Turner, F., McCabe, M., Boxer, C., Thomas, J.M., & Barrett, J.H. (2004). A quality-of-life study in high-risk (thickness >Z or 2 mm) cutaneous melanoma patients in a randomized trial of 1-cm versus 3-cm surgical excision margins. *J Investig Dermatol Symp Proc*, 9(2), 152-9.

Nguyen, T.A., Feldstein, S. I., Shumaker, P.R., & Krakowski, A. C. (2015). A review of scar assessment scales. *Semin Cutan Med Surg*, 34(1), 28-36.

Norton, D. (1996). Calculating the risk: reflections on the Norton Scale. *Adv Wound Care*, 9(6), 38–43.

Norton, D., McLaren, R., & Exton-Smith, A.N. (1962). *An Investigation of Geriatric Nursing Problems in Hospital*. London: National Corporation for the Care of Old People (1st Ed).

Oakley, W., & Caterall, C.F. (1956). Aetiology and management of lesions of the feet in diabetes. *BMJ*, 2(4999), 953–955.

Oduncu, H., Hoppe, A., Clarck, M., & Williams, R. J. (2004). Analysis of skin wound images using digital color image processing: a preliminary communication. *Int J Low Extrem Wounds*. 3(3), 151–156.

Omar, A.A., Mavor, A.I., Jones, A.M., & Homer-Vanniasinkam, S. (2004). Treatment of venous leg ulcers with Dermagraft. *Eur J Endovasc Surg*, 27(6), 666–672.

OpenCV, (2012). OpenCV library. Retrieved April 2, 2017, from http://www.opencv.org/.

Oyibo, S.O., Jude, E.B., Tarawneh, I., Nguyen, H.C., Harkless, L.B., & Boulton, A.J. (2001). A comparison of two diabetic foot ulcer classification systems: The Wagner and the University of Texas wound classification systems. *Diabetes Care*, 24(1), 84–88.

Palumbo, P.J., & Melton, L.J. (1985). *Peripheral vascular disease and diabetes*. In: Harris MI, Hamman RF, eds. *Diabetes in America*. Washington, DC: U.S. Govt. Printing Office, 85-1468.

Pancorbo, P.L., Garcia, F.P., Lopez, I.M., & Alvarez Nieto, C. (2006). Risk assessment scales for pressure ulcer prevention: a systematic review. *J Adv Nurs*, 54(1), 94-110.

Papanikolaou, P., Lyne, P., & Anthony, D. (2007). Risk assessment scales for pressure ulcers: A methodological review. *Int J Nurs Studies*, 44(2), 285–296.

Patterson, D.R., Everett, J.J., & Bombardier, C.H. (1993). Psychologic effects of severe burn injuries. *Psychol Bull*, 113(2), 362-378.

Patterson, D.R., Ptacek, J.T., Cromes, F., Fauerbach, J.A., & Engrav, L. (2000). The 2000 Clinical Research Award. Describing and predicting distress and satisfaction with life for burn survivors. *J Burn Care Rehabil*, 21(6), 490-498.

Pereira, S. M., Frade, M. A. C., & Rangayyan, R. M. (2013). Classification of colour images of dermatological ulcers. *IEEE J Biomed Health Inform*, 17(1), 136–142.

Peshko, O. (2005). Surface reconstruction from structured-light images for radiation therapy. MSc Thesis, McMaster University.

Piacquadio, D., & Nelson, D.B. (1992). Alginates: a “new” dressing alternative. *J Dermatol Surg Oncol*, 18(11), 992–995.

PictZar, (2007). PictZar Digital Planimetry Software. Retrieved December 2, 2016, from http://www.pictzar.com/.

Plassman, P., & Jones, T. (1998). MAVIS: a non-invasive instrument to measure area and volume of wounds. *Med Eng Phys*, 20(5), 332-338.

Plassmann, P. (1995). Measuring wounds. *J Wound Care*, 4(6), 269–272.

Plassmann, P., & Jones, B.F. (1992). Measuring Leg Ulcers by Colour Coded Structured Light. *J Wound Care*, 1(3), 35-38.

Plassmann, P., & Jones, T.D. (2003). Improved active contour models with application to measurement of leg ulcers. *JEI*, 12(2), 317-326.

Plassmann, P., Melhuish, J.M., & Harding, K.G. (1995). Problems of assessing wound size, University of Wales College of Medicine, Cardiff CF4 4XN, Wales, United Kingdom. Retrieved November 21, 2016, from http://webcache.googleusercontent.com/search?q=cache:I41PIwBn7uIJ:www.ibrarian.net/navon/paper/PROBLEMS_OF_ASSESSING_WOUND_SIZE.pdf%3Fpaperid%3D4354599+&cd=3&hl=pt-PT&ct=clnk&gl=pt

Polverini, P.J., Cotran, R. S., Gimbrone Jr, M. A., & Unanue, E.R. (1977). Activated macrophages induce vascular proliferation. *Nature*, 269(5631), 804–806.

Pories, W., Schear, E., Jordan, D., & Chase, J. (1966). Human wound healing. *Surgery*, 59(5), 821-824.

Powers, P.S., Sarkar, S., Goldgof, D.B., Cruse, C.W., & Tsap, L.V. (1999). Scar assessment: current problems and future solutions. *J Burn Care Rehabil*, 20(1), 54–60.

Ramos-e-Silva, M., & Ribeiro de Castro, M.C. (2002). New dressings, including tissue-engineered living skin. *Clin Dermatol*, 20(6), 715-23.

Ratliff, C.R., & Rodeheaver, G.T. (2005). Use of the PUSH tool to measure venous ulcer healing. *Ostomy Wound Management*, 51(58–60), 62–63.

Rees, R.S., Robson, M.C., Smiell, J.M., & Perry, B.H. (1999). Becaplermin gel in the treatment of pressure ulcers: a phase II randomized, double-blind, placebo-controlled study. *Wound Repair Regen*, 7(3), 141–147.

Reiber, G.E., Lipsky, B.A., & Gibbons, G.W. (1998). The burden of diabetic foot ulcers. *Am J Surgery*, 176 (Suppl 2A), 5–10.

Reichel, S.M. (1958). Shearing force as a factor in decubitus ulcers in paraplegics. *JAMA*, 166(7), 762–763.

Rennert, R., Golinko, M., Kaplan, D., Flattau, A., & Brem, H. (2009). Standardization of Wound Photography Using the Wound Electronic Medical Record. *Adv Skin Wound Care*, 22(1), 32-38.

Ribu, L., Hanestad, B.R., Moum, T., Birkeland, K., & Rustoen, T. (2007). A comparison of the health-related quality of life in patients with diabetic foot ulcers, with a diabetes group and a nondiabetes group from the general population. *Qual Life Res*, 16(2), 179–189.

Robson, M.C., & Smith, P.D. (2001). *Topical use of growth factors to enhance healing*. In: Falanga V (Ed), *Cutaneous wound healing*. London: Martin Dunitz Ltd, 379–398.

Robson, M.C., Phillips, L.G., Thomason, A., Robson, L.E., & Pierce, G.F. (1992). Platelet-derived growth factor BB for the treatment of chronic pressure ulcers. *Lancet*, 339(8784), 23–25.

Rodgers, L.C., Bevilacqua, N.J., Armstrong, D.G., & Andros, G. (2010). Digital Planimetry results in more accurate wound measurements: a comparison to standard ruler measurements. *J Diabetes Sci Technol*, 4(4), 799-802.

Rojas, A.I., & Phillips, T.J. (2001). *Venous ulcers and their management*. In: Falanga V (Ed), *Cutaneous wound healing*. London: Martin Dunitz Ltd, 263–286.

Roques, C., & Teot, L. (2007). A critical analysis of measurements used to assess and manage scars. *Int J Low Extrem Wounds*, 6(4), 249-253.

Saxena, V., Hwang, C.W., Huang, S., Eichbaum, Q., Ingber, D., & Orgill, D.P. (2004). Vacuum-assisted closure: microdeformations of wounds and cell proliferation. *Plast Reconstr Surg*, 114(5), 1086–1098.

Schoonhoven, L. (2003). Prediction of Pressure Ulcers: Problems and Prospects. PhD Thesis, University Medical Centre, Utrecht.

Shai, A., & Maibach, H I. (2005). *Wound Healing and Ulcers of the Skin: Diagnosis and Therapy - The Practical Approach*. New York: Springer Science and Business Media.

Shai, A., Maibach, H. I., & Ebooks, C. (2005). *Ulcer Measurement and Patient Assessment*, In *Wound Healing and Ulcers of the Skin: Diagnosis and Therapy - the Practical Approach*, ed Dordrecht: Springer-Verlag Berlin and Heidelberg GmbH and Co. KG, 89-102.

Sharifi, M., Fathy, M., & Mahmoudi, M.T. (2002). A Classified and Comparative Study of Edge Detection Algorithms. In proceedings of the International Conference on Information Technology: Coding and Computing, April 8-10, 117-120.

Shaw, J., & Bell, P. (2011). Wound Measurement in diabetic foot ulceration. In: Global Perspective on Diabetic Foot Ulcerations. Thanh Dinh (Ed), ISBN 978-953- 307-727-7. Retrieved June 2, 2017, from http://cdn.intechweb.org/pdfs/24689.pdf.

Shaw, J.E., & Boulton, A.J.M. (1997). The pathogenesis of diabetic foot problems. *Diabetes*, 46(Suppl. 2), 58–61.

Shea, J.D. (1975). Pressure sores: classification and management. *Clin Orthop Relat Res*, (112), 89–100.

Sheehan, P., Jones, P., Caselli, A., Giurini, J.M., & Veves, A. (2003). Percent change in wound area of diabetic foot ulcers over a 4-week period is a robust predictor of complete healing in a 12 week prospective trial. *Diabetes Care*, 26(6), 1879–1882.

Sheffield, C.G., Irons, G.B., Mucha, P. Jr, Malec, J.F., Ilstrup, D.M., & Stonnington, H.H. (1988). Physical and psychologic outcome after burns. *J Burn Care Rehabil*, 9(2), 172-177.

Shirakawa, M., & Isseroff, R.R. (2005). Topical negative pressure devices: use for enhancement of healing chronic wounds. *Arch Dermatol*, 141(11), 1449–1453.

Singer, A.J., & Clark, R.A. (1999). Cutaneous wound healing. *N Engl J Med*, 341(10), 738–746.

Singer, A.J., Arora, B., Dagum, A., Valentine, S., & Hollander, J.E. (2007). Development and validation of a novel scar evaluation scale. *Plast Reconstr Surg*, 120(7), 1892–1897.

Singer, A.J., Mach, C., Thode Jr., H.C., Hemachandra, S., Shofer, F.S., & Hollander, J.E. (2000). Patient priorities with traumatic lacerations. *Am J Emerg Med*, 18(6), 683-686.

Smith, G.M., Tompkins, D.M., Bigelow, M.E., & Antoon, A.Y. (1988). Burn-induced cosmetic disfigurement: Can it be measured reliably? *J Burn Care Rehabil*, 9(4), 371-375.

Sociedade Portuguesa de Diabetologia (1997). Sociedade Portuguesa de Diabetologia. Retrieved June 20, 2017, from http://www.spd.pt/.

Soo, C., Sayah, D. N., Zhang, X., Beanes, S.R., Nishimura, I., Dang, C., Freymiller, E., & Ting, K. (2002). The identification of novel wound-healing genes through differential display. *Plast Reconstr Surg*, 110(3), 787–797.

Sørensen, J. A., Jemec, G. B. E., & Yderstraede, K. B. (2015). Methods to assess area and volume of wounds – a systematic review. *Int Wound J*, 13(4), 540-553.

Steed, D.L. (1995). Clinical evaluation of recombinant human platelet-derived growth factor for the treatment of lower extremity diabetic ulcers. Diabetic Ulcer Study Group. *J Vasc Surg*, 21(1), 71–78.

Sterling, C. (1996). Methods of wound assessment documentation: a study. *Nurs Stand*, 11(10), 38–41.

Stotts, N.A., Rodeheaver, G. T., Thomas, D. R., Frantz, R. A., Bartolucci, A.A., Sussman, C., & MaklebustAn, J. (2001). Instrument to Measure Healing in Pressure Ulcers: Development and Validation of the Pressure Ulcer Scale for Healing (PUSH). *J Gerontol A Biol Sci Med Sci*, 56(12), 795–799.

Sullivan, T., Smith, J., Kermode, J., McIver, E., & Courtemanche, D.J. (1990). Rating the burn scar. *J Burn Care Rehabil*, 11(3), 256–60.

Tallman, P., Muscare, E., Carson, P., Eaglstein, W.H., & Falanga, V. (1997). Initial rate of healing predicts complete healing of venous ulcers. *Arch Dermatol*, 133(10), 1231–1234.

Thawer, H.A., Houghton, P.E., Woodbury, G., & Keast, D. (2002). A comparison of computer-assisted and manual wound size measurement. *Ostomy Wound Manage*, 48(10), 46–53.

Thomas, D.R., Rodeheaver, G.T., Bartolucci, A.A., Franz, R.A., Sussman, C., Ferrell, B.A., & Maklebust, J. (1997). Pressure ulcer scale for healing: derivation and validation of the PUSH tool. *Adv Wound Care*, 10(5), 96–101.

Torra, J.E. (1997). Valorar el riesgo de presentar úlceras por presión. Escala de Braden. *Rev Enferm*, 224, 23–30.

Van de Kar, A.L., Corion, L.U., Smeulders, M.J., Draaijers, L.J., Van der Horst, C.M., & Van Zuijlen, P.P. (2005). Reliable and feasible evaluation of linear scars by the Patient and Observer Scar Assessment Scale. *Plast Reconstr Surg*, 116(2), 514-522.

Van der Wal, M.B., Verhaegen, P.D., Middelkoop, E., & Van Zuijlen, P.P. (2012). A clinimetric overview of scar assessment scales. *J Burn Care Res*, 33(2), 79-87.

Van Houtum, W.H., Lavery, L.A., & Harkless, L.B. (1996). The impact of diabetes related lower-extremity amputations in the Netherlands. *J Diabetes Complications*, 10(6), 325–330.

Van Loey, N.E., & Van Son, M.J. (2003). Psychopathology and psychologic problems in patients with burn scars: Epidemiology and management. *Am J Clin Dermatol,* 4(4), 245-72.

Van Zuijlen, P.P., Angeles, A.P., Kreis, R.W, Bos, K.E., & Middelkoop, E. (2002). Scar assessment tools: implications for current research. *Plast Reconstr Surg*, 109(3), 1108-1122.

Van Zuijlen, P.P., Vloemans, J.F., Van Trier, A.J., Suijker, M.H., Van Unen, E., Groenevelt, F., & Middelkoop, E. (2001). Dermal substitution in acute burns and reconstructive surgery: a subjective and objective long-term follow-up. *Plast Reconstr Surg*, 108(7), 1938-1946.

Varma, A., Varma, A., Jakkampudi, H. M., & Raj, A. N. J. (2016) Vision based Pus Segmentation and Area Estimation of Wound using Android Application. *Indian J Sci Technol*, 9(3), 1-7.

Vascotto, S.G., Beug, S., Liversage, R.A., & Tsilfidis, C. (2005). Identification of cDNAs associated with late dedifferentiation in adult newt forelimb regeneration. *Dev Dyn*, 233(2), 347–355.

Venturi, M.L., Attinger, C.E., Mesbahi, A.N., Hess, C.L., & Graw, K.S. (2005). Mechanisms and clinical applications of the vacuum-assisted closure (VAC) device: a review. *Am J Clin Dermatol*, 6(3), 185–194.

Veredas, F., Mesa, H., & Morente, L. (2010). Binary tissue classification on wound images with neural networks and bayesian classifiers. *IEEE Trans Med Imag*, 29(2), 410-427.

Vermeulen, H., Ubbink, D. T., Schrender, S. M., & Lubbers, M. J. (2007). Inter- and intra-observer (dis)agreement among nurses and doctors to classify colour and exudation of open surgical wounds according to the Red-Yellow-Black scheme. *J Clin Nurs*, 16(7), 1270-1277.

Veves, A., Falanga, V., Armstrong, D.G., & Sabolinski, M.L. (2001). Graftskin, a human skin equivalent, is effective in the management of noninfected neuropathic diabetic foot ulcers: a prospective randomized multicenter clinical trial. *Diabetes Care*, 24(2), 290–295.

Vivanco, J., Haydaman, J., Hamel, C., McLeod, R. D., & Friesen, M. R. (2012). Development of wound care software for smartphones and tablets. *Wounds Int*, 3(3), 13-14.

Wagner, F.W. Jr. (1981). The dysvascular foot: a system for diagnosis and treatment. *Foot Ankle*, 2(2), 64–122.

Wagner, F.W. Jr., (1986). *The diabetic foot and amputation of the foot*. In Surgery of the Foot. Mann R.A. (ed) Mosby, St Louis, 421- 455 (5th Ed).

Wai-Han, C., Kit-Wai, C., French, P., Yim-Sheung, L., & Lai-Kwan, T. (1997). Which pressure sore risk calculator? A study of the effectiveness of the Norton scale in Hong Kong. *Int J Nurs Stud*, 34(2), 165–169.

Wang, L., Pedersen, P. C., Strong, D. M., Tulu, B., Agu, E., & Ignotz, R. (2015). Smartphone-Based Wound Assessment System for Patients with Diabetes. *IEEE Trans Biomed Eng*, 62(2), 477-488.

Wannous, H., Lucas, Y., Treuillet, S., & Albouy, B. (2008). A complete 3D wound assessment tool for accurate tissue classification and measurement. In Proc. IEEE 15th Conf. Image Process, 2928–2931, October 12-15.

Wannous, H., Treuillet, S., & Lucas, Y. (2010). Robust tissue classification for reproducible wound assessment in telemedicine environments. *J Electron Imaging*, 19(2), 023002.

Wannous, H., Treuillet, S., & Lucas. Y. (2007). Supervised tissue classification from color images for a complete wound assessment tool. In 29th Annual International Conference of the IEEE, Engineering in Medicine and Biology Society, 6031-6034, Lyon, France, August 23-26.

Waterlow, J. (1988). The Waterlow Card for the prevention and management of pressure sores: towards a pocket policy. *Care Sci Pract*, 6(1), 8–12.

Waterlow, J. (1998). The history and use of the Waterlow Card. *Nurs Times*, 94(7), 63–69.

Wendelken, M. E., Berg, W. T., Lichtenstein, P., & Markowitz, L. (2011). Wounds Measured from Digital Photographs Using Photo-digital Planimetry Software: Validation and Rater Reliability. *Wounds*, 23(9), 267-75.

Weststrate, J.T., Hop, W.C., Aalbers, A.G., Vreeling, A.W., & Bruining, H.A. (1998). The clinical relevance of the Waterlow pressure sore risk scale in the ICU. *Intensive Care Med*, 24(8), 815-820.

Whitaker, J.C. (2000). *The Resource Handbook of Electronics*. Boca Raton: CRC Press (1st Ed).

Whittington, K.T., & Briones, R. (2004). National Prevalence and Incidence Study: 6-Year sequential acute care data. *Adv Skin Wound Care*, 17(9), 490–494.

Xu, R.X. (2004). *Burns regenerative medicine and therapy*. Switzerland, Basel: S Karger AG (1st Ed).

Yeong, E.K., Mann, R., Engrav, L.H., Goldberg, M., Cain, V., & Costa, B. (1997). Improved burn scar assessment with use of a new scar-rating scale. *J Burn Care Rehabil*, 18(4), 353-355.

Young, D. (2016) Circle Hough Transform. Retrieved May 28, 2017, from https://www.mathworks.com/matlabcentral/fileexchange/26978-hough-transform-for-circles?focused=6019428&tab=function.

Zhan, C., & Miller, M.R. (2003). Excess length of stay, charges, and mortality attributable to medical injuries during hospitalization. *JAMA*, 290(14), 1868–1874.

Zheng, H., Bradley, L., Patterson, D., & Galushka M. (2004). New protocol for leg ulcer tissue classification from colour images. Proceedings of the 26th Annual International Conference of the IEEE Engineering in Medicine and Biology Society, San Francisco, CA, 1:13891392, September 1–4.